Spatiotemporal Variability in the Invasion Dynamics of the Gypsy Moth

Jonathan Anthony Walter
West Chester, Pennsylvania

Bachelor of Science, Gettysburg College, 2010

A Dissertation presented to the Graduate Faculty
of the University of Virginia in Candidacy for the Degree of
Doctor of Philosophy

Department of Environmental Sciences

University of Virginia
December, 2014

Acknowledgements

While only one name appears on the cover, dissertations are hardly one-person jobs and this one is no exception. Above all, I'd like to thank my advisor, Kyle Haynes, for his tremendous support and mentorship. I also received valuable guidance from the members of my committee: Howie Epstein, Todd Scanlon, and Janis Antonovics. I would like to extend thanks to several people with whom I collaborated on studies comprising my dissertation: Bill Fagan, Marci Meixler, Thomas Mueller, Ariel Firebaugh, Derek Johnson, and Patrick Tobin. Several people provided field or technical assistance on one or more components of this work: Tim Park, Laurel Cepero, Kate LeCroy, Clare Rodenberg, Brianna Collins, Drew Robison, Staige Davis, Mary-Ann Baner, Geno Luzader, Laura Blackburn, and Matt O'Connell. This work also benefitted greatly from conversations among the Terrestrial Ecology and Plant-Animal Interactions groups at UVa, and particular thanks go to Manuel Lerdau, Jeff Atkins, Dave Carr, T'ai Roulston, and Rosemary Malfi. Financial and logistical support for this work came from Blandy Experimental Farm, the University of Virginia Department of Environmental Sciences, the USDA Forest Service, the Gypsy Moth Slow the Spread Foundation, Inc., and the National Science Foundation. Access to field sites was facilitated by the Smithsonian Conservation Biology Institute, the 500-Year Forest Foundation, Rick Helms and Carolyn Phillips, John and Mary Alley, and John Hourigan. I would also like to thank my friends and family, whose positive effects on my graduate school experience cannot be measured. This achievement reflects the culmination of many small actions that began long before I knew what ecology was, let alone wanted to be an ecologist. For providing me innumerable opportunities for learning and growth, and themselves frequently being the vehicle of that learning, I'd like to thank my parents, Jim and Paula Walter. I'd also like to thank the Department of Environmental Studies at Gettysburg College, particularly John "Doc" Commito and Rud Platt, for honing my interest in ecology and the study of the environment.

Table of Contents

Abstract

The spread of invasive species has severe ecological and economic consequences, making it critical to understand the processes driving range expansion. A contemporary challenge in invasion ecology is to understand mechanisms generating observed spatial and temporal patterns of spread, which are inconsistent with classical models that predict rates of spread that are constant through space and time. Using the invasion of North America by the gypsy moth, this dissertation address four questions concerning mechanisms underlying spatiotemporal variability in the spread of invasive species, each representing a separate chapter: 1) Are observed temporal fluctuations in gypsy moth invasion rate driven by high-amplitude population fluctuations in established populations? 2) Does topography, by altering reproductive timing, affect population growth rates in spreading gypsy moth populations? 3) Does the configuration of gypsy moth habitat on the landscape affect gypsy moth mate finding and population growth? And 4) what general patterns of invasion dynamics result from spatial and temporal heterogeneity in environmental conditions?

In the first study, I combined time series analysis with a simulation model to find that yearly fluctuations in the invasion rate of the gypsy moth were driven by cycles in established populations, which affected the number of immigrants arriving to nascent populations near the invasion front via long-distance human-mediated transport. In the second study, I integrated empirical data and simulation models to demonstrate that the growth of nascent gypsy moth populations is strongly slowed by increases in elevation, and slowed more modestly by increases in the elevational variability (hilliness) of landscapes. These reductions in population growth are driven by topographically induced changes in the timing of reproductive maturation that result in mating failure. For example, moths developing at low elevations reach reproductive age before moths at higher elevations, isolating potential mates in time. Mating failure may also result from spatial isolation of potential mates; for example, boundaries between forest and non-forest habitat may act as barriers to movement. In the third study, I evaluated whether mating failure may be increased in landscapes where forest habitat is patchily distributed. Field experiments showed that gypsy moths strongly resist leaving forest patches and that mate-location probabilities decay more quickly in the non-forested matrix than in forested habitats. A simulation model predicted that increased spread rates would accompany increases in the abundance of forest habitat and the connectivity of forest patches, and an empirical analysis of gypsy moth spread rates was consistent with the model predictions. The second and third studies are among the first to show how environmental heterogeneity affects the severity of the Allee effect, a phenomenon causing slow population growth and extinctions in small populations. In the fourth study I used a theoretical model to investigate general responses of invasions to spatial heterogeneity in the severity of the Allee effect. Patterns of spread in landscapes with varying Allee effect severity depended on the spatial configuration of Allee variability, and depended also on an interaction between long-distance dispersal and the severity of the Allee effect.

This dissertation makes several contributions to applied and theoretical invasion ecology. These studies support ongoing efforts to slow the spread of the gypsy moth by improving predictions of risk of future gypsy moth spread. My findings also suggest that range expansion may be slowed by suppression of gypsy moth outbreaks. More generally, this work provides novel insights into two potentially widespread mechanisms causing variations in the severity of Allee effects, and suggests that such variations are an underappreciated source of variability in the dynamics of biological invasions.

1. Introduction

Globally, invasive species have severe ecological and economic consequences (Vitousek et al. 1996, Mack et al. 2000, Mooney and Hobbs 2000, Pimentel et al. 2005). Although there is continuing debate within the field over a precise definition, in general invasive species are those that have been transported to a location where they do not historically occur, that have become established in their new habitat, that spread from their initial point(s) of introduction, and substantially impact the ecosystems they invade (Lockwood et al. 2007). Introductions of exotic species to new habitats have risen as a consequence of growth in global commerce and are likely to continue to increase (Simberloff et al. 2013). Invasive species have been implicated in the loss of native biodiversity and in altering the structure and function of ecosystems (Mack et al. 2000, Simberloff et al. 2013). Many invasive species have become forest or agricultural pests, are nuisances to homeowners, or restrict outdoor recreation (Lockwood et al. 2007, Aukema et al. 2011). As a consequence of the dramatic impacts of invasive species, it is critical to understand the processes governing their establishment and spread.

The Spread of Biological Invasions

A contemporary challenge in invasion ecology is to understand the processes giving rise to spatial and temporal patterns in the spread of invasive species. Spatiotemporal patterns observed in nature do not conform to classical models of invasions, which formalized that range expansion is a function of population growth and dispersal, but also predict rates of spread that are constant through time and space (Fisher 1937, Skellam 1951). These classical models, however, do not incorporate several characteristics of real-world invasions that are predicted to generate different spatiotemporal patterns in spread. These characteristics include: cyclical

population fluctuations; stratified dispersal, in which both local and long-distance dispersal occurs within the same population; and Allee effects, which result in slow growth and extinction of small populations. Many spread models also disregard environmental heterogeneity, which may influence both population growth and dispersal and, as a result, influence spread. Hence, it is not yet clear how these different processes give rise to spread patterns in real landscapes, particularly when observed patterns might reflect interactions between multiple processes.

Spread models often assume that the rate of population growth is constant through time, or follows a simple generalized pattern such as a logistic curve, but fluctuations in the population growth rate–such as those resulting from environmental stochasticity, climatic oscillations, or trophic interactions (Hanski et al. 1993, Stenseth et al. 2002)–can produce episodes of advance and retreat of the invasion front (Neubert et al. 2000). When the population growth rate varies stochastically, the location of the range boundary is predicted to fluctuate, but the mean rate of spread converges on the prediction obtained using the mean population growth rate (Neubert et al. 2000). Not only can the population growth rate vary temporally, certain species exhibit high-amplitude, "boom-or-bust" population cycles. Understanding the effect of such cycles on spread may be particularly important because outbreaking species can be especially damaging. Neubert et al. (2000) found that when the population growth rate alternates between two values (e.g. a "good" and a "bad" state) with period *p*, the location of the invasion front fluctuates with the same period *p*. Johnson et al. (2006) also modeled range expansion in a population exhibiting high-amplitude population cycles, but their conclusions differed from those of Neubert et al. (2000) in that range boundary fluctuations occurred at half of the period length of population cycles. Another source of uncertainty in the role of population cycles in invasions is that the dynamics of nascent, low-density populations near a species' range boundary

may differ from longer-established populations behind the invasion front that undergo periodic outbreaks (Bjørnstad et al. 2008). Hence, the connections between population cycles and temporal patterns of spread, including the mechanisms potentially linking outbreaking populations to those at the invasion front, remain unresolved.

Outbreaking populations behind the invasion front could be mechanistically linked to nascent populations near the invasion front in systems exhibiting stratified dispersal. Stratified dispersal occurs when both local and long-distance "jump" dispersal occur side-by-side within a population (Shigesada et al. 1995). Long-distance dispersal can be the result of stage structure or polymorphism in dispersal capability within a population, but is thought to occur widely due to transport of an exotic species due to human activity (Shigesada et al. 1995, Neubert and Caswell 2000). Accidental human transport results when individuals, often as egg masses or seeds, are unnoticed hitchhikers on shipping materials, firewood or nursery stock, in vehicles or recreational equipment, or during household moves (Bigsby et al. 2011). Stratified dispersal is predicted to produce invasions in which the rate of spread accelerates through time rather than remaining constant (Shigesada et al. 1995).

The Allee Effect and Spread

One population dynamic phenomenon thought to have a strong impact on the establishment and spread of exotic species is the Allee effect. Originally developed to describe how cooperation between animals of the same species can result in increased per-capita fitness (Allee 1931), the Allee effect now refers to any positive correlation between population size (or density) and individual fitness (Stephens et al. 1999, Courchamp et al. 1999). Such effects of population size on fitness may result from mechanisms including mate (or pollen) limitation, inbreeding depression, breakdown of cooperative defense or foraging behaviors, and failure to

satiate predators (Kramer et al. 2009). Allee effects have been detected in a variety of taxonomic groups, including several families of plants and animals (Kramer et al. 2009). This taxonomic diversity, as well as the ubiquity of processes that can give rise to Allee effects, suggests that they may occur widely even though they have been difficult to detect in natural populations (Gregory et al. 2010, Ugeno 2013, Berec and Mrkvička 2013).

The concept of the Allee effect has also developed to distinguish between component Allee effects, in which increasing population size results in improvements in a particular aspect of fitness, and demographic Allee effects, in which improvements in fitness components with increasing population size result in an increase in the population growth rate (Stephens et al. 1999). Component Allee effects may not always translate into demographic Allee effects if, for example, increases in one component of fitness at higher densities is compensated for by reduced competition at low densities. Because the spread of biological invasions is intrinsically related to rates of population growth, this dissertation is explicitly concerned with demographic Allee effects, and it is implied that further use of the term "Allee effect" refers to the demographic variety.

Demographic Allee effects can be further characterized as being either weak or strong. In the case of a strong Allee effect, there is a threshold population size–termed the Allee threshold–below which the population growth rate is below the replacement rate and the population will likely decline to extinction. When Allee effects are weak, the rate of population growth is slowed while the population is small, but the population is likely to persist (Wang and Kot 2001, Taylor and Hastings 2005, Courchamp et al. 2008). Although the presence of an Allee threshold, and the population size at which it occurs, has obvious implications for population persistence, the full impact of Allee effects on population dynamics is a result of both the Allee

threshold and the rate at which increases in population size result in increases in the population growth rate (i.e., the slope of the relationship between population size and growth rate). I refer to the combination of Allee threshold and slope as the "severity" of the Allee effect since by convention the "strength" of the Allee effect denotes the presence or absence of an Allee threshold.

A rich body of theory predicts that Allee effects play a critical role in the establishment and spread of biological invasion. Strong Allee effects may act as filters that prevent exotic species from becoming established because the founder population size is below the Allee threshold (Leung et al. 2004, Lockwood et al. 2007, Courchamp et al. 2008). If a population is able to establish itself, increasing Allee effect severity is predicted to slow rates of spread and may contribute to the formation of stable range boundaries (Wang and Kot 2001, Keitt et al. 2001, Hastings et al. 2005). In contrast to classical models of invasion, when Allee effects are present spread is predicted to begin slowly and accelerate through time (Lewis and Kareiva 1993, Kot et al. 1996). Despite the apparent importance of Allee effects to the dynamics of biological invasions, relatively few empirical studies on the role of Allee effects in invasions have been published (Veit and Lewis 1996, Leung et al. 2004, Tobin et al. 2007b).

Recently, a small number of articles have highlighted how the severity of Allee effects may vary due to heterogeneity in environmental conditions (Tobin et al. 2007b, Kramer and Drake 2010, Kramer et al. 2011), and in one instance, regional differences in the Allee threshold were related to differences in the mean rate of range expansion (Tobin et al. 2007b). Due to the small number of studies on the subject, the understanding of the mechanisms underlying variation in Allee effect severity is extremely limited. Variation in Allee effect severity is likely, however, to occur widely because many of the types of mechanisms that produce Allee effects

display spatial and temporal variability. Furthermore, these empirical results showing variations in Allee effect severity stand in contrast to ecological theory, which has largely considered Allee effect severity to be fixed across time and space for a given population. Thus, further research is needed to understand how environmental characteristics and changes in biotic interactions alter the severity of Allee effects and how different patterns of Allee effect variation impact the spread of biological invasions.

Objectives

This dissertation investigates the role of population cycles and spatial variation in the severity of Allee effects in shaping spatiotemporal patterns of invasive spread using the invasion of North America by the gypsy moth (*Lymantria dispar*, Lepidoptera: Lymantriidae) as a model system. Specifically, I address four major research questions, each forming a separate chapter of the dissertation:

1) Are observed temporal fluctuations in gypsy moth spread rate driven by high-amplitude population fluctuations in established populations? Although the gypsy moth continues to expand its range over the long term, year-to-year fluctuations show periods of stasis, advance, and retraction of the range boundary. It is thought that population cycles in established populations contribute to this behavior, but the mechanisms linking established populations where high-amplitude cycles occur to nascent populations at the invasion front are not understood. I investigate the influence of gypsy moth population outbreaks on temporal patterns of gypsy moth spread by combining an analysis of spread and defoliation time series with insights from a simulation model.
2) Does topography, by altering reproductive timing, affect population growth rates in spreading gypsy moth populations? Successful reproduction necessitates that potential mates co-occur in space and time, but in many populations not all individuals are reproductively active at the same time. In insects such as the gypsy moth, developmental rates are temperature-dependent and thus topography may impact reproductive timing by driving local variations in thermal conditions. First, I use a simulation model to investigate how the effects of topography on gypsy moth reproductive timing influence population growth and

the severity of Allee effects. These results are then confronted with an empirical analysis of population growth rates in low-density populations near the invasion front.

3) Does the abundance and configuration of gypsy moth habitat on the landscape affect rates of gypsy moth spread? Rates of mating success may be influenced by effects of habitat characteristics on dispersal behavior. Individuals may alter their rates of movement in different habitat types, or avoid crossing edges between habitat types. I use field experiments to quantify the likelihood of adult male gypsy moths crossing forest edges to move into the non-forest matrix and the distance-decay of mate location probabilities in forested and non-forested habitats, and then use these results to inform development of a model simulating gypsy moth population spread in heterogeneous landscapes. These results are coupled with an empirical analysis of patterns of gypsy moth spread.

4) What general patterns of invasion dynamics result from spatial heterogeneity in the severity of Allee effects? In the second and third studies of my dissertation, I demonstrated two mechanisms by which geographical differences in environmental conditions could alter the severity of Allee effects. In light of the fact that environmental conditions vary widely in space and time, and evidence suggesting that Allee effects may occur widely, variation in the severity of Allee effects may be an underappreciated source of variability in the dynamics of biological invasions. To make general predictions for how spatial heterogeneity in the severity of Allee effects impacts patterns of range expansion, I develop a model simulating a population spreading through a landscape where the severity of Allee effects varies with several different spatial configurations representing null models and real-world patterns.

In the concluding chapter, I argue that this dissertation makes several important contributions to the field of ecology and the management of the gypsy moth invasion. This project contributes to efforts to slow the spread of the gypsy moth by improving predictions of invasion risk and suggesting a management intervention that could slow the rate of spread. This dissertation also highlights the importance of environmental heterogeneity to the dynamics of spreading populations. In particular, it provides evidence for two mechanisms generating spatial variability in the severity of Allee effects and suggests that variation in the severity of Allee effects may be a widespread and underappreciated source of variability in the dynamics of biological invasions.

The Gypsy Moth in North America

The gypsy moth is a highly polyphagous forest-defoliating pest native to Eurasia. Gypsy moths are noted for their cyclical, spatially synchronous population outbreaks, which are capable of producing widespread forest defoliation. Gypsy moth outbreaks reduce forest productivity (Clark et al. 2010), alter nutrient cycling (Riscassi and Scanlon 2009, Scanlon et al. 2010) , and alter the structure of forest communities (Doane and McManus 1981, Manderino et al. 2014). Population outbreaks are also a homeowner nuisance, disrupt outdoor recreational activities, and can contribute to timber losses. The total annualized cost of gypsy moths in the United States, including expenditures by the federal, state, and local governments, homeowner expenditures, and the loss of value to residential property and the timber industry is estimated at $253.5 million (Aukema et al. 2011). Gypsy moth outbreaks also occur in their native range, spanning Western Europe to Japan (Milenkovic et al. 2010).

The gypsy moth was introduced to North America in 1869 in Medford, Massachusetts, by Etienne Leopold Trouvelot, an artist, astronomer and amateur entomologist who was interested in hybridizing gypsy moths with other silk-producing caterpillars to improve resistance to a protozoan disease (Liebhold et al. 1989). Several insects escaped from the room where he was rearing them. Early efforts at eradication failed, and the gypsy moth became established and has spread, at spatially and temporally variable rates, over much of northeastern North America (Liebhold et al. 1992). Today, the gypsy moth's established range stretches from southern Nova Scotia and New Brunswick, Canada as far south as Virginia, USA, and as far west as eastern Minnesota, USA (USDA Forest Service 2014).

The gypsy moth makes an ideal model system for investigating spatiotemporal patterns of population dynamics and spread in an invasive species. Its status as a forest pest has prompted

research leading to a detailed knowledge of its basic biology as well as extensive monitoring of population dynamics and spread. Information on spread and the dynamics of nascent populations near the invasion front are provided through the gypsy moth Slow the Spread program (STS), which annually deploys >100,000 pheromone-baited gypsy moth traps over an area surrounding the leading edge of the invasion front. The dynamics of longer-established gypsy moth populations, located further behind the invasion front, can be approximated using spatially explicit records of gypsy moth defoliation derived from aerial surveys (Liebhold and Elkinton 1989, Johnson et al. 2006a, Haynes et al. 2012).

Prior studies indicate that gypsy moth spread is constrained by a combination of resource availability and climatic suitability. In the north of its range, suboptimal temperatures restrict spread (Liebhold et al. 1992, Sharov et al. 1999), while to the south spread is restricted by supraoptimal temperatures that inhibit larval development (Tobin et al. 2014). The gypsy moth feeds on over 300 species of trees and shrubs, but its most commonly-occurring preferred host species, on which gypsy moths have the highest survivorship and fecundity, are predominantly in the genera *Quercus* and *Populus* (Liebhold et al. 1995). The gypsy moth currently occupies only approximately 1/3 of the area in North America where its preferred host species are abundant (Morin et al. 2005).

Within limits imposed by host tree availability and climate, Allee effects and stratified dispersal are thought to be major forces contributing to patterns of spread (Liebhold et al. 1992, Liebhold and Tobin 2006, Johnson et al. 2006b, Tobin et al. 2009b). In this system, two mechanisms of Allee effects have been identified: predation (Bjørnstad et al. 2010) and mating failure (Robinet et al. 2007, 2008, Contarini et al. 2009). Small mammals, such as the white-footed mouse (*Peromyscus leucopus*) are major predators on gypsy moth pupae and are thought

to have a type-II predator functional response to gypsy moths (Elkinton et al. 2004). In the type-II response, predation rates, as a proportion of the population predated upon, are highest when prey density is lowest; theoretical and empirical studies support that the type-II functional response produces Allee effects in the prey species (Gascoigne and Lipcius 2004, Angulo et al. 2007, Kramer and Drake 2010). Mating failure Allee effects are thought to occur for reasons intrinsic to a species reproductive biology (Berec et al. 2007). In the case of the gypsy moth, one factor contributing to mating failure at low densities is that populations tend to exhibit protandry, meaning that males tend to mature and become reproductively active earlier than females (Robinet et al. 2007, 2008).

In the gypsy moth, stratified dispersal results from a combination of natural and anthropogenic processes. Local dispersal occurs largely through passive, wind-borne dispersal of early-instar larvae, a process termed "ballooning" because the larvae produce silk threads that increase their buoyancy in air currents. In North America adult females do not fly, meaning that most local spread occurs during the larval stage. Long-distance gypsy moth dispersal is thought to occur primarily through accidental movement of gypsy moth life stages by humans. Gypsy moths commonly lay their egg masses on firewood or recreational vehicles and equipment and so may be inadvertently transported ahead of the invasion front through commerce, recreation, and household moves (Liebhold et al. 1992, Bigsby et al. 2011). Long-distance dispersal may also occur if, during storms, gypsy moths become entrained in wind currents that transport them long distances (Tobin and Blackburn 2008, Frank et al. 2013). This phenomenon is thought to explain in part rapid rates of spread in Wisconsin (Tobin and Blackburn 2008, Frank et al. 2013), but is not though to occur widely in other parts of the gypsy moth's range.

Rates of gypsy moth spread vary in time and space (Liebhold et al. 1992, Tobin et al. 2007b, 2007a). Two recent studies have provided important insights into the causes of this variability, but questions remain. Johnson et al. (2006b) advanced understanding of temporal spread patterns by showing that pulsed invasion by the gypsy moth—cyclical periods of advance and stasis of the range boundary—could result from the combination of population cycles, stratified diffusion, and Allee effects. Periodic advance of the invasion front was hypothesized to occur based on the time it took nascent populations to grow large enough to send out enough emigrants to form viable populations. Precise connections between population cycles and spread, however, are not yet clear. For example, Johnson et al. (2006b) did not investigate temporal lags between population cycles and invasion pulses, or the distance over which population cycles influenced range expansion, which could yield inferences into the mechanisms contributing to observed patterns. In a study from the following year, Tobin et al. (2007b) used a novel approach for quantifying the Allee threshold to show that in the gypsy moth the severity of Allee effects varies from year-to-year and that the time-averaged Allee threshold differs between regions. This study did not, however, investigate ecological mechanisms that might cause the Allee threshold to vary and did not resolve patterns of spread occurring at local spatial scales, where mechanisms leading to variation in Allee effects are likely to operate.

2. Population cycles produce periodic range boundary pulses[1]

Abstract

Classical theories of biological invasions predict constant rates of spread that can be estimated from measurable life history parameters, but such outcomes depend strongly on assumptions that are often unmet in nature. Subsequent advances have demonstrated how relaxing assumptions of these foundational models results in other spread patterns seen in nature, including invasions that accelerate through time, or that alternate among periods of expansion, retraction, and stasis of range boundaries. In this paper, we examine how periodic population fluctuations affect temporal patterns of range expansion by coupling empirical data on the gypsy moth invasion in North America with insights from a model incorporating population cycles, Allee effects, and stratified diffusion. In an analysis of field data, we found that gypsy moth spread exhibits pulses with a period of 6 years, which field data and model simulations suggest is the result of a 6-year population cycle in established populations near the invasion front. Model simulations show that the development of periodic behavior in range expansion depends primarily on the period length of population cycles. The period length of invasion pulses corresponded to the population cycle length, and the strength of invasion pulses tended to decline with increases in population cycle length. A key insight of this research is that dynamics of established populations, behind the invasion front, can have strong effects on spread. Our findings suggest that coordination between separate management programs targeting low-density spreading and established outbreaking populations, respectively, could increase the efficacy of efforts to mitigate gypsy moth impacts. Given the variety of species experiencing population

[1] This study was conducted in collaboration with Derek Johnson, Patrick Tobin, and Kyle Haynes.

fluctuations, Allee effects, and stratified diffusion, insights from this study are potentially important to understanding how the range boundaries of many species change.

Introduction

Classical invasion theory formalizes that range expansion is a function of population growth and dispersal (Fisher 1937, Skellam 1951). These early models predict constant rates of spread that can be estimated analytically from measurable life history parameters, but such outcomes depend strongly on both explicit and implicit assumptions in the model framework (Hastings et al. 2005). For example, the model of Skellam (1951) assumes that all individuals disperse and reproduce simultaneously, that the redistribution of individuals fits a Gaussian distribution, that there is no variation in dispersal abilities of individuals, and that population growth is exponential. It is clear that such assumptions are violated in many cases, although some systems approximate these assumptions closely enough that actual rates of range expansion are consistent with predictions from the models of Fisher and Skellam (Fisher 1937, Skellam 1951, Andow et al. 1990). Subsequent theory has advanced our understanding of, among other characteristics of real biological invasions, the effects of non-Fickian diffusion (i.e., not occurring through Brownian motion) (Kot et al. 1996, Clark 1998), environmental fluctuations and demographic stochasticity (Neubert et al. 2000), and forms of density dependence (Lewis and Kareiva 1993, Kot et al. 1996, Keitt et al. 2001, Taylor and Hastings 2005).

When classical invasion models underestimate observed rates of spread, it is often inferred that long-distance dispersal is more frequent than what is assumed to occur under a Gaussian distribution of dispersal (Hastings et al. 2005). Indeed, data from a variety of plant and animal taxa show that dispersal in nature often follows a leptokurtic probability distribution, sometimes having a "fat" (exponentially unbounded, i.e., approaching zero slower than the

exponential decay function) tail (Kot et al. 1996, Clark 1998). Models incorporating leptokurtic dispersal kernels predict faster rates of spread than a Gaussian dispersal kernel, and when the distribution is exponentially unbounded the rate of spread accelerates through time (Kot et al. 1996, Clark 1998). Accelerating rates of range expansion can also result from stratified diffusion, in which both neighborhood diffusion and long-distance "jump" dispersal occur within a species (Shigesada et al. 1995).

Similarly, relaxing assumptions about population growth also affects patterns of range expansion. When invaders experience demographic Allee effects, invasions begin slowly and accelerate following a period of establishment (Lewis and Kareiva 1993, Kot et al. 1996). A demographic Allee effect describes the case in which there is a positive relationship between population density and the population growth rate, sometimes resulting in a threshold density below which the population growth rate is below the replacement level (Stephens et al. 1999). Allee effects are thought to inhibit establishment and slow the spread of many biological invasions (Lewis and Kareiva 1993, Taylor and Hastings 2005, Courchamp et al. 2008).

Fluctuations in the population growth rate, such as those resulting from environmental stochasticity, can produce episodes of advance and retreat of the invasion front (Neubert et al. 2000). Neubert et al. (2000) found that when the population growth rate alternates between two values (e.g. a "good" and a "bad" state) with period *p*, the location of the invasion front fluctuates with the same period *p*. When stochastic, rather than periodic, variations in the population growth rate were introduced to the model, the rate of spread converged on the mean prediction (Neubert et al. 2000).

Both classical invasion theory and more recent advances reveal an intimate connection between population processes and the spread rate. However, the evidence that new models yield

more realistic descriptions of natural systems often comes from the ability of such models to coarsely reproduce characteristics of range expansion such as a mean spread rate (Lubina and Levin 1988, Andow et al. 1990, Kot et al. 1996, Neubert and Caswell 2000). Empirical tests of the effects of population processes on spread patterns are few, due in part to the difficulties of monitoring the abundance of a species through time and over large areas. These challenges are particularly evident in low-density populations such as those occurring at the edge of a species' range (Ehler 1998, Fagan et al. 2002).

One exception to the "data problem" is the invasion of North America by the gypsy moth, *Lymantria dispar* (L.), which has become a model system for understanding the dynamics of biological invasions due to extensive monitoring of range expansion (Tobin et al. 2004, 2007b) and the ability to use aerial survey defoliation data as a proxy for population outbreaks to study the cyclical fluctuations of established populations (e.g. Liebhold and Elkinton 1989, Johnson et al. 2006a, Bjørnstad et al. 2010, Haynes et al. 2012). Liebhold et al. (1992) demonstrated the inadequacy of Skellam's classic equation to describe the spatiotemporal characteristics of range expansion by the gypsy moth. One conclusion of this work was the importance of long-distance transport to gypsy moth spread, resulting in stratified diffusion (Liebhold et al. 1992, Liebhold and Tobin 2006, Tobin and Blackburn 2008, Bigsby et al. 2011, Frank et al. 2013). Gypsy moth population dynamics also exhibit spatially synchronous high-amplitude fluctuations (Peltonen et al. 2002), oscillating between a low-density phase during which gypsy moths are barely detectable and population outbreaks during which extremely high densities of larvae cause spatially extensive tree defoliation. Previous studies have shown that gypsy moth population cycles have a primary period length of 8-10 years and a 4-5 year secondary period, with forest type, elevation, and predation pressure potentially contributing to variations in the period length

(Johnson et al. 2006a, Bjørnstad et al. 2010, Haynes et al. 2012). Allee effects are thought to be an important feature of the dynamics of low-density gypsy moth populations, for example at range boundaries (Tobin et al. 2007b, 2009b) or following an outbreak crash (Bjørnstad et al. 2010). Allee effects in the gypsy moth system have been observed to result from mate-finding failure at low densities (Robinet et al. 2008, Tobin et al. 2009b, 2013, Contarini et al. 2009) and small mammal predation (Elkinton et al. 1996, 2004, Bjørnstad et al. 2010).

Johnson et al. (2006b) combined these features—a cycling population, stratified dispersal, and an Allee effect—into a model of gypsy moth invasion dynamics. The model reproduced "invasion pulses" characteristic of gypsy moth range expansion, as represented in county quarantine records (U.S. Code of Federal Regulations, Title 7, Chapter III, Section 301.45-3). Invasion pulses were defined as "regularly punctuated range expansions interspersed among periods of range stasis" (Johnson et al. 2006b). Although the model agreed with empirical data, range dynamics differed from the general predictions of Neubert et al. (2000) in that gypsy moth invasion pulses occurred at ≈½ the period length of the population cycle. Hence, the precise nature of connections between population cycles and fluctuations in the rate of range expansion remains unresolved and is largely untested empirically. For example, Johnson et al. (2006b) did not investigate temporal lags between population cycles and invasion pulses, or the distance over which population cycles influenced range expansion.

In this paper, we analyze time series of gypsy moth defoliation and year-to-year displacement of gypsy moth range boundaries to explore connections between gypsy moth population cycles and range expansion. These findings are interpreted in light of insights from a spread model to understand relationships between population cycling and year-to-year temporal variations in invasion speed. In the model, period length and strength of population cycles were

varied to simulate weakly to strongly cyclic populations across a range of period lengths. We hypothesize that periodic temporal fluctuations in the gypsy moth invasion rate are driven by population cycles occurring in established populations near the invasion front. We also hypothesize that cyclically fluctuating populations tend to produce pulsed invasion dynamics, the definition of which we extend to include the possibility of range retraction. Studies by Johnson et al. (2006b) and Neubert et al. (2000) made different predictions regarding the period length of range boundary fluctuations relative to the length of population cycles, and one difference between these studies is that population fluctuations were weaker in Johnson et al. (2006b). Given this discrepancy, we further predict that the period length of invasion pulses depends on the strength of population cycles.

Methods

Study Area

We focused our study on gypsy moth spread in the Piedmont, Blue Ridge, Ridge and Valley, Central Appalachian, and Western Allegheny Plateau ecoregions of West Virginia, Virginia, and North Carolina. Spatially extensive, temporally continuous trapping data from the deployment of pheromone-baited traps date to 1989, the longest such record for any region in the United States. We excluded eastern Virginia (i.e. the Southern Plain and Atlantic Coastal Plain ecoregions) from this analysis because of markedly different invasion dynamics in which the spread of gypsy moth populations appears to be restricted by supraoptimal temperatures during the larval and pupal period (Tobin et al. 2014). Major forest type groups in our study region include oak-hickory, maple-beech-birch, spruce-fir, and oak-pine, with the oak-hickory group covering the largest percentage (59%) of the study area (USDA Forest Service 2008). From the

late 1980s to mid 2000s the mean rate of gypsy moth spread in West Virginia, Virginia, and North Carolina was ≈7 km yr^{-1} (Tobin et al. 2007a).

Measuring Invasion Rates

We measured yearly invasion rates based on data from the deployment of pheromone-baited traps from the gypsy moth Slow the Spread program (STS) and its precursors (Tobin et al. 2012). Under such programs, ≈15,000 pheromone traps are deployed annually along the leading edge of the invasion front in our study area. Traps are generally placed ≈2 km apart, but in some areas are as little as 0.25 km or as much as 3-8 km apart (Tobin et al. 2004). Although they capture only males, pheromone-baited traps are highly effective at sampling very low to medium densities (Schwalbe 1981, Elkinton and Cardé 1983), providing an effective means of delineating spreading populations.

Invasion rates were estimated using the "boundary displacement" method (Sharov et al. 1995b, Tobin et al. 2007a). To estimate population boundaries, we first interpolated, from each year's trap catch data from 1989 to 2012, a continuous surface of gypsy moth abundance over a network of 1×1 km lattice cells using median indicator kriging (Isaaks and Srivastava 1989) in GSLIB (Deutsch and Journel 1992); this approach accommodated for the exact locations of traps changing from year to year. Because some gypsy moth populations are treated under the STS program in an effort to eliminate newly formed colonies ahead of the invasion front (Tobin et al. 2004), trap catch data within 1.5 km of a treated area were excluded prior to kriging; generally, ≤2% of the area was treated each year.

From the interpolated surface of each year, we then estimated the 10-moth population boundary using an optimization algorithm that spatially delineated areas at which the expected catch per pheromone-baited trap was 10 moths (Sharov et al. 1995b). The 10-moth population

boundary was chosen as a proxy for the range boundary because it has been shown to be relatively more stable than other population boundaries (Sharov et al. 1995b). We measured the distance from a point fixed in space (39.39 °N, 77.16 °W) to the boundary along transects radiating from the fixed point at 0.25° intervals (Tobin et al. 2007b). The year-to-year displacement along each transect was measured and averaged across the study area to obtain a yearly invasion rate.

Geographically Referenced Outbreak Data

The periodic characteristics of gypsy moth outbreaks were assessed by analyzing an archive of defoliation survey maps covering the northeastern United States over a period of up to 38 years (1975-2012) (Liebhold et al. 1997, USDA Forest Service 2013). These maps were digitized and compiled into a geographical information system (GIS). We calculated the total annual area of defoliation within 10 zones representing distances from the mean position of the 10-moth population boundary from 1989-2012: 0-50 km, 50-100 km, 100-150 km, 150-200 km, 200-300 km, 300-400 km, 400-500 km, 500-600 km, 600-700 km, and 700-800 km. Because the gypsy moth invasion did not advance into Virginia and West Virginia until 1982, no defoliation was recorded near the invasion front at the beginning of the defoliation record; hence, shorter time series were used for 0-50 km (1990-2012), 50-100 km (1990-2012), 100-150 km (1986-2012), 150-200 km (1986-2012), and 200-300 km (1978-2012).

Wavelet Analysis

We used wavelet analysis (Torrence and Compo 1998) to detect the periodic characteristics of time series of gypsy moth invasion rates and gypsy moth defoliation. Similar to Fourier analysis, wavelet analysis may be used to extract frequency information from a signal,

but wavelet analysis can also be applied to signals where the frequency and amplitude of oscillations vary through time (Torrence and Compo 1998). Wavelet analysis measures how well oscillating periodic functions ("wavelets") approximate a time series. The wavelet transform, which measures the correspondence between a wavelet function and the data, is computed as the integral of the amount of overlap as the wavelet function is slid across the time series. The dominance of signals of different period length in the time series data is determined by comparing the power (square of the wavelet transform) of wavelets of varying scale (width), using a known relationship between scale and period length (Torrence and Compo 1998). We used the Morlet wavelet, a modified sine wave that is localized in time by damping it with a Gaussian envelope (Farge 1992, Grenfell et al. 2001). Prior to performing wavelet analysis, the distribution of observations in each time series was normalized and standardized to have zero mean and unit variance (Torrence and Compo 1998). To correct for a bias toward producing higher power values for low-frequency (long period length) signals, we divided the wavelet power by the wavelet scale, as suggested by Liu et al. (2007). When using wavelet analysis, significance levels for wavelet spectra are determined by comparing the actual spectrum against a null model that uses a random process to produce synthetic data sharing statistical characteristics with the original time series (Torrence and Compo 1998, Cazelles et al. 2014). The outcome of the significance test depends strongly on the process used to generate the null model (Cazelles et al. 2014), and Cazelles et al. (2014) identified the hidden Markov model (HMM) algorithm as effectively balancing conservatism and computational efficiency. Consequently, we chose the HMM algorithm to generate the null models for our statistical tests of wavelet power.

We used two complementary extensions of wavelet analysis to investigate relationships between invasion and defoliation time series: the cross-wavelet spectrum and wavelet coherence (Cazelles et al. 2007). The cross-wavelet spectrum indicates wavelengths at which both time series have common wavelet power, corresponding to the relative importance of shared variation at each wavelength. Wavelet coherence indicates consistency in phase differences between both time series and is similar to a cross-correlation, except that it allows detection of relationships at specific wavelengths. Values of wavelet coherence range from 0 (independent time series) to 1 (phase-locked time series), and consistent phase differences suggest causal relationships between time series. Monte Carlo simulation experiments were used to test for statistical significance in the cross-wavelet spectrum and wavelet coherence (Cazelles et al. 2007). As for the univariate wavelet analyses, the null model was developed using an HMM algorithm, and time series were normalized and standardized to unit variance prior to analysis. Time series of defoliation prior to 1990, which is the first year of the invasion rate time series, were truncated to match the length of the invasion rate time series. We computed wavelet coherency and cross-wavelet spectra for the invasion rate time series paired with time series of defoliated area within each zone corresponding to different distances from the invasion front. Wavelet analyses were performed in MATLAB release 2011b (MathWorks, Inc., Natick, Massachusetts), using code developed by Cazelles et al. (2007).

Mechanistic Model of Gypsy Moth Spread

We simulated gypsy moth spread by spatially extending a mechanistic gypsy moth population dynamics model developed by Dwyer et al. (2004), and incorporating modifications by Bjørnstad et al. (2010) and Haynes et al. (2012). The original Dwyer et al. (2004) model simulated the combined effects of the gypsy moth nucleopolyhedrosis virus (*Ld*NPV) and

generalist small-mammal predators on gypsy moth population dynamics. Development of the model was informed by extensive field and lab experiments on viral transmission (Dwyer and Elkinton 1993, Dwyer et al. 1997) and experimental data on interactions with small mammal predators (Elkinton et al. 1996). An important modification by Bjørnstad et al. (2010) was to model the effects of *Ld*NPV and predators sequentially, with viral infection imposed during the larval stage and predation imposed during the pupal stage. These modifications accord with the timing of these mortality sources in field populations. Prior studies have shown the model produces an Allee effect at low densities (Bjørnstad et al. 2010) and periodic fluctuations in gypsy moth density across 4 orders of magnitude (Dwyer et al. 2004, Bjørnstad et al. 2010, Haynes et al. 2012) as observed in field populations of the gypsy moth (Berryman 1991).

In the model, the density of larvae in year *t* is calculated as

$$\widetilde{N}_t = \lambda N_{t-1}, \quad (1)$$

where λ is the mean number of female larvae produced per adult female and N_{t-1} is the density of adult females in year *t-1*. The fraction of these larvae that are infected and killed by *Ld*NPV, $I(\widetilde{N}_t, \tilde{Z}_t)$, depends on densities of larvae $\widetilde{N}_t$ and viruses $\tilde{Z}_t$. The fraction of larvae killed by *Ld*NPV is given by

$$1 - I\left(\widetilde{N}_t, \tilde{Z}_t\right) = \left(1 + \frac{\bar{v}}{\mu k}\left(\widetilde{N}_t I\left(\widetilde{N}_t, \tilde{Z}_t\right) + \rho \tilde{Z}_t\right)\right)^{-k}, \quad (2)$$

where μ is the rate at which cadavers lose infectiousness, ρ is the susceptibility of hatchlings relative to later-stage larvae, $\bar{v}$ is the average transmission rate, and *k* is the inverse squared coefficient of variation of transmission rate (Dwyer et al. 2000, 2004). The density of individuals surviving to the pupal stage is then

$$N'_t = \widetilde{N}_t\left(1 - I\left(\widetilde{N}_t, \tilde{Z}_t\right)\right), \quad (3)$$

and viral density in generation t+1 can then be calculated as

$$\tilde{Z}_{t+1} = f\tilde{N}_t I\left(\tilde{N}_t, \tilde{Z}_t\right), \quad (4)$$

where *f* is the over-winter growth rate of the pathogen.

The largest source of mortality of pupae in low-density gypsy moth populations is predation by small mammals (Elkinton and Liebhold 1990, Elkinton et al. 1996). Though results from empirical studies differ as to whether predation on gypsy moth pupae by small mammals follows a type-II or a type-III functional response (Schauber et al. 2004, Elkinton et al. 2004), following Bjørnstad et al. (2010) we modeled predation on gypsy moth pupae using a type-II functional response with parameter values pinpointed by Haynes et al. (2012) to yield outbreak dynamics similar to those found by Dwyer et al. (2004) when using a type-III predator functional response. Our model of adult gypsy moth dynamics is then

$$N_t = N'_t \exp\left(-\frac{abP}{N'_t + b}\right) e^{v_t} . \quad (5)$$

Here, *P* is the predator density, *a* determines the maximum fraction of prey killed and *b* determines the half-saturation point (the density at which the number of prey killed is half the maximum killed). The term $\exp(v_t)$ incorporates stochastic variation in population growth into equation 5, with v_t representing a zero-mean, unit-variance normally distributed random variable.

We spatially extended the model over a two-dimensional 50 cell by 750 cell landscape with locations linked by dispersal. Local, short-distance dispersal was simulated by randomly determining if a grid cell would serve as a source population in each generation with probability *Sr* and then transporting a constant proportion, p_{sr}, of the source population to a new cell. Short-distance dispersers moved to neighboring cells using rook (8-cell) continuity. Similarly, long distance transport of egg masses was implemented by randomly selecting source population grid cells in each generation with probability *Lr* and transporting a constant proportion, p_{lr}, of the

source population to a new cell. The displacement in the *x* and *y* directions of long distance dispersal events was determined by independently drawing random values from a normal distribution with mean = 0 and standard deviation = 1, and multiplying these values by the scalar value *Ld*. In our simulations, we set $Sr = 0.1$, $p_{sr} = 0.01$, $Lr = 0.01$, $p_{lr} = 0.01$, and $Ld = 15$.

Given prior knowledge of the importance of long-distance transport to gypsy moth invasion dynamics (Liebhold et al. 1992, Liebhold and Tobin 2006, Bigsby et al. 2011, Frank et al. 2013), we used parameter values for *Lr* and p_{lr} thought to be realistic for the system, assuming that each grid cell is approximately 1×1 km. Because gypsy moth females are flightless, short-distance spread occurs mainly through "ballooning," passive wind-borne dispersal by neonates. The empirical estimate of the diffusion coefficient for larval ballooning is 0.003 km^2 $generation^{-1}$ (Liebhold and Tobin 2006), suggesting that on average few individuals would disperse to a new grid cell in a given year. To achieve this in the model, rather than prescribe a very small proportion from all grid cells to disperse we chose to balance the probability of short distance dispersal, *Sr*, and the proportion of short-distance dispersers, p_{sr}, so that over the entire landscape the same number of individuals would disperse as if individuals dispersed from every population in every generation. This substantially reduced the computational demands of the model. We also examined the degree to which our results were sensitive to the values of these parameters (Appendix A1).

We were primarily interested in how patterns of gypsy moth spread would change when populations cycled with different period lengths and strengths of cyclicity. Haynes et al. (2012) showed that varying the predator density, *P*, primarily affected the period length of population cycles, while varying the per-capita rate of growth, λ, primarily affected the strength of cyclicity. Hence, we varied *P* and λ to simulate weakly to strongly cycling populations with period lengths

of 6, 8, 10, and 12 years (Table 1). The intermediate value of $\lambda = 74.6$ represents an empirical estimate of gypsy moth fecundity (Dwyer et al. 2004). The values of additional parameters in equations 2 and 4 were empirically derived (Elkinton et al. 1996, Dwyer et al. 2004; $\bar{v} = 0.9$, $\mu = 0.32$, $k = 1.06$, $\rho = 0.8$, and $f = 21.33$). The minimum viral density was set at 0.0001, which functioned to prevent extinctions of NPV and may mimic rescue effects due to dispersal (Schauber 2001).

We used the model to simulate data on spread that were analogous to the field data, with the spread rate in the *y* direction determined from year-to-year differences in the position of the invasion front. For each year *t*, we fit a smoothing spline to the row-average population size along a transect from $y = 1$ to $y = 750$ in which the initial density was contained within cells corresponding to row $y = 1$; cells were populated by randomly drawing from a normal distribution. The position of the invasion front at time *t* was estimated to be the largest value of *y* with a mean population size (determined from the smoothing spline) above a threshold density. We examined the sensitivity of periodic behavior of range boundaries to the value of this threshold by varying it by orders of magnitude between 10^{-9} and 10^{-5} (Appendix A2). Though in any given simulation the density of source populations fluctuated over four orders of magnitude, the density at the nadir of population cycles declined from 10^{-5} to 10^{-7} as we increased *P*, making these densities reasonable thresholds for delineating the extent of spread. Simulations were run for 250 generations, with data on spread and population size taken only from the last 100, allowing 150 generations of run-up time to reach non-transient spread dynamics. As with the field data, global wavelet spectra were used to describe the periodic behavior of the invasion time series of the simulated data. Here, we report the mean global wavelet spectra of 100 model

iterations. Model simulations and analyses were conducted in MATLAB release 2014a (MathWorks, Inc., Natick, Massachusetts).

Results

Empirical Analysis

Between 1989 and 2012, the gypsy moth expanded its range in our study area at an average rate of 2.6 km yr^{-1}, but in a single year the range contracted as much as 24.0 km or expanded as much as 18.8 km (Figure 1). Wavelet analysis indicated a dominant ≈6-year period in invasion rate (Figure 1). Time series of area defoliated by the gypsy moth confirmed the occurrence of periodic outbreaks (Figure 2), but dominant periods in the defoliation time series varied with distance from the invasion front (Figure 3). The 0-50 km, 50-100 km, and 100-150 km zones, representing distances from the invasion front, showed high and significant wavelet power at ≈6 years, matching the period of invasion pulses, but the strongest cross wavelet power and wavelet coherence were found between invasion rate and defoliation 50-100 km from the invasion front. In combination, the cross-wavelet spectrum and wavelet coherence indicated that the invasion rate and defoliation at 50-100 km from the invasion front share high wavelet power at an ≈6-10 year period and that there was a consistent phase difference between the two time series over these wavelengths (Figure 4). Phase differences between invasion rate and defoliation at 50-100 km from the invasion front (represented by the angle of the phase arrows in Figure 4) indicate that the defoliation cycle tends to lead the invasion rate by ≈1 year. Defoliation time series in other zones showed relatively less cross-wavelet power and wavelet coherence with invasion rate (Figure 4). Although our time series are relatively short for applying wavelet

analysis (22-38 years), we found statistically significant wavelet metrics that were unaffected by edge effects, even using 22 year time series (Figure 4).

Model Results

Periodic behavior of spread depended mainly on the period length and very little on the strength of population cycles (Figure 5). The largest peaks in wavelet power for the simulated invasion time series coincided with the period length of population cycles, and the magnitude of these peaks, corresponding to the strength of invasion pulses, tended to decline as period length increased. Smaller, secondary peaks in wavelet power occurred at ½ of the population cycle length (and ¼ of length of cycles 8 years or longer), and secondary peaks tended to increase in power as λ increased (Figure 5). These patterns were insensitive to variability in parameters controlling short-distance dispersal, while the magnitude of peaks in wavelet power, but not their period length, was sensitive to parameters controlling long-distance dispersal (Appendix A1). In Figure 5, the population density of the range boundary was set at 10^{-7}, matching the order of magnitude of gypsy moth density at the nadir of population cycles under the highest predator densities. Simulation outcomes were somewhat sensitive to the choice of the population density threshold defining the range boundary (Appendix A2). Increasing the population density that defined the range boundary tended to shift invasion pulses toward shorter period lengths (Appendix A2).

Discussion

Cyclical or "pulsed" behavior in gypsy moth range dynamics appears to coincide with population cycles in established populations near the invasion front. In the empirical analysis, yearly invasion rate showed a dominant 6-year period, which was matched by dominant 6-year

period lengths in defoliated area within 0-50 km, 50-100 km, and 100-150 km from the invasion front. Interestingly, cross-wavelet power and coherency between population cycles and yearly rates of range expansion were strongest at 50-100 km from the invasion front, suggesting that outbreaking populations within this zone are an important source of immigrants to the invasion front through long-distance dispersal. Over period lengths of ≥6 years, the time series were out of phase by ≈1 year, with punctuated forward movements of the invasion front lagging one year behind peaks in the defoliated area.

The strength of cross-wavelet power and wavelet coherence between defoliation 50-100 km from the invasion front and the invasion rate suggests that populations within these distances may contribute the most immigrants to the invasion front. Although populations 0-50 km and 100-150 km from the invasion front also shared a 6-year dominant cycle length with invasion pulses, the number of immigrants contributed to the invasion front is likely a function of gypsy moth density (host population size) and distance from the invasion front. Compared to populations 50-100 km from the invasion front, less defoliation occurred within 0-50 km, likely due to the gypsy moth's more recent establishment. Defoliation within 0-50 km from the invasion front generally occurred in small patches and tended to have a lower total area, whereas longer-established populations further from the invasion front produced more widespread areas of defoliation; hence populations 0-50 km from the invasion front may contribute fewer immigrants to the invasion because of their lower overall density. Populations 100-150 km from the invasion front may provide fewer immigrants to the invasion front than those 50-100 km from the invasion front because the probability of long distance transport events likely decays with distance.

Our observation that pulses in invasion tended to occur 1 year after peaks in population density 50-100 km behind the invasion front may be explained by human-mediated long distance dispersal. It is thought that this mode of dispersal primarily involves the anthropogenic movement of egg masses. Egg masses are present for approximately 8 months out of the year and are sessile, and thus are more readily transported through household goods, firewood, and other cargo (Liebhold and Tobin 2006, Hajek and Tobin 2009, Bigsby et al. 2011). Thus, eggs transported beyond the invasion front in a given year would eventually emerge as adults in the following year, during which adult males would be recorded in pheromone-baited traps.

Our model reproduced observed patterns of cyclical pulses in range expansion. This agreement between theory and empirical data provides strong evidence that gypsy moth invasion pulses are driven by population cycles in established populations behind the invasion front. More generally, cyclical patterns of spread in the model depended primarily on the period length of population fluctuations, with invasion pulses occurring with the same period length as the population cycles. However, the strength of invasion pulses, indicated by the magnitude of the peak in wavelet power, declined as population cycles lengthened. These results add nuance to previous theoretical predictions regarding invasions with fluctuating source populations. Our findings largely agree with those of Neubert et al. (2000), in which range boundaries also fluctuated with the same period length as the population, but Neubert et al. (2000) did not evaluate how the strength of range boundary fluctuations could be affected by the period length and strength of population fluctuations. Given that in Neubert et al. (2000) populations alternated between two states, the added realism of modeling a continuously fluctuating population, as in this study, strengthens inferences about how periodic population fluctuations affect invasive spread.

In the empirical analysis, our finding of 6-year period lengths for both invasion and defoliation differs from previous studies, which have found invasion pulses with a 4-year period and population cycles with 8-10 year dominant and 4-5 year subharmonic periods (Johnson et al. 2006a, 2006b, Haynes et al. 2009, 2013). There are several reasons why this study may have observed different dynamics than previous works. Johnson et al. (2006b) observed invasion pulses with a 4-year period using yearly gypsy moth quarantine records covering the entire invasion from 1960 to 2002, which may primarily reflect spread patterns prior to the implementation of the gypsy moth Slow the Spread program; pilot Slow the Spread programs in our study region began in 1989, and the entire invasion front, from Wisconsin to North Carolina, was not managed until 1996 (Tobin et al. 2004). Moreover, determining invasion rates from a field measurement of population size, as we have done, provides a more accurate picture of spread dynamics than county quarantine records that are coarser in spatial scale and most importantly cannot show retraction of range boundaries. Prior research has demonstrated spatial (Haynes et al. 2009, 2012, 2013) and temporal (Allstadt et al. 2013) variation in the periodic behavior of gypsy moth population dynamics, so the dynamics in the time period and area studied here may differ from the overall, spatiotemporally averaged dynamics of the system. These prior studies of gypsy moth population cycles have focused on New England, New York, and Pennsylvania (where the gypsy moth has been established longer, leaving a longer record for analysis), whereas our analysis focused on Virginia and West Virginia given our interest in linking defoliation to spatially detailed trapping records that quantify spread dynamics.

Another difference between this study and Johnson et al. (2006b) is that, in the Johnson et al. (2006b) model, weakly cycling populations with a 9-10 year period length produced invasion pulses with a 4-year dominant period. Johnson et al. (2006b) used a phenomenological

second-order autoregressive (AR[2]) model to simulate population cycles in the established area, in contrast to the mechanistic population model used here. Because AR(2) models are commonly used to simulate cycling populations, further research should investigate how the properties of different population models contribute to differences in resultant invasion dynamics, and whether invasion pulses generally occur at ≈1/2 the population cycle length, as in Johnson et al. (2006b), or at the full population cycle length, as in this study.

Collectively, our results demonstrate a link between cycles in source populations and pulsed range expansion, and show how variations in the periodic behavior of source populations can yield different temporal patterns of range expansion. These results have immediate implications for management as the gypsy moth range continues to expand. Existing efforts to slow the spread of the gypsy moth focus on treatment of isolated populations formed by long-distance dispersal (Tobin et al. 2004). Our findings suggest a conceptual model of gypsy moth spread in which population cycles in the moth's established range lead to pulses in the number of immigrants reaching nascent populations. Pulsed influxes of immigrants, in turn, may be critical to the persistence and growth of nascent populations, in which population growth is known to be limited by Allee effects (Tobin et al. 2009b). The importance of cyclical fluctuations in the density of source populations to pulsed invasion suggests that a strategy of suppressing outbreaks in source populations may be an effective means of slowing invasive spread. In addition to the Slow the Spread program, which exclusively manages gypsy moth spread along its leading population front, gypsy moth outbreaks in the areas where the species is already well established are largely managed under federal and state cooperative suppression programs (Tobin et al. 2012) separate from the Slow the Spread program. Our results suggest that coordination between these two separate management programs (Slow the Spread and cooperative

suppression) could be mutually beneficial: spread rates along the expanding front would be reduced, which would effectively reduce the area infested by the gypsy moth that could experience outbreaking populations.

Our results also contribute to a broader understanding of how population fluctuations affect range expansion, specifically in cases where the combination of stratified diffusion and Allee effects is also present. In particular, this study indicates that cyclical population behavior gives rise to corresponding cyclical variations in spread, and suggests an important role of long-distance dispersal in the development of invasion pulses. Given the variety of species exhibiting population cycles (Symonides et al. 1986, Hanski et al. 1993, Johnson et al. 2010), that stratified diffusion may potentially be widespread (Andow et al. 1990, Shigesada et al. 1995), and that Allee effects slow the growth of low-density populations of many taxa (Kramer et al. 2009), these insights are potentially important to understanding how the range boundaries of many species change.

Tables & Figures:

Table 1: Population parameters used in model simulations. Parameters were tuned to simulate weakly to strongly cycling populations at period lengths of 6, 8, 10, and 12 years.

	Values			
Parameter	**6-year**	**8-year**	**10-year**	**12-year**
λ = 50 (Per-capita rate of increase: weak population cycles)				
P (predator density)	0.16	0.61	0.75	0.82
λ = 74.6 (Per-capita rate of increase: normal population cycles)				
P (predator density)	0.16	0.69	0.85	0.95
λ = 100 (Per-capita rate of increase: strong population cycles)				
P (predator density)	0.16	.74	0.9	0.98

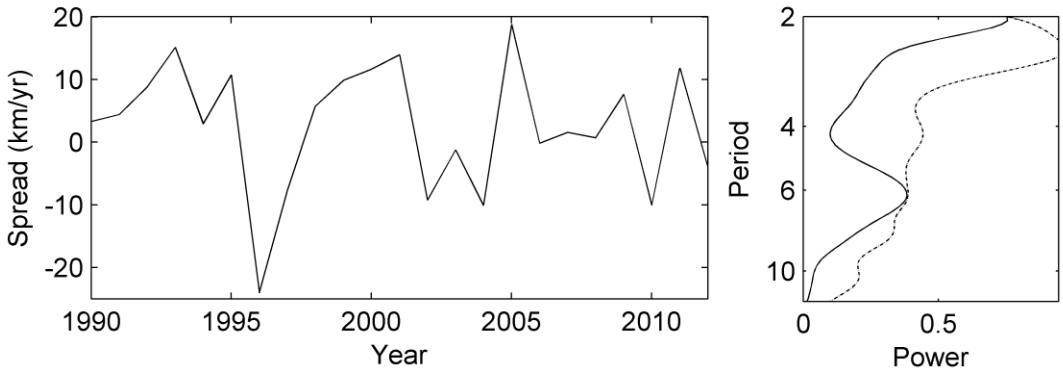

Figure 1: Time series of gypsy moth invasion rate (left) and global wavelet spectrum of the invasion rate time series (right). Invasion rate represents year-to-year displacement of the 10-moth population boundary. For the wavelet spectrum, solid lines indicate the power of the real series and dashed lines indicate the null hypothesis. Periods where the solid lines cross the dashed lines indicate significant wavelet power at that period.

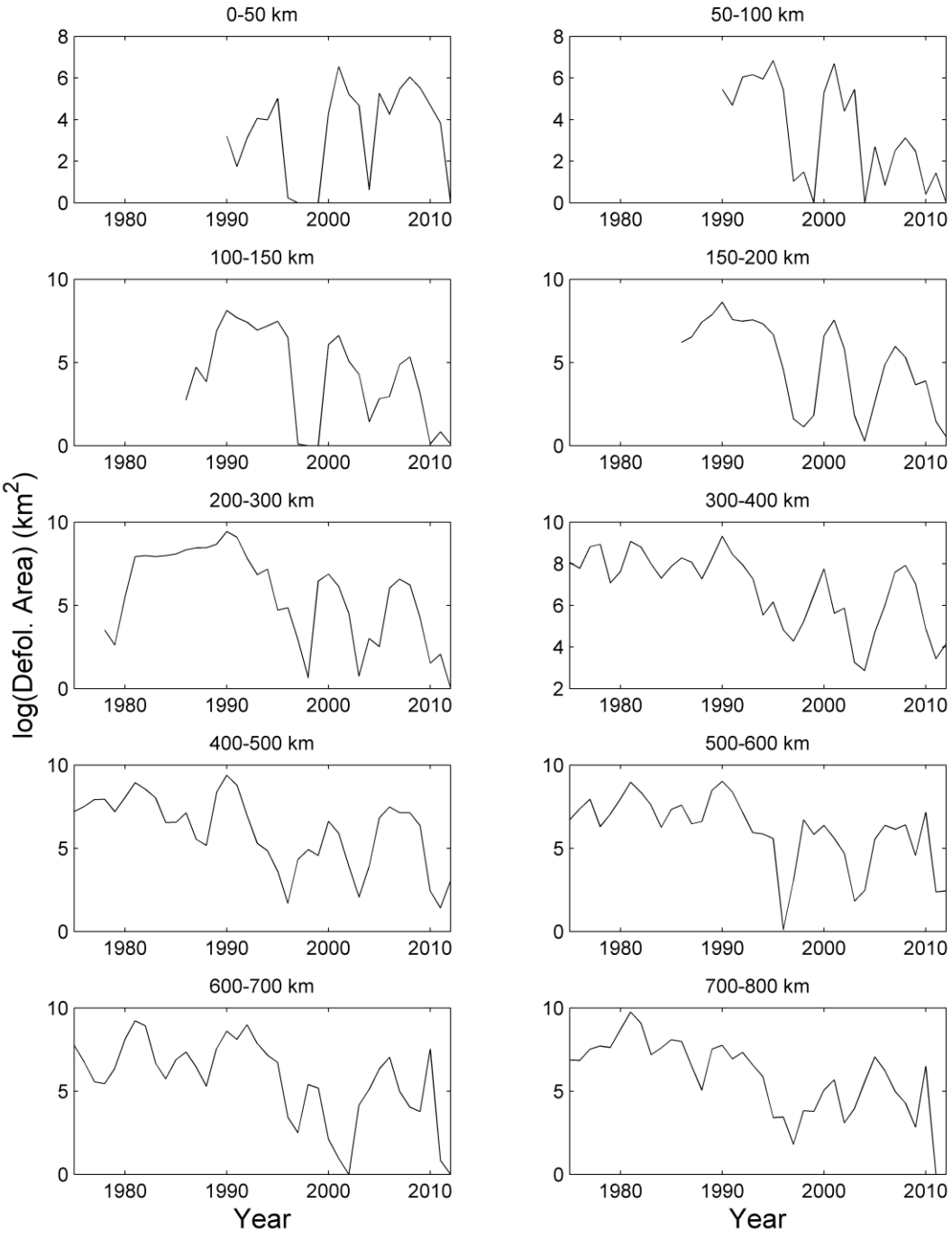

Figure 2: Time series of area defoliated by gypsy moths over a range of distances from the invasion front. Defoliation time series are $\log(x + 1)$ transformed.

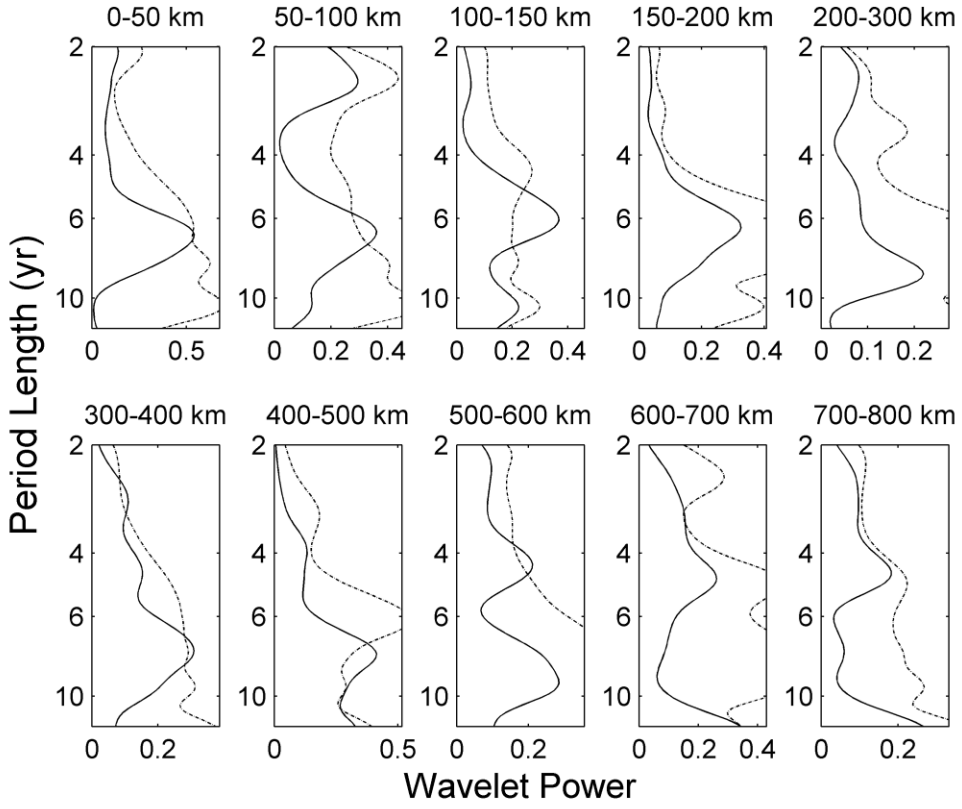

Figure 3: Global wavelet spectra for time series of defoliation at a range of distances from the invasion front. Solid lines indicate the power of the real series and dashed lines indicate the null hypothesis. Periods where the solid lines cross the dashed lines indicate significant wavelet power at that period.

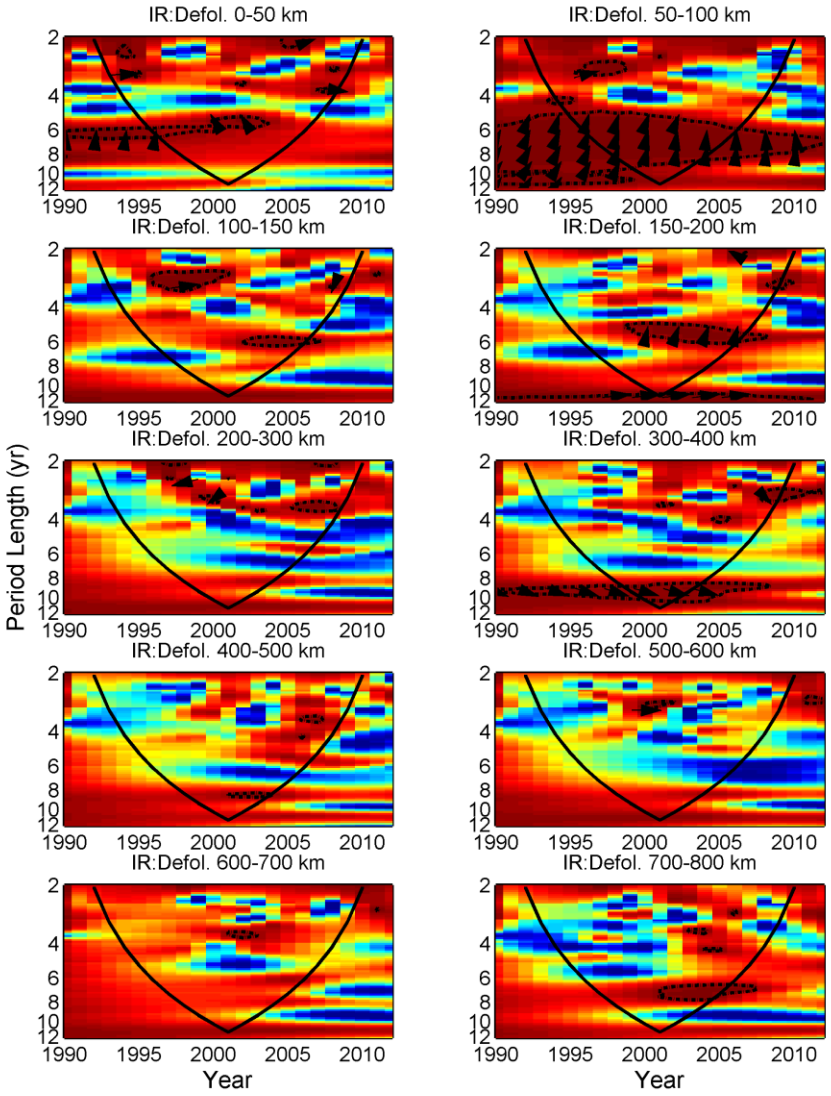

Figure 4: Wavelet coherency plots for invasion rate and defoliation. "Hotter" colors (e.g., red) indicate higher coherency: period lengths having statistically significant coherence and cross-wavelet power are outlined in black, with arrows indicating phase differences within these regions of statistical significance. Rightward-facing arrows denote series in-phase, leftward-facing arrows denote series perfectly out of phase. Upward-tilted arrows denote defoliation leading invasion rate by a fraction of period length. The black "v" shaped lines denote the cone of influence, outside of which results may be influenced by edge effects.

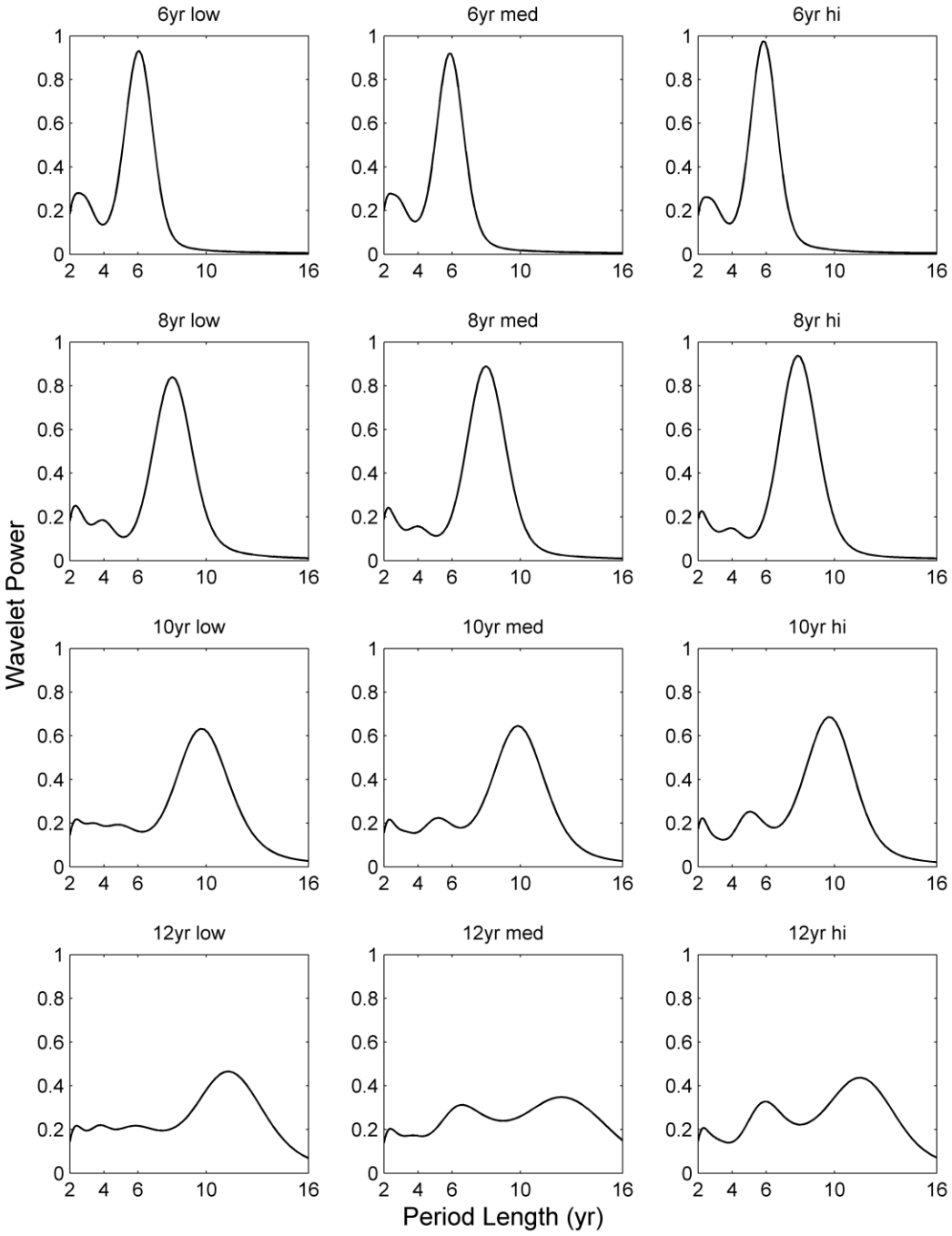

Figure 5: Averaged (n = 100) global wavelet spectra for model-simulated range expansion with populations exhibiting weak, normal, and strong population cycles with period lengths of 6, 8, 10, and 12 years.

3. How topography induces reproductive asynchrony and alters gypsy moth invasion dynamics[2]

Abstract

Reproductive asynchrony, a temporal mismatch in reproductive maturation between an individual and potential mates, may contribute to mate-finding failure and Allee effects that influence the establishment and spread of invasive species. Variation in elevation is likely to promote variability in maturation times for species with temperature-dependent development, but it is not known how strongly this influences reproductive asynchrony or the population growth of invasive species. We examined whether spatial variation in reproductive asynchrony, due to differences in elevation and local heterogeneity in elevation (hilliness), can explain spatial heterogeneity in the population growth rate of the gypsy moth, *Lymantria dispar* (L.), along its invasion front in Virginia and West Virginia, USA. We used a spatially explicit model of the effects of reproductive asynchrony on mating success to develop predictions of the influences of elevation and elevational heterogeneity on local population growth rates. Population growth rates declined with increased elevation and more modestly with increased elevational heterogeneity. As in earlier work, we found a positive relationship between the population growth rate and the number of introduced egg masses, indicating a demographic Allee effect. At high elevations and high heterogeneity in elevation, the population growth rate was lowest and the density at which the population tended to replace itself (i.e., the Allee threshold) was highest. An analysis of 22 years of field data also showed decreases in population growth rates with elevation and heterogeneity in elevation that were largely consistent with the model predictions. These results highlight how topographic characteristics can affect reproductive asynchrony and

[2] This chapter has been published as: Walter, J.A., M.S. Meixler, T. Mueller, W.F. Fagan, P.C. Tobin, & K.J. Haynes (2014). How topography induces reproductive asynchrony and alters gypsy moth invasion dynamics. *Journal of Animal Ecology*. doi: 10.1111/1365-2656.12272

influence mate-finding Allee effects in an invading non-native insect population. Given the dependence of developmental rates on temperature in poikilotherms, topographic effects on reproductive success could potentially be important to the population dynamics of many organisms.

Introduction

Invasions by non-native species are significant threats to biodiversity and ecosystem function (Mack et al. 2000, Pimentel et al. 2005). One factor influencing the establishment and spread of introduced species is the Allee effect (Lewis and Kareiva 1993, Fagan et al. 2002, Taylor and Hastings 2005). A demographic Allee effect describes a positive relationship between population growth rate and population size (Stephens et al. 1999). Underlying mechanisms of Allee effects include inbreeding depression, failure to satiate predators, inability to acquire prey, and failure to locate mates at low population densities (Kramer *et al.* 2009). In the case of a strong Allee effect, the population is unable to replace itself when below some minimum population density, termed the Allee threshold (Stephens et al. 1999, Courchamp et al. 1999). Recent studies have detected spatiotemporal variability in the Allee threshold due to heterogeneity in biotic and abiotic conditions (Tobin et al. 2007b, Kramer et al. 2011). Variability in the strength of Allee effects may appear as changes in the Allee threshold density or in the slope of the relationship between population growth rate and population density. Despite the importance of this phenomenon to invasion ecology, there are relatively few empirical studies concerning Allee effects in biological invasions (Veit and Lewis 1996, Leung et al. 2004, Tobin et al. 2007b), partly due to the challenges of measuring low-density populations in which Allee effects occur.

One common cause of Allee effects is mate-finding failure (Gascoigne *et al.* 2009), which can be influenced by reproductive asynchrony (Calabrese and Fagan 2004, Robinet et al. 2008). Reproductive asynchrony describes a temporal mismatch in reproductive maturity between an individual and potential mates, which—though potentially adaptive in higher-density populations as it may promote outbreeding (Morbey and Ydenberg 2001), decrease female waiting (Morbey and Ydenberg 2001), and hedge against environmental stochasticity (Post *et al.* 2001)—could limit mating opportunities in low-density populations (Calabrese and Fagan 2004). Considering the population-level temporal distribution of reproductive activity, reproductive asynchrony may reduce fitness in low-density populations if the temporal distribution of reproductive activity for either sex is wide, or if males and females tend to mature at different times (i.e. protandry or protogyny) (Calabrese and Fagan 2004, Calabrese et al. 2008, Larsen et al. 2013).

The degree of reproductive asynchrony in a population may show trends with elevation and latitude (Robinet et al. 2007, Larsen et al. 2013), and another factor that would increase temporal dispersion in reproductive activity is if individuals from different locations–near enough to be linked by dispersal–developed at different times due to differences in microclimate. Consequently, factors leading to variability in phenology across spatial gradients could influence mating success. In taxa with temperature-dependent developmental rates (e.g., poikilotherms), heterogeneity in elevation could affect mating success by promoting spatial variability in the emergence of sexually mature adults, but this hypothesis has not been explored.

The gypsy moth, *Lymantria dispar* (L.) (Lepidoptera: Lymantriidae), is an ideal model organism for examining the influence of topography on mating success and the consequences for invasion dynamics. Introduced to North America outside Boston, MA, in 1869, its current North

American range stretches from Nova Scotia to Wisconsin, and Ontario to Virginia (Tobin et al. 2012), and range expansion continues at variable rates (Tobin, Liebhold & Roberts 2007a). Under the gypsy moth Slow-the-Spread programme, >100,000 pheromone-baited traps are deployed annually over >200,000 km^2 along the invasion front (Tobin et al. 2012). Data from this programme are currently available from the Central Appalachian region from 1988 to 2012, providing a unique opportunity to study the population dynamics governing this invasion within a topographically diverse region.

A prior analysis of Slow-the-Spread data revealed an Allee threshold below which populations declined to extinction and demonstrated how spatial variation in the Allee threshold influenced the rate of spread (Tobin *et al.* 2007b). Mate finding failure is thought to be an important cause of Allee effects in this system (Tobin *et al.* 2009b). Gypsy moth females in North America are not capable of flight and attract flying males using a pheromone. Empirical studies have consistently documented that female mating success increases with male moth density (Sharov et al. 1995a, Tcheslavskaia et al. 2002, Tobin et al. 2013). Along the invasion front, females frequently go unmated (Contarini *et al.* 2009), and reproductive asynchrony is thought to be one potential cause of mate finding failure (Robinet *et al.* 2007, 2008).

Across the range of the gypsy moth in North America, thermal gradients due to elevation and latitude produce variation in phenology (Regniere and Sharov 1998, Tobin et al. 2009a). Differences in protandry (the degree to which males tend to mature earlier than females) and the temporal dispersion of maturation times have been linked to geographic trends in mating success (Robinet, Liebhold & Gray 2007). While the authors do not explicitly discuss elevation, findings by Robinet, Liebhold & Gray (2007) indicate a reduction in mating success as elevation increases in the Central Appalachian region (see Fig. 4 in Robinet, Liebhold & Gray 2007).

Mating success may decline with elevation if adult emergence becomes increasingly asynchronous, for instance because of increased day-to-day temperature variability at high elevations (Whiteman 2000). A pattern of increased phenological variability in mountainous areas has also been empirically observed (Regniere and Sharov 1998).

Despite the importance of Allee dynamics to the spatial spread of the gypsy moth (Johnson *et al.* 2006b), the underlying causes of geographic variation in the dynamics of low-density populations (e.g. Tobin *et al.* 2007b) remain unknown. We investigated the degree to which elevation and elevational heterogeneity, by influencing reproductive asynchrony, could affect geographic variability in the growth of gypsy moth populations. We extended a spatially explicit model to simulate phenology and mate finding in topographically variable landscapes, and then connected these theoretical findings to an analysis of 22 years of field-collected population density data. We made two hypotheses about the population growth rate of gypsy moths along the invasion front, where populations have not become fully established and densities are low. These are: a) population growth rates will decrease as elevation increases because gains in elevation increase reproductive asynchrony, and b) population growth rates will decrease as local elevational heterogeneity (hilliness) increases because such heterogeneity causes potential mates from different elevations to become sexually mature at different times.

Methods

Study System

The gypsy moth is a polyphagous forest defoliating pest native to Eurasia. In North America, female gypsy moths are flightless, thus natural population spread occurs mainly though passive wind-borne dispersal of neonates, during which larvae typically disperse tens to

hundreds of meters (Mason and McManus 1981). Long-distance transport, over distances up to hundreds of kilometers, occurs mainly through accidental movement of gypsy moth life stages by humans (Liebhold and Tobin 2006). Because females are sessile, successful mating depends on a free-flying male locating a mature female. Consequently, rates of mating success are affected by local male moth density (Contarini et al. 2009, Tobin et al. 2013). Adult males could disperse up to1-3 km, but typical dispersal distances are on the order of tens to hundreds of meters (Mastro 1981). Prior research indicates adult phenology can affect mating success, which is reduced by increases in protandry and temporal dispersion of reproductive maturation times (Robinet *et al.* 2007, 2008). Both of these phenological characteristics vary due to temperature gradients across the range of the gypsy moth, with temporal dispersion of reproductive maturation (measured as the standard deviation [SD] of the maturation distribution) ranging at least 2.3 to 4.5 days and protandry ranging at least 3 to 5 days (Robinet *et al.* 2007).

Study Area

We focused our study on a ≈100,000 km^2 area centered over Virginia and West Virginia, where elevation ranges from 95 to >1900 meters above sea level (Figure 1). This area spans portions of the Piedmont, Blue Ridge, Northern Ridge and Valley, Central Appalachian and Western Allegheny Plateau ecoregions. Major forest type groups include oak-hickory, maple-beech-birch, spruce-fir, and oak-pine. The oak-hickory group covers the largest percentage (59%) of the study area (USDA Forest Service 2008). The mean gypsy moth spread rate in this area from the late 1980s to 2000s was ≈7 km yr^{-1} (Tobin *et al.* 2007a). Continuous trapping records from the deployment of pheromone-baited traps, which attract adult males, from this area date to 1988.

Population Growth Model

We extended the model of Robinet *et al*. (2008) to examine how elevation and heterogeneity in elevation influence gypsy moth mating success and population growth. Their model was developed to study the effects of reproductive asynchrony (protandry and temporal dispersion of adult maturation) on gypsy moth mating success. In the model's original form, *N* egg masses were introduced at the center of a 0.5×0.5 km region devoid of the species. Then, neonates of both sexes dispersed in two spatial dimensions (*x* and *y*) at time *t* based on the simple diffusion equation:

$$\frac{\partial U}{\partial t}(x, y, t) = D\left(\frac{\partial^2 U}{\partial x^2}(x, y, t) + \frac{\partial^2 U}{\partial y^2}(x, y, t)\right), \quad (1)$$

where the diffusion coefficient $D = 0.003$ km^2 (Liebhold and Tobin 2006) and U is the standardized population density. Individuals were assigned to locations based on probabilities generated by the diffusion equation. Egg-to-adult mortality was implemented by randomly choosing surviving individuals at a realistic survivorship rate of 0.05 (Elkinton and Liebhold 1990). The timing of reproductive maturation was simulated using Gaussian functions with peak male maturation fixed at an arbitrary day. Both the temporal dispersion of the maturation period and the amount of protandry were varied to assess their effects. Mating success depended on spatial and temporal overlap of potential mates. The probability of a female attracting a given male (p_i) at a given distance (x) and time lag between male and female maturation (i = 0, 1, or 2 days) was estimated using the negative exponential equation:

$$p_i(x) = a_i \exp(-b_i x), \quad (2)$$

where a_i and b_i are parameters fitted based on release-recapture experiments simulating mate finding (Robinet *et al.* 2008). Mortality of adult males was implicitly accounted for in the mate

attraction function. Mate finding at lags ≥ 3 days was ignored given the short life spans of adult males. Females were assumed to be reproductively active only on the day of their emergence due to high rates of mortality (Sharov et al. 1995a). Robinet *et al.* (2007) showed that the effect of variation in female longevity on mating success was small. The model was run for a single generation and mating success was measured in terms of the population growth rate, which was defined as the number of fertilized egg masses produced after 1 generation divided by the number of introduced egg masses.

To predict spatial variation in population growth resulting from differences in topography across our study region, we made three adjustments to the Robinet *et al.* (2008) model. We expanded the size of the model landscape to 1×1 km to match the spatial grain of gypsy moth pheromone-baited trap records (see *Growth Rates in Field Populations* below), we introduced egg masses at locations selected randomly from a uniform distribution rather than a fixed point to mimic human-mediated long-distance transport (Liebhold and Tobin 2006), and we prescribed gypsy moth phenology to vary as a function of elevation and latitude, rather than controlling these parameters directly.

Relationships between elevation and latitude and three aspects of gypsy moth phenology –the day of peak male maturation, the SD (temporal dispersion) of the male maturation period, and the degree of protandry–were determined based on predictions from the gypsy moth life stage model (GLS) (Gray 2004). GLS is a composite of phenology models for the egg (Gray et al. 2001), early larval (Logan et al. 1991), and late larval to adult stages (Sheehan 1992). GLS predicts developmental timing using stage-specific and, where applicable, sex-specific developmental responses to temperature. One key feature of GLS is that, rather than specifying

egg mass fertilization at an arbitrary date, it uses an optimization procedure to estimate fertilization dates that are realistic to that particular climate (Gray 2004).

For the day of peak male maturation and temporal dispersion of male maturation, predictions for 2001-2011 were generated by applying the GLS model to meteorological records interpolated over the network of 1×1 km lattice cells using BioSIM software (Regniere and Saint-Amant 2008). BioSIM interpolates meteorological records, adjusting for latitude, longitude, and elevation. As phenological predictions vary according to annual weather variations, we calculated the average day of peak maturation and average temporal dispersion over the 12-year period. These mean predictions were regressed against the mean elevation and northing (analogous to latitude) of the lattice cell. We considered linear, quadratic, and exponential relationships and the model having the lowest AIC value was selected. To quantify effects of elevation and latitude on protandry, we obtained GLS model predictions used by Robinet, Liebhold & Gray (2007) for 77 weather stations in our study area and estimated the mean amount of protandry (days from peak male to peak female abundance) for 1961-2000 at each weather station. We applied the same criterion as above to determine the equation that best described the effects of elevation and latitude on protandry. As in Robinet et al. (2008), we assumed the temporal dispersion in maturation follows a normal distribution, and the female distribution has the same SD as the males', but is shifted in time due to protandry.

To model variation in population growth rate, we divided the study region into 1×1 km lattice cells and represented the topography present in each cell using a 10 m-resolution digital elevation model (DEM) (United States Geologic Survey 2002). The phenologies of introduced egg masses were determined based on relationships with elevation and latitude determined above, with elevation taken from the 10m DEM at the location of the egg mass and using the

mean latitude of the lattice cell. Our model was run on a stratified random sample of 2,200 out of 106,928 lattice cells to improve computational tractability. We randomly selected 200 cells from each of 11 intervals of heterogeneity in elevation, which was computed as the SD of elevation (represented by the 10m DEM) within each lattice cell. The 11 intervals were: 0-10, 10-20, 20-30, 30-40, 40-50, 50-60, 60-70, 70-80, 80-90, 90-100 and >100 m. Standard deviation of elevation in selected lattice cells ranged from 0 to 158 m and mean elevation ranged from 129 to 1,508 m.

For each selected 1×1 km lattice cell, we estimated mating success in terms of the population growth rate over 1 generation. Following Robinet et al. (2008), we estimated the finite rate of population growth (λ) according to $\lambda = E_t / E_{t-1}$, where E_t is the number of fertilized egg masses after one generation (gypsy moth females oviposit 1 egg mass each) and E_{t-1} is the number of introduced egg masses. To assess dependence between initial egg mass density and the population growth rate, landscapes were initially seeded with 3, 5, 7, 9, 11, 13, 15, 20, 25, 30, 35, or 40 egg masses. Each egg mass was assumed to contain 300 eggs with a 1:1 sex ratio (Robinet *et al.* 2008). Model simulations and analysis were conducted in R version 3.0.1 (R Core Team 2014).

Growth Rates in Field Populations

We also examined the influences of elevation and local heterogeneity in elevation on growth rates in field-collected data across the network of 1×1 km lattice cells described above. Growth rates were estimated using spatially referenced trap data from the gypsy moth Slow-the-Spread programme. The pheromone-baited traps used in this programme are effective at collecting males at very low densities (Schwalbe 1981), providing a means to identify the earliest stages of an invading gypsy moth colony. We used trap catch data collected in Virginia and

West Virginia annually from 1988 to 2009 as a proxy for the true population density. The number of traps in the study area averaged 11,150 per year. Most traps were placed ≈2 km apart, although some are placed as much as 3-8 km apart or as little as 0.25 km apart (Tobin *et al.* 2007a). Because the exact location of traps changed from year-to-year, median indicator kriging (Isaaks and Srivastava 1989) was used to interpolate a continuous surface of gypsy moth abundance over the network of 1×1 km lattice cells using GSLIB software (Deutsch and Journel 1992). From the center of each lattice cell, we extracted the estimated number of male moths per trapping area for each year. Because some gypsy moth populations are treated under the Slow-the-Spread programme in an effort to eliminate newly formed colonies (Tobin et al. 2012), trap catch data within 1.5 km of a treated area were excluded. Generally, ≤ 2% of the area was treated each year.

We determined the population growth rate in each lattice cell by fitting the geometric population growth equation $N_t = \lambda_m N_{t-1}$ to a time series of trap catch densities using ordinary least squares regression. The population growth rate λ_m describes the proportional change in the number of gypsy moth males (N) captured between time $t-1$ and time t. We limited our analysis to estimated densities between 0 and 50 moths per trapping area to focus on growth of low-density populations. Fifty moths is below this region's mean carrying capacity of 673 moths per trap, yet above the region-wide Allee threshold of 21 moths per trap (Tobin *et al.* 2007b). We used values greater than the 21-moth-per-trap threshold to allow for the possibility that the Allee threshold might vary locally. Some lattice cells had very low estimated trap catch in one or more years before a gypsy moth was actually captured in the cell, which is an artifact of the interpolation method. Thus, N values < 0.1 were considered to be 0. We ignored data prior to the last year in which $N = 0$ because N commonly fluctuated between 0 and very low densities (< 2

moths) for ≈3-5 years prior to gypsy moths consistently being present in a lattice cell. In exploratory analyses, including data in which *N* fluctuated between 0 and non-zero values resulted in poor fits of the population growth equation. Furthermore, the geometric growth model precludes population growth following a generation with zero individuals. We further excluded grid cells meeting certain non-mutually-exclusive criteria, primarily removing cells in which gypsy moth was present at the beginning of our study period or cells with too little data (See Appendix B1 for details).

We used generalized additive models (GAMs) to assess the influence of elevation, elevational heterogeneity, and density of preferred host trees on population growth rates. GAMs combine properties of generalized linear models and additive models, allowing the replacement of linear regression coefficients with nonparametric smooth functions such as splines (Hastie and Tibshirani 1986). Using smoothed estimates for covariates is advantageous because it allows detection of nonlinear relationships, such as those between environmental covariates and aspects of gypsy moth population dynamics (Sharov et al. 1997, Haynes et al. 2012). In GAMs, smooth functions are penalized for increased nonlinearity to balance model fit and complexity. To further guard against overfitting we increased the penalty for increasing spline degrees of freedom to 1.4 (Kim and Gu 2004). We specified the gamma distribution for the dependent variable and the log link function to improve normality of the model residuals. We also examined measures of concurvity (i.e., a generalized case of colinearity allowing for curvilinear relationships) between predictor variables to ensure the analysis did not suffer from severe model identifiability issues. Concurvity statistics are bounded between 0 and 1, with 0 indicating no concurvity and 1 indicating complete lack of model identifiability.

Elevation and elevational heterogeneity (SD[elevation]) were calculated using the 10 m DEM as above. Because we found nonlinear effects of elevation on day of peak maturation and temporal dispersion (Figure 2a,b), we also tested whether the effects of elevational heterogeneity on population growth could become stronger at high elevations by including an interaction effect between elevational heterogeneity and elevation. The density of gypsy moth preferred host trees, which includes 79 tree species, was obtained from Morin *et al.* (2005) and is expressed as the basal area of preferred species (m^2 ha^{-1}) at 1 km resolution. A correlogram indicated population growth rates were positively autocorrelated over a distance of ≈58 km (Appendix B2). Spatial autocorrelation in population growth rate was accounted for in the GAM by including the distance-weighted mean of the growth rate as a term in the model. Here, points > 58 km from the focal point were assigned a weight of zero. Otherwise, the weight (w_{ij}) was calculated based on the fitted relationship between autocorrelation and distance:

$$w_{ij} = (0.8608 - 1.175e^{-5}(d_{ij}))^2, \quad (3)$$

where d_{ij} is the straight-line distance between the focal point *i* and point *j* (Anselin and Bera 1998). The distance-weighted mean growth rate, $\overline{\lambda_m}$, was then calculated as:

$$\overline{\lambda_m} = \frac{\sum_{j=1}^{n} w_{ij}\lambda_j}{\sum_{j=1}^{n} w_{ij}}. \quad (4)$$

Correlogram analyses were implemented using the "ncf" package in R version 3.0.1 (R Core Team 2014).

Following Wood & Augustin (2002), we used a backwards selection protocol to arrive at a parsimonious model. We began with the full model:

$$\lambda_m = s(elev) + s(SD(elev)) + s(hostba) + s(\overline{\lambda_m}) + te(elev, SD(elev)), \quad (5)$$

in which the growth rate was predicted by elevation, SD of elevation, density of preferred host trees, the distance-weighted mean growth rate, and an interaction between elevation and SD of

elevation. Here, *s* indicates smooth spline functions of the covariates and *te* indicates a tensor product smooth. Wood & Augustin (2002) suggested a variable should be dropped from the model if it meets all of the following criteria: 1) the estimated degrees of freedom for that term are close to 1, 2) the confidence region for the smooth function includes zero for all values of the independent variable, and 3) the generalized cross-validation (GCV) score for the full model decreases if the term is removed. Because of the subjectivity of the first criterion, we removed terms based only on the second and third criteria. In practice, this method is more conservative than the one suggested by Wood & Augustin (2002) because it less likely to retain variables. GAMs were implemented using the "mgcv" package (Wood 2006) in R version 3.0.1 (R Core Team 2014).

Results

Parameterizing the Population Growth Model

When analyzing phenological predictions to parameterize our simulation model, we selected the candidate model with the lowest AIC value (Appendix B4). The most parsimonious relationship between the day of peak male maturation and elevation was peak = 899.2 - 4.218e^{-4}(northing [m]) + 5.983e-11(northing[m])^2 + 1.766e^{-2}(elevation [m]) + 2.255e^{-5}(elevation [m])^2 (R^2 = 0.953) (Figure 2a). Here, elevation is the DEM value at the coordinates where an egg mass is introduced and northing was measured at the center of the 1×1 km landscape in a custom coordinate system (Appendix B3). The selected relationship (R^2 = 0.870) for the dispersion (SD) of the male maturation distribution was dispersion = 23.09 - 1.358e^{-5}(northing [m]) + 2.067e^{-12}(northing[m])^2 + 1.172(exp(elevation [km])) (Figure 2b). The amount of protandry, in days, was estimated as protandry = -3.639e^{-3} + 1.112e^{-3}(elevation[m]) + 8.401e-^{7}(northing[m]) (R^2 =

0.318) (Figure 2c). Tables ranking each of the candidate models by AIC value are located in Appendix B4. In the model, we allowed for variability from these relationships by adding to each estimate normally distributed random error, with SD determined from regression residuals. These values were 2.61, 0.224, and 0.406 days for the day of peak male maturation, the temporal dispersion of the maturation period, and protandry, respectively.

Population Growth Model Predictions

For all densities of introduced egg masses, the modeled mean population growth rate declined with increases in elevation (Figure 3a, Appendix B5). The population growth rate declined more modestly with increases in elevational heterogeneity (SD[elevation]), and the effect was nearly imperceptible when < 20 egg masses were introduced (Figure 3b, Appendix B5) but grew as the number of introduced egg masses increased. We also found a positive effect of the number of introduced egg masses on the population growth rate, indicating the presence of a demographic Allee effect. Increases in elevation and elevational heterogeneity increased the number of introduced egg masses at which population growth reach the replacement rate of $\lambda = 1$ (Figure 3). Additional plots showing trends and variability in the effects of elevation and elevational heterogeneity on population growth rates can be found in Appendix B5.

Growth Rates in Field Populations

Estimates of the growth rates of invading gypsy moth populations based on pheromone-baited trap catch data varied from $\lambda_m = 0.044$ to $\lambda_m = 23.0$, with a mean (± SD) of 1.16 ± 1.28. Distance-weighted mean growth rate, density of preferred host trees, elevation, and SD(elevation) met our model selection criteria and were retained in the GAM, but the interaction term between elevation and elevational heterogeneity was removed because the confidence

intervals overlapped zero for all values of the covariates. Estimates of concurvity between each term and the rest of the model were 0.278 for distance-weighted mean growth rate, 0.359 for density of preferred host trees, 0.546 for elevation, and 0.289 for SD(elevation). The adjusted R^2 for the full model was 0.314. Population growth rates generally decreased with increases in elevation (Figure 4a). The relationship between SD(elevation) and the growth rate was nonlinear, with the growth rate increasing with SD(elevation) in the flattest landscapes (0 < SD[elevation] < 10 m) and exhibiting little or no relationship across landscapes of intermediate hilliness (10 m < SD[elevation] < 100 m; Figure 4b). The most sustained trend was a negative relationship between the growth rate and SD(elevation) in the hilliest landscapes (SD[elevation] > 100 m). There was also a weak and generally negative relationship between the growth rate and basal area of preferred gypsy moth host trees (Figure 4c). Inclusion of the distance-weighted mean growth rate term strongly reduced spatial autocorrelation in the GAM residuals (Appendix B2).

Discussion

In this study, a model simulating the effects of thermal regime on reproductive asynchrony predicted that increasing elevation and local heterogeneity in elevation (hilliness) negatively affect the growth rates of low-density gypsy moth populations. As in Robinet *et al.* (2008), our simulations predicted the existence of a demographic Allee effect and also supported our novel hypotheses, with populations in landscapes at the highest elevations and with the hilliest topographies suffering the lowest growth rates (Figure 3). Consistent with these theoretical predictions, an analysis of field data collected near the invasion front showed that population growth rates declined with increasing elevation (Figure 4a). High local elevational heterogeneity also tended to reduce population growth rates, though this relationship was not

entirely consistent (Figure 4b). The general agreement between theory and field data support the hypothesis that topographic characteristics, acting through effects on reproductive asynchrony, influence the growth of gypsy moth populations along the margins of its range. Negative demographic consequences of reproductive asynchrony have been documented for a variety of insect species (Calabrese et al. 2008, Régnière et al. 2013), and in the gypsy moth there is a particularly clear link between reproductive asynchrony and the Allee effect (Robinet *et al.* 2007, 2008). Despite this, few studies have addressed specific causes of variability in Allee dynamics (but see Kramer *et al.* 2011), and we are not aware of any other studies addressing elevation or elevational heterogeneity as drivers of reproductive asynchrony and Allee effects.

The relatively strong decline in gypsy moth population growth rates with increasing elevation may be explained by increased protandry and temporal dispersion in maturation times (Figures 2b-c), likely due to increased variability in temperature at high elevations (Whiteman 2000). Previously, Robinet *et al.* (2007, 2008) showed that high levels of protandry and temporal dispersion of maturation times can reduce gypsy moth population growth rates by limiting mate finding. This study demonstrates how these phenological characteristics map onto real landscapes and shows clear implications for understanding the dynamics of gypsy moth spread.

We also hypothesized that elevational heterogeneity would negatively affect the population growth rate given that, in steeply undulating landscapes, potential mates are exposed to different thermal conditions at different elevations. The resulting phenological differences lower mating success by locally increasing temporal dispersion in maturation times; in other words, these phenological differences effectively reduce the number of males available to mate with each female, *ergo* reducing mating success and the population growth rate. However, this

effect was weak compared to the effect of elevation on population growth. Allowing different egg masses to develop under different thermal conditions effectively widens the population-level distribution of reproductive maturation, which others found to have less influence on mating success than protandry (Robinet *et al.* 2007, 2008). Here, phenological differences between egg masses caused by elevational heterogeneity were not large relative to the width of the maturation distribution of a single egg mass, weakening the resulting effect on population growth. We predict that elevational heterogeneity may more strongly influence population growth in species whose individual reproductive period is shorter relative to their ability to locate mates in space, whose phenology displays greater sensitivity to temperature, or who inhabit landscapes with very high elevational heterogeneity.

In simulated populations, the slope of the relationship indicated a stronger decline in population growth rates with increases in elevation and elevational heterogeneity when more egg masses were introduced (Figure 3, Appendix B5). For elevational heterogeneity, this is likely because the average distance between egg masses was so high that dispersal limitation largely prevented mating between individuals from different egg masses. In other words, isolation in time was less significant when there was already substantial isolation in space. This effect may influence observed relationships between elevation and population growth rate given that higher elevation sites tend also to have more elevational variability.

In field populations, the relationship between elevational heterogeneity and the population growth rate did not strictly conform to the predictions of the simulation model. The model predicted a linear decline in the population growth rate with increasing elevational variability, but in field populations there was a positive relationship across a narrow range of the flattest landscapes, no relationship in landscapes of intermediate hilliness, and a negative

relationship in the hilliest landscapes. Although the decline in population growth rate in very heterogeneous landscapes is significant (Figure 4b), it is based < 2% of the dataset (124 grid cells with SD[elevation] ≥ 100). One possible explanation for the positive relationship between population growth rate and hilliness in the flattest landscapes is that a slight amount of reproductive asynchrony may be beneficial if it allows some individuals to escape episodic disturbances such as severe weather events (Post *et al.* 2001). Because the mortality rate was constant in the simulation model, we were not able to address this potential benefit of a small amount of asynchrony.

The basal area of preferred host-tree species was expected to positively influence gypsy moth population growth rates because gypsy moths exhibit higher survivorship and fecundity when feeding on preferred hosts (Hamilton and Lechowicz 1991). Indeed, the development of gypsy moth outbreaks is strongly influenced by the density of preferred host tree species (Gottschalk 1993, Johnson et al. 2006a). However, the relationship between host tree density and the dynamics of low-density populations is unclear. One study from the lower peninsula of Michigan observed a positive relationship between the rate of gypsy moth spread and the density of preferred host trees (Sharov *et al.* 1999). However, another study across the entire invasion front, from Wisconsin to North Carolina, showed no relationship between the persistence of low density populations and host tree density (Whitmire and Tobin 2006). One possible explanation is that, although population growth to outbreak densities is dependent upon the density of preferred hosts (Gottschalk 1993), population growth in low-density gypsy moth populations is more strongly influenced by drivers of Allee effects such as mate-finding failure because low-density populations require a relatively low abundance of resources.

In interpreting empirical relationships between growth rate, elevation, elevational heterogeneity, and host tree basal area, potential relationships between these variables should be noted. In many landscapes, the greatest elevational variability may occur at the highest elevations, and due to patterns of human development these may also be the most heavily forested sites. In this case, GAMs fitted using the procedures implemented in the R package "mgcv" have been shown to be robust to concurvity (Wood 2008), and concurvity metrics did not suggest severe model identifiability issues in our data. However, given that gypsy moths require some amount of suitable host, an increase in host tree density with elevation and elevational heterogeneity should make it *more difficult* to detect negative effects of elevation and elevational heterogeneity on population growth rates.

Other factors influencing gypsy moth survivorship or mating success may also confound or counter the relationships found in this study. For example, small mammals, which are important predators of gypsy moth pupae (Hoffman Gray *et al.* 2008), may be less abundant at high elevations (Yahner and Smith 1991, Brooks et al. 1998). Similar to the effect of elevation on host tree basal area, this elevational gradient in predation pressure would make it more difficult to detect negative effects of elevation on population growth rates. In addition, topography may bias the movement of some insects (Pe'er *et al.* 2004), but whether this applies to the gypsy moth is unknown. Theory predicts that populations subject to strong Allee effects exhibit a critical occupied area, in addition to a critical density, for persistence (Lewis and Kareiva 1993). This prediction was empirically confirmed for the gypsy moth (Vercken *et al.* 2011). This finding could have implications for our results if factors such as topography or forest patchiness constrain the area of a population by limiting movement, or if the size of favorable habitat patches tends to vary along topographic gradients. The extent to which these

may occur is not known. The findings of Vercken et al. (2011) also underscore that the population dynamics of nearby grid cells may not be independent of each other, but our efforts to control for spatial autocorrelation minimized spatial non-independence.

One notable difference between the results of the simulation model and observed rates of population growth is that observed rates were generally above the replacement rate $\lambda = 1$, while growth rates in the model only exceeded $\lambda = 1$ at relatively high densities. This difference is due in part to data filtering in the empirical analysis removing unsuccessful colonization events; however, it may also result from the model considering isolated populations, whereas nascent populations near the gypsy moth invasion front receive immigrants from well-established populations behind the front (Tobin and Blackburn 2008). We also note that observations filtered for having too few years of usable data, or where trap catch was zero in 2009, were located ahead of the leading edge of the invasion, indicating that failure to establish was largely dependent on distance from the invasion front, not on local ecological factors.

Although we and others (Tobin *et al.* 2007b) have detected spatial variability in the strength of Allee effects in the gypsy moth, we interpret our results as indicating that gypsy moth reproductive biology could lead to an Allee threshold at a fixed "effective density" of reproductive adults considering both space and time. Reproductive asynchrony, then, relates total density over the entire reproductive period to effective density such that, holding the total density over the entire reproductive period constant, increasing reproductive asynchrony decreases the effective density. Other factors, such as wind effects on pheromones or male flight, would operate in a similar manner, introducing error into the relationship between total density and effective density. Supporting this interpretation, Tobin *et al*. (2007b) detected regional variability in the Allee threshold using season-long pheromone-baited trap catch

records, even though the relationship between daily male moth density and female mating success is broadly consistent across regions (Contarini *et al.* 2009). This apparent discrepancy may be explained by regional differences in weather that influence immigration rates (Tobin and Blackburn 2008, Frank et al. 2013), producing variations in the effective population density not reflected in density measures based on season-long trap catch records.

Understanding how and why spatiotemporally variable environmental characteristics influence the dynamics of populations subject to Allee effects may have broad implications for conserving threatened species and managing biological invasions (Courchamp et al. 2008, Tobin et al. 2011). Specifically, our findings suggest that future rates of gypsy moth spread could be partially predicted based on topography. Considering the link between Allee effects and invasion rate (Lewis and Kareiva 1993), our findings indicate that, all else being equal, the areas at highest risk of invasion by gypsy moths are at low elevations and have little elevational heterogeneity. Consistent with this prediction, unusually high invasion rates have been observed in Wisconsin (Tobin *et al.* 2007a), where elevation and elevational heterogeneity are low relative to the Central Appalachians, but other factors, particularly transport of gypsy moths, may differ between the two regions (Bigsby et al. 2011, Frank et al. 2013). Very low invasion rates have been observed in Ohio, Indiana, and Illinois (Tobin *et al.* 2007b) where elevation and elevational heterogeneity are also low relative to our study area, but this is likely explained by much lower density of host trees in heavily agricultural areas (Morin *et al.* 2005). Thus, there could be a crucially important interplay between topography and resource availability in the invasion dynamics of the gypsy moth, which has immediate implications to management efforts seeking to reduce gypsy moth spread. More generally, the evidence presented by this study underscores that reproductive asynchrony may affect the invasion dynamics of poikilotherms, particularly

other non-native insects that also can be subject to the challenges of mate-finding failure at low densities.

Figures

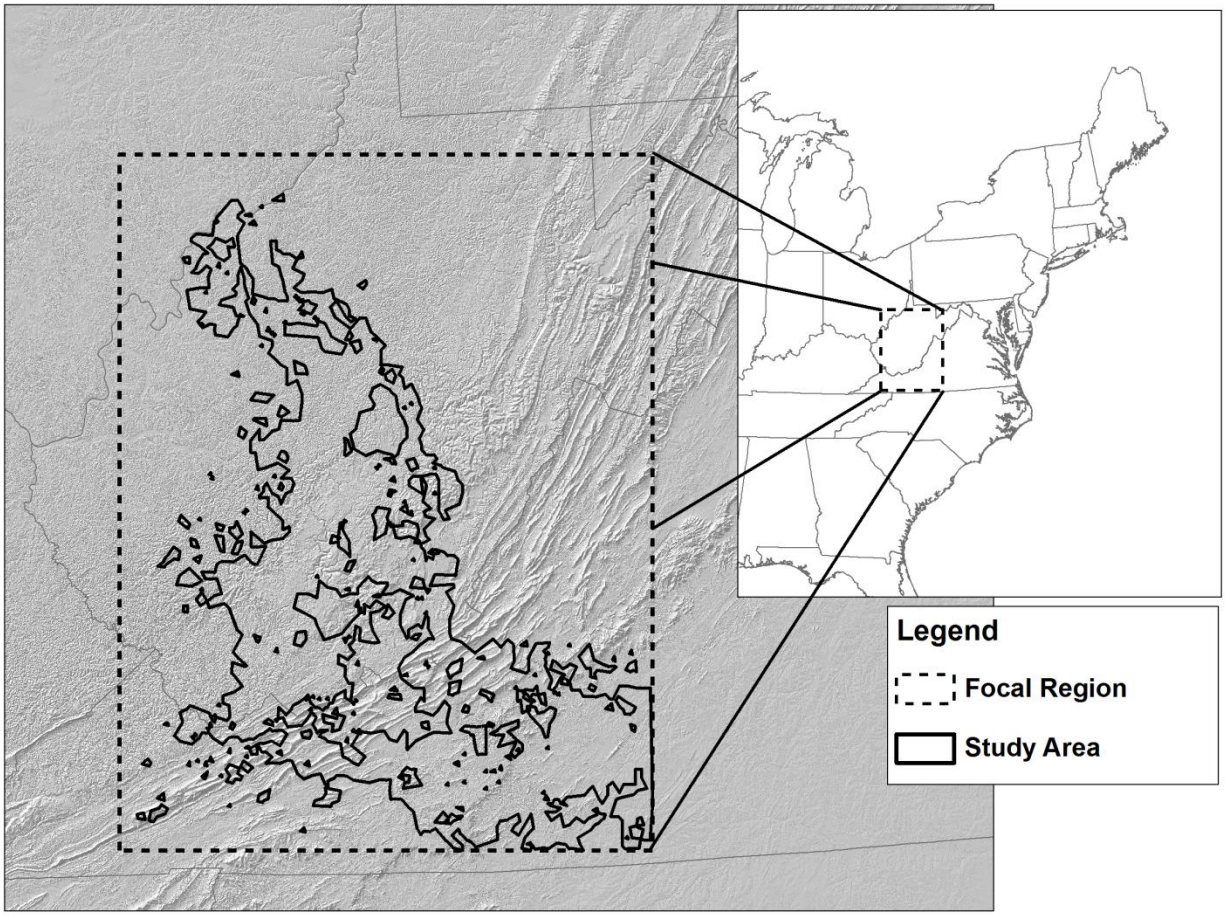

Figure 1: Study area map. A hillshade layer illustrates topography. The "Focal Region" defines the geographic area in which effects of topography on mating success were modeled. The "Study Area" outlines grid cells retained for the empirical analysis after filtering to remove cells where the gypsy moth was present prior to the beginning of monitoring and where there were too few data (see *Growth Rate in Field Populations* in Methods).

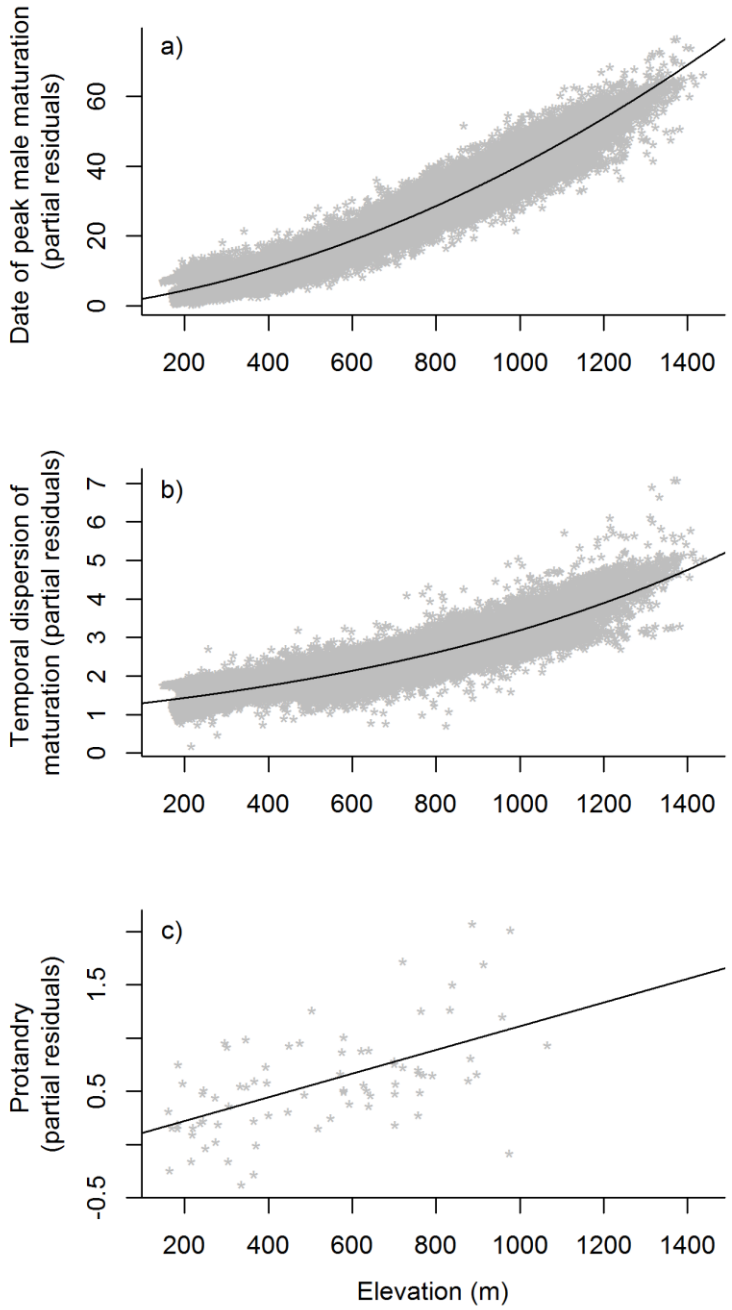

Figure 2: Relationships between elevation and a) day of peak male maturation, b) dispersion (SD) of the population-wide distribution of male maturation, and c) protandry.

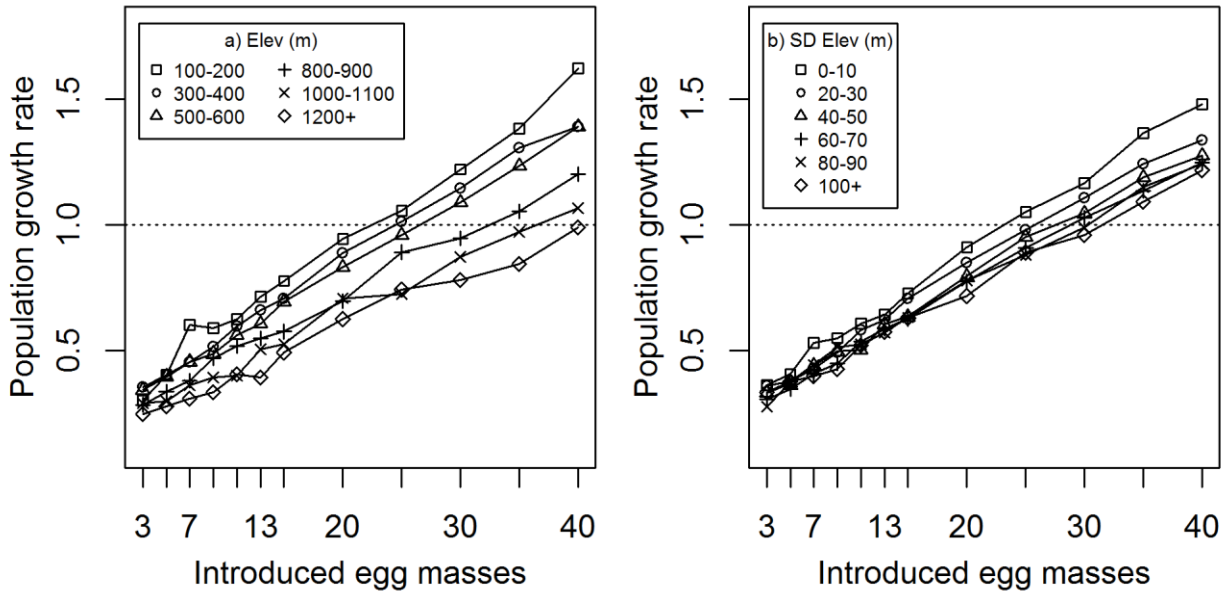

Figure 3: The mean population growth rate increased as the number of introduced egg masses increased from 3 to 40, with the population growth rate increasing more slowly with increases in a) elevation, and b) heterogeneity in elevation (SD of elevation). For visual clarity, a selection of ranges of elevation and elevational variability are shown, but the pattern remains consistent across all levels of elevation and elevational variability in the focal region.

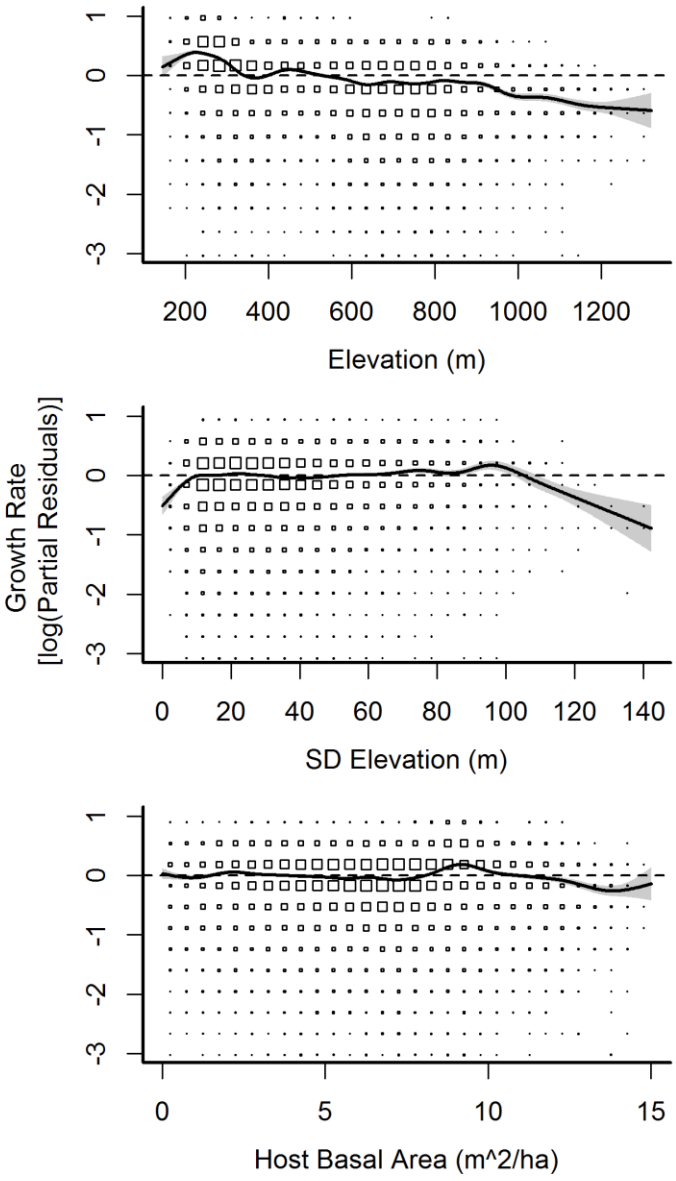

Figure. 4: Spline fit plots from GAM analysis describing relationships between growth rate and (top) elevation (spline with 18.8 df), (middle) SD of elevation (spline with 16.1 df) and (bottom) basal area of preferred host trees (spline with 15.8 df). Grey regions are confidence bounds (± 2 standard errors). X-axes are scaled in units of the linear predictor; Y-axes represent partial residuals on a logarithmic scale. Partial residuals were binned using equal-width intervals and are plotted using squares scaled according to the number of residuals in that bin.

4. Effects of landscape structure on the spread of the gypsy moth[3]

Abstract

Understanding how landscape heterogeneity affects patterns of range expansion is a critical challenge of modern ecology. Allee effects are thought to slow population spread, and recent findings indicate that environmental heterogeneity can drive variations in the severity of Allee effects but few studies have elucidated the mechanisms causing such variations or their impacts on spread in heterogeneous landscapes. This study combined field experiments, simulation modeling, and analysis of empirical spread patterns to investigate how landscape structure affects the spread of the gypsy moth in Virginia and West Virginia. In experiments designed to assess mate finding in complex landscapes, we found that adult gypsy moths resist leaving forest patches and that mate finding probabilities decayed more rapidly over distance in the non-forest matrix than in the forest. These findings informed the development individual-based simulations of gypsy moth spread in complex landscapes, which indicated that population persistence and spread increase as forested area and the aggregation of forest patches increased. These results reflect effects of landscape structure on gypsy moth mortality and mate finding, which collectively exacerbate a mating failure Allee effect. Our model predictions were evaluated against empirical patterns of gypsy moth spread, which showed relationships between spread rate and landscape structure consistent with our model predictions. These results highlight cross-scale interactions in which local processes (e.g. survivorship, mate finding) scale up to landscape-level patterns and elucidate potentially widespread mechanisms by which landscape structure may affect Allee effects and gypsy moth spread.

[3] This study was conducted in collaboration with Ariel Firebaugh, Patrick Tobin, and Kyle Haynes.

Introduction

Invasions by exotic species have severe ecological (Vitousek et al. 1996, Mooney and Hobbs 2000) and economic (Pimentel et al. 2005) consequences. As a result, understanding the ecological processes governing their establishment and spread is critical. Theoretical and empirical evidence indicates that the establishment and spread of introduced species can be influenced by demographic Allee effects (Wang and Kot 2001, Wang et al. 2002, Leung et al. 2004, Taylor et al. 2004, Tobin et al. 2007b), defined as a positive relationship between population size or density and the per-capita population growth rate when population sizes are low (Stephens et al. 1999, Courchamp et al. 1999). Mechanisms of Allee effects include mating failure, the breakdown of cooperative feeding or defense behaviors, inbreeding depression, and failure to satiate predators (Kramer et al. 2009). In some populations in which Allee effects occur, the population is unlikely to replace itself when below some minimum population density termed the Allee threshold; this is called a strong Allee effect (Wang and Kot 2001). As low-density populations are common at a species' initial introduction and at the edges of its range, Allee effects are thought to provide a barrier to newly introduced species becoming established, as well as slowing the spread of established invasions (Keitt et al. 2001, Courchamp et al. 2008, Tobin et al. 2011).

Ecologists have typically considered the Allee effect to be a fixed quantity, but a small number of recent studies have highlighted how variability in environmental conditions can alter the Allee threshold density and/or the rate at which increases in the population density result in increases in the population growth rate (Tobin et al. 2007b, Kramer and Drake 2010, Kramer et al. 2011, Walter et al. 2014). To differentiate from the "strength" of Allee effects, which by convention denotes whether or not there is an Allee threshold, we term this combination the

"severity" of the Allee effect. Two such studies have focused on how environmental variability impacts rates of mate-finding failure, a common cause of Allee effects. Kramer et al. (2011) showed that temperature influenced the Allee threshold in populations of a freshwater copepod due to the tendency of increasing temperature to increase rates of mate encounter by enhancing swimming speed and the ability to follow pheromone trails. Walter et al. (2014) showed that topography, by influencing variability in developmental timing, impacts rates of mating failure and the severity of Allee effects at the leading edge of the gypsy moth's invasion of North America. Similar to the way Allee effect severity has typically been considered a fixed value, most theoretical predictions regarding the spread of invasions are made in hypothetical homogeneous landscapes, disregarding the heterogeneity present in the real world (With 2002).

Given that successful mating necessitates that potential mates be both reproductively active at the same time and able to locate each other in space, the severity of mating failure Allee effects could also be influenced by effects of landscape structure on movement behaviors. Individuals may move relatively freely within continuous patches of suitable habitat, but their movements may be restricted if they resist crossing edges into unsuitable habitat (i.e., the matrix) (Stamps et al. 1987, Haynes and Cronin 2006), or if distances between patches of suitable habitat are large relative to the organism's dispersal capabilities (Collingham and Huntley 2000, Cronin 2003, Matter et al. 2005). Hence, mating success may be particularly limited when individuals are distributed among different patches with edges and the matrix acting as barriers separating potential mates.

The abundance and spatial configuration of suitable habitat could also influence mating success and spread if it affects mortality rates of dispersers attempting to locate mates. For individuals seeking mates, increasing isolation of patches of suitable habitat could increase

metabolic costs and mortality risk (Bonte et al. 2012). For example, predation rates may differ between suitable and matrix habitat types (Kauffman et al. 2007, Cronin and Reeve 2014), resulting in altered mortality rates among individuals crossing through the matrix in search of mates. The presence of matrix habitat types may affect mortality rates for other reasons, such as differences in resource availability or intolerable abiotic conditions (Bonte et al. 2012). We reason that mating failure and dispersal mortality may also interact by reducing the proportion of a population surviving to reproductive age. When rates of mortality are affected by landscape structure, increasing mortality rates of pre-reproductive life stages (relative to a homogeneously suitable landscape) reduces the available pool of potential mates, likely leading to lower mating success.

As a result of impacts on movement behavior and mortality, landscape structure may influence the severity of mating failure Allee effects and contribute to geographic patterns of invasive spread; however, connections between landscape structure, Allee effects, and spread have not been explored. The gypsy moth's invasion of North America is an ideal system in which to investigate these connections because prior research provides strong evidence for a mate-finding Allee effect (Robinet et al. 2007, 2008, Contarini et al. 2009, Walter et al. 2014), and for a critical population area below which gypsy moth populations are unlikely to persist (Vercken et al. 2011). In addition, long-term spatially explicit data on population abundance over large areas permit uniquely detailed analysis of spread in real landscapes. Despite this, prior research concerning the effect of landscape structure on gypsy moth population dynamics is quite limited (Vandermeer et al. 2001, Hoffman Gray et al. 2008), and we are not aware of any studies directly assessing the effects of landscape structure on gypsy moth spread.

In this paper, we used a three-pronged approach to evaluate how landscape structure affects the spread of the gypsy moth invasion. We first used a field survey and field-based behavioral and mass-release-recapture experiments to assess how landscape structure affects gypsy moth movement and mate finding. Data from the field experiments was then used to build a spatially explicit individual-based model of gypsy moth spread in spatially heterogeneous environments. Finally, predictions from the simulation model were tested against empirical data on gypsy moth spread. We hypothesized that gypsy moths would resist leaving forest patches and locate mates over shorter distances in non-forest versus forest habitats. We further predicted that these effects would scale up to affect population dynamics and spread, resulting in increased Allee effect severity and slowed spread in increasingly patchy landscapes.

Methods

Study System

The gypsy moth is a highly polyphagous forest-defoliating pest that has been invading North America since its introduction near Boston, Massachusetts in 1869 (Tobin et al. 2009b). Gypsy moths feed on over 300 species of trees and shrubs in North America, but performance of gypsy moths feeding on these species varies (Liebhold et al. 1995). Species most preferred by the gypsy moth are predominantly in the genera *Quercus*, *Populus*, and *Larix*. In North America, gypsy moth females are flightless, and successful mating depends on a free-flying male locating a mature female via a combination of a mating pheromone and visual cues (Doane 1976). Because females are not capable of flight, two main modes of range expansion are passive wind-borne dispersal of early-instar larvae, termed "ballooning," and accidental long-distance transport of egg masses by humans (Mason and McManus 1981, Liebhold et al. 1992).

Long-distance transport of other life stages can also occur during storms, but this is thought to occur widely only in Michigan and Wisconsin (Tobin and Blackburn 2008, Frank et al. 2013).

Study Area

We focused our study on an area of West Virginia and Virginia spanning the Western Allegheny Plateau, Central Appalachian, Northern Ridge and Valley, Blue Ridge, and Piedmont ecoregions. Continuous trapping records from the deployment of pheromone-baited traps, which facilitate estimation of gypsy moth range boundaries (see *Empirical Spread Rates* below) are most complete in this region. Although records in this region date to 1989, spatial coverage of the trapping program became more widespread in 1997, so we focused our analysis on the time period 1997-2012. Major forest type groups include oak-hickory, maple-beech-birch, spruce-fir, and oak-pine, with the oak-hickory group comprising the majority of the study area. Due to the gypsy moth's high degree of polyphagy and the near-ubiquity of suitable host tree species in our study area we assumed all forest was suitable habitat. All other land cover types were assumed to comprise the non-forest matrix.

Field Experiments and Sampling

Two experiments and a field survey were used to assess the responses of adult male gypsy moths to landscape structure and to predict their ability to locate mates in landscapes consisting of patches of suitable habitat embedded in a matrix of unsuitable habitat. We assumed that rates of mate finding were a function of two components: distances traveled to locate mates through forest vs. non-forest matrix, and the rate at which adult males emigrate from forest patches by crossing the forest-matrix edge. We used mass-release-recapture methods to compare dispersal kernels of male mate-searching flight in forest and the non-forest matrix. For each trial

of the mass-release-recapture experiment, between 240 and 280 virgin, lab-reared, newly emerged (<24 hours) adult male gypsy moths were released at the center of a rectangular grid of traps baited with female mating pheromone, and recapture rates from the traps were used to estimate the distance-decay of mate finding probabilities. Releases began in late morning and trap catches were recorded 1, 2, and 3 days following the release to also account for how mate finding probabilities decay over time. Three replicate releases were conducted at each of three sites of two habitat types, for a total of 36 trials. Agricultural fields and an old field represented the non-forest matrix, and forest sites had a mature canopy with few large gaps. For each trapping grid, traps were separated by 70 m along grid axes, with no trap at the release point, and grid sizes ranged from 3x7 traps to 9x7 traps because of variability in the size of fields and woodlots used for these experiments. The distance of the furthest trap from the release point ranged from 198 m to 350 m. The seventy-meter inter-trap distance was chosen to minimize interference between adjacent pheromone baited traps (Elkinton and Cardé 1983, 1988). Traps were hung ≈ 1.5 m off the ground on garden stakes; prior research shows that gypsy moth recapture may be maximized in traps 1 to 2 m from the ground (Mastro 1981). Each trap contained a pheromone lure and an insecticide strip to kill moths that entered.

Moths used in the mass-release-recapture experiment were reared to adulthood from pupae obtained from the USDA APHIS Otis laboratory. Pupae were placed in quart-size cardboard cups and stored in a climate-controlled room at ≈24 °C until they were needed for experiments. Transport and experimentation with invasive gypsy moths was permitted by the USDA under permit # P526P-11-01295 to Dr. Kyle Haynes. One condition of the permit was that release of our experimental lab-reared adult male gypsy moths could not occur while wild gypsy moth populations were reproductively active to prevent experimental males from

supplementing the wild population by mating with wild females. As such, trials were conducted during two periods: late May to early June, and late July through August. Experiments took place in 2011 to 2013 and all trials began on sunny days with forecast daily highs above 23°C and no heavy rain forecast for the duration of the trail. Our three forested sites were located at Blandy Experimental Farm (Boyce, VA), the Smithsonian Conservation Biology Institute (Front Royal, VA), and a privately owned forest in Albemarle County, VA. We located two non-forested matrix sites on different parts of Blandy Experimental Farm, and one on privately owned farm land in Onondaga County, NY.

We fit a variety of equations representing Gaussian, leptokurtic, and fat-tailed distributions to the trap catch data to quantitatively describe the dispersal kernel representing distance-decay of mate finding probabilities (Table 1) (Kot et al. 1996). We fit each kernel equation to the day 1 recapture data for each replicate release, and selected the equation that best described the data from each release by ranking the equation fits according to their AIC values. Prior to kernel fitting, trap recapture was converted to proportions of the total number of released moths, and distances from the release point were corrected for drift. The *x* component of drift was calculated as:

$$\hat{\beta}_x = [(\sum x_i)/n]/t, \quad (1)$$

i.e., the average *x*-coordinates (x_i) of *n* recaptured moths, divided by the time (*t*) between release and recapture (Turchin 1998). The *y* component of drift was calculated in the same manner. The overall best kernel equation was determined by averaging the AIC ranks across all replicates. We also considered whether the best equation differed between forest and non-forest releases, potentially indicating a different characteristic shape of the dispersal kernel between the habitat types, but we were unable to establish that the dispersal kernel differed between habitat types

because the differences we observed appeared to be related to differences in the grid size (detail regarding the effect of grid size on kernel fits can be found in Appendix C1). After selecting the best kernel equation, we determined its fitted parameter values for each replicate release and then averaged the parameter values first within site and then within habitat type to arrive at an average kernel describing the distance-decay of mating probabilities in forest and non-forest habitats. Too few recaptures occurred on days 2 and 3 for a robust comparison of kernel equation fits or of habitat differences in dispersal kernels, so we assumed that the best kernel equation for the day 1 data applied to days 2 and 3 as well, and averaged the fitted parameter values first within site and then across all sites regardless of habitat type. Dispersal kernel analyses were conducted using R version 3.0.1 (R Core Team 2014).

In our second field experiment, we investigated how frequently male gypsy moths cross forest edges into the non-forest matrix. Here, newly emerged virgin male gypsy moths were released at a well-defined forest edge and their habitat choice was assessed based on where they first alighted after a period of short (>5 seconds) but sustained flight. Moths that did not fly after a period of 10 minutes or that were lost from view were coded as "no choice." Moths were released one at a time from a 0.76 m high platform using a pulley apparatus that allowed the experimenter to observe each trial from a distance of ≈5 meters to minimize the effect of the experimenter's presence on moth behavior (see Appendix C2 for an image of the release apparatus). Replicate releases were performed at 4 forest edges at Blandy Experimental Farm (Boyce, VA, USA), with each forest edge approximately facing a different cardinal direction to account for the effects of solar illumination; all trials were conducted between 11:00 AM and 2:00 PM. Moths used in this experiment were selected from the same group of lab-reared moths

as was used in the dispersal kernel experiment above. Prior to release, moths selected for the edge choice experiment were stored in a dark cooler to keep them calm.

To confirm that our experimental results were predictive of male mate finding patterns in wild populations, we used pheromone-baited traps to sample wild gypsy moth abundances at 14 locations at Blandy Experimental Farm during the summer of 2011. These sites represented open fields dominated by grasses and forbs (6 sites), mid-succession areas dominated by shrubs and trees < 5 m (3 sites), and patches of mature forest (5 sites) with varying size and species composition. Open field and mid-succession sites varied in their distance from a forest patch. Traps were deployed from early June to late July, spanning the adult reproductive period of wild gypsy moths. We deployed one pheromone-baited trap to each location and recorded the total number of gypsy moths captured per trap, identified dominant vegetation, and measured the size of forest patches and distance of non-forest sites from the nearest forest patch using ArcGIS version 10.1 (Environmental Systems Research Institute, Redlands, CA).

Spread Model

We simulated gypsy moth spread in heterogeneous landscapes by modifying a mate-finding model originally developed by Robinet et al. (2008). In its original form, the model was used to assess how mate finding and Allee effects were affected by reproductive asynchrony. To investigate how the amount and distribution of forest habitat in affects gypsy moth spread, we made three main modifications to the model of Robinet et al. (2008): we extended the model to run for multiple generations, with females mated in generation t providing egg masses to generation t+1, we introduced egg masses to the model in a manner that simulated a spreading range boundary, and we used our field experiments to inform the estimation of mate-finding probabilities in heterogeneous landscapes.

Landscapes used in the model simulations were generated using a modification of the midpoint displacement algorithm (Saupe 1988) that produced rectangular landscapes. This allowed us to randomly generate landscapes while controlling the proportion of the landscape comprised of suitable habitat, as well as *H*, the degree of aggregation of habitat grid cells on the landscape. Landscapes consisted of a 33×165 grid, with each grid cell representing a 30×30 m area to match the spatial grain of data from the National Land Cover Database (Fry et al. 2011), which was used to measure habitat fragmentation of real landscapes (see *Empirical Spread Rates* below). After generating the landscape, the first three columns (x = 1:3) were uniformly assigned to be suitable habitat and were seeded with egg masses to simulate spread out of a continuous forested area.

We began by simulating the introduction of 33 egg masses containing 300 individuals each at a 1:1 sex ratio. Thirty-two were assigned to random locations within the forest boundary on the left edge of the landscape and one egg mass was assigned to a random location anywhere in the landscape to simulate the effects of long-distance dispersal, which in this system is a result of unintended anthropogenic dispersal of egg masses lain on vehicles or human goods. Then, larvae of both sexes dispersed in two spatial dimensions (x and y) at time t based on the simple diffusion equation:

$$\frac{\partial U}{\partial t}(x, y, t) = D\left(\frac{\partial^2 U}{\partial x^2}(x, y, t) + \frac{\partial^2 U}{\partial y^2}(x, y, t)\right), \quad \text{(eqn.1)}$$

where the diffusion coefficient D = 0.003 km^2 generation^{-1} (Liebhold and Tobin 2006) and U is the standardized population density. Individuals were assigned to locations based on probabilities generated by the diffusion equation. Larvae dispersing into non-forest grid cells were killed based on the assumption that those landing outside forests would not be able to complete their life cycle and emerge as adults. Egg-to-adult mortality of remaining individuals

was implemented by randomly choosing surviving individuals at a realistic survivorship rate of 0.05 (Elkinton and Liebhold 1990). The timing of reproductive maturation was simulated using Gaussian functions with peak male maturation fixed at an arbitrary day. The temporal dispersion of maturation was fixed at 3.5 days and the amount of protandry (i.e., the degree to which males tend to mature earlier than females) was fixed at 3 days, which are realistic values for our study area (Robinet et al. 2007, Walter et al. 2014). Mating success depended on spatial and temporal overlap of potential mates. If potential mates were located in the same forest patch, the probability of a female attracting a given male (p_i) at a given distance (x) and time lag between male and female maturation (t = 0, 1, or 2 days) was estimated using the equation:

$$p_i(x) = a_{ft} \exp\left(-b_{ft}\sqrt{x}\right), \quad \text{(eqn. 2)}$$

where a_{ft} and b_{ft} are parameters fitted based on release-recapture experiments simulating mate finding, with *f* denoting the use of values of *a* and *b* for mate finding in the forest, as determined from our field experiments. If potential mates were located in different forest patches, the probability of mate attraction became:

$$p_i(x) = ca_{mt} \exp\left(-b_{mt}\sqrt{x}\right), \quad \text{(eqn. 3)}$$

where *c* is the likelihood that adult males cross a forest edge (moving from forest to non-forest) and *m* denotes the use of values of *a* and *b* for the non-forest matrix. Here, we assume that the edge is completely permeable when crossing from the matrix to the forest. Distinct forest patches were identified using a single-pass implementation of connected components labeling (Chang et al. 2004). Mortality of adult males was implicitly accounted for in the mate attraction function. Mate finding at lags ≥ 3 days was ignored given the short life spans of adult males. Females were assumed to be reproductively active only on the day of their emergence due to high rates of mortality (Sharov et al. 1995a). Robinet *et al.* (2007) showed that the effect of

variation in female longevity on mating success was small. Each generation began with egg masses introduced as in the first generation, plus any egg masses contributed by successfully mated females in the previous generation. The model was run for up to 20 generations, but was stopped following a generation in which no females mated successfully (i.e., the population went extinct).

Although in our field experiment gypsy moth males never chose to fly to the field when released at a forest edge (see below), the probability of crossing forest edges, *c* was set conservatively at 0.25 based on field experiments in which pheromones traps were placed on both sides of a forest edge, males were released at the forest edge, and recaptures of males in the matrix was used to estimate rates of edge crossing (Thompson 2014). In Thompson (2014), mate attraction occurred over 25 m, a shorter distance than could occur between forest patches in our model. Given this, and the fact that connected components labeling allows for convoluted patch shapes, meaning that the shortest path between two mates in the same patch may cross forest boundaries, our model is likely to underestimate the effects of landscape structure on mate finding. More complex models of movement, however, come with computational costs that would have made our simulations intractable.

We conducted several experiments with the model. In the first, we employed a factorial design in which we directly controlled the proportion of suitable habitat and degree of aggregation of suitable habitat (*H*). The proportion of suitable habitat was varied among 0.1, 0.25, 0.5, and 0.75 and *H* was varied among 0.25, 0.5, and 0.75. For each of the 12 combinations, we conducted 50 replicate simulations and recorded the number of simulations in which the population went extinct before 20 generations had passed and, for the simulations lasting 20 generations, measured how far the invasion had spread accross the landscape. Spread

was measured by fitting a smoothing spline to the mean number of egg masses per grid cell in each column *y* and determining the largest value of *y* where the egg mass density was greater than or equal to one egg mass per square kilometer.

We also manipulated the effects of landscape structure on larval mortality and mate finding to evaluate how each of these processes contributes to predicted patterns of gypsy moth spread. In one alternate model, we examined what would happen if dispersal were not affected by landscape structure by setting the edge-crossing probability to 1 and using the forest kernel regardless of whether mates were in the same patch. In a second alternate model, we examined what would happen if mortality were not affected by landscape structure by allowing gypsy moths to survive to adulthood regardless of whether they landed in a forest or a non-forest grid cell as larvae. Mating probabilities of males maturing in a non-forest grid cell were based on the open field kernel, with complete permeability of edges when crossed from matrix to forest. Because the model that did not impose mortality on individuals landing in the matrix had much greater computational costs, it was run for 20 replicates rather than 50.

In another simulation experiment, we asked which landscape metric(s) best predict simulated gypsy moth spread rates. Landscape metrics quantify aspects of landscape structure, and while many are based on similar values (e.g. the area and perimeter of patches of a particular habitat type) and are often correlated with each other, they have different strengths, weaknesses, and interpretations (Hargis et al. 1998). Here, we used 200 replicate simulations in which we specified the proportion of suitable habitat and *H* to vary independently and randomly between 0 and 1, and computed the following metrics for each of the generated landscapes: proportion habitat, proportion like adjacencies, proportion core habitat, effective mesh size, largest patch index, aggregation index, landscape shape index, patch cohesion index, patch density, edge

density, and the splitting index (McGarigal et al. 2002) (Table 2). Given possible nonlinearities in the effects of landscape structure on invasive spread (With and Crist 1995, With 2002, Skelsey et al. 2012), we used generalized additive models (GAMs) (Wood 2006) to determine relationships between landscape metrics and spread. GAMs combine properties of generalized linear models and additive models to replace regression coefficients with nonparametric smooth functions (Hastie and Tibshirani 1986). Using smoothed estimates for covariates facilitates detection of non-linear relationships, but smooth functions are penalized for increased nonlinearity to balance model fit and complexity. To further prevent overfitting, we increased the penalty on spline degrees of freedom to 1.4 (Kim and Gu 2004). We specified the gamma distribution for the dependent variable and log link function to improve normality of model residuals. We ranked models containing each landscape metric by AIC value and considered those with AIC differences <10 to have support (Burnham and Anderson 2002). GAMs were implemented using the package "mgcv" and landscape metrics were calculated using the "SDMTools" package in R (R Core Team 2014).

Empirical Spread Rates

Empirical rates of gypsy moth spread were measured based on data from the deployment of pheromone-baited traps from the gypsy moth Slow the Spread program (STS) (Tobin et al. 2012). Under the program, ≈15,000 pheromone traps are deployed annually along the leading edge of the invasion front in our study area. Traps are generally placed ≈2 km apart, but in some areas are as little as 0.25 km or as much as 3-8 km apart (Tobin et al. 2004). Despite capturing only males, pheromone-baited traps are highly effective at sampling very low to medium densities (Schwalbe 1981, Elkinton and Cardé 1983), providing an effective means of delineating spreading populations.

The "boundary displacement" method (Sharov et al. 1995b, Tobin et al. 2007a) was used to estimate invasion rates. To estimate population boundaries, we first interpolated, from trap catch data for each year from 1997 to 2012, a continuous surface of gypsy moth abundance over a network of 1×1 km lattice cells using median indicator kriging (Isaaks and Srivastava 1989) in GSLIB (Deutsch and Journel 1992). This approach accommodated for the exact locations of traps changing from year to year. Because some gypsy moth populations are treated under the STS program in an effort to eliminate newly formed colonies ahead of the invasion front (Tobin et al. 2004), trap catch data within 1.5 km of a treated area were excluded prior to kriging; generally, ≤2% of the area was treated each year. We then estimated the 10-moth population boundary from the interpolated surface for each year using an optimization algorithm that spatially delineated areas at which the expected catch per pheromone-baited trap was 10 moths (Sharov et al. 1995b). The 10-moth population boundary was chosen to estimate the range boundary because it has been shown to be relatively more stable than other population boundaries (Sharov et al. 1995b). We measured the distance from a point fixed in space (39.39 °N, 77.16 °W) to the boundary along transects radiating from the fixed point at 0.25° intervals (Tobin et al. 2007b). The mean spread rate along each transect was quantified by measuring the year-to-year displacement along the transect and averaging the annual displacements over the study period.

We then analyzed how landscape structure affected gypsy moth spread rates along these transects using landscape metrics identified to be important in the simulations, while controlling for the effects of elevation, elevational heterogeneity, May maximum temperature, and the abundance of preferred host trees. Elevation and elevational heterogeneity are thought to impact rates of mate finding by inducing reproductive asynchrony (Walter et al. 2014), while

supraoptimal temperatures during the larval stage may restrict spread (Tobin et al. 2014). We assessed the effects of these variables on spread using generalized additive models (GAMs). As before, we increased the penalty on spline degrees of freedom to 1.4 to prevent overfitting (Kim and Gu 2004).

To determine values for each predictor of gypsy moth invasion rates, we considered a 1 km-wide area centered on each transect with length determined by the minimum and maximum position of the invasion front along that transect during 1997-2012. The 1km width minimizes overlap between adjacent transect areas and also approximates the width of the landscapes used in simulations. Elevation and elevational heterogeneity were calculated by finding the mean and standard deviation of a 30 m resolution digital elevation model (United States Geologic Survey 2002) within each transect area. The mean density of preferred host trees along each transect was determined using data from Morin et al. (2005) and is expressed as the basal area of preferred species (m^2 ha^{-1}) at 1 km resolution. The mean May maximum temperature was determined using 800m resolution downscaled 1981-2010 climate normals from the PRISM Climate Group (Prism Climate Group 2012). A selection of landscape metrics that were good predictors of spread rates in the above simulations was calculated based on NLCD land cover data (Fry et al. 2011). Here we considered binary landscapes where all forest was considered suitable habitat and all non-forested land cover types were considered unsuitable. Landscape metrics were computed using FRAGSTATS (McGarigal et al. 2002), while other computations involving spatial data were made in ArcGIS version 10.1 (Environmental Systems Research Institute, Redlands, CA).

We also controlled for spatial autocorrelation in invasion rates by including a distance-weighted mean invasion rate as a covariate in the GAM. From calculating the spatial

autocorrelation in invasion rates among transects, we determined that autocorrelation among transects declined to zero approximately linearly over 66 transects; hence, transects more than 66 positions from the focal transect *i* were assigned a weight of zero, and transects less than or equal to 66 positions from transect *i* were assigned weight according to an equation parameterized to mimic the observed autocorrelation function: $w_{ij} = 0.706 - 0.0128d_{ij}$. Here, w_{ij} is the weight of transect *j* relative to focal transect *i*, and d_{ij} is the distance between them in number of transects (Anselin and Bera 1998). The weighted mean invasion rate was then:

$$\overline{IR}_w = \frac{\sum_{j=1}^{n} w_{ij} IR_j}{\sum_{j=1}^{n} w_{ij}}. \qquad \text{(eqn. 4)}$$

We used a combination of AIC values and a backwards selection protocol to arrive at a parsimonious model (Wood & Augustin 2002). First, because in our simulations we found support for multiple landscape metrics as good predictors of gypsy moth spread (see below), and because these metrics tend to be highly correlated with one another, we first compared the AIC values of full models containing one landscape metric and all other covariates:

$$IR = s(\text{elev}) + s(\text{sd[elev]}) + s(\text{hostba}) + s(\text{may tmax}) + s(\text{lscp}) + s(\overline{IR}_w), \qquad \text{(eqn. 5)}$$

where *s* represents a penalized regression spline. We selected the full model (containing one landscape metric) based on AIC values and then tested the full model for concurvity, a generalization of colinearity that allows for non-linear relationships, among the set of predictor variables. When high levels of concurvity were detected, we removed from the model one of the correlated variables at a time, continuing with the reduced model having the lowest AIC value, until pairwise concurvity metrics among remaining predictor variables were reduced below 0.6. Because GAMs fitted using the methods in R package "mgcv" have been shown extremely robust to concurvity (Wood 2008), <0.6 was deemed acceptable. We then applied a backward selection criterion to arrive at a parsimonious model. Wood & Augustin (2002) suggested that a

variable should be dropped from a GAM if it meets three criteria: 1) the estimated degrees of freedom for that term are close to 1, 2) the confidence region for the smooth function overlaps zero for all values of the predictor variable, and 3) the generalized cross-validation score for the full model decreases when the term is removed. Because the first criterion is subjective we removed terms based only on the second and third criteria. This modification is less likely to retain variables, making it more conservative than the method of Wood & Augustin (2002). GAMs were implemented using the "mgcv" package (Wood 2006) in R version 3.0.1 (R Core Team 2014).

Results

Field Experiments and Sampling

In the mass-release-recapture experiments, we recaptured an average of 25.4% moths per release. We found the dispersal kernel that best described the distance-decay of mate-finding probabilities was fat-tailed (i.e., decaying to zero more slowly than a negative exponential function), and described by the equation $p = a \exp(-b\sqrt{x})$, where a and b are fitted parameters and x is the displacement distance (Table 1). Mate finding probabilities decayed more quickly with increasing distance in the non-forest matrix than in the forest (Figure 1). Although the 95% confidence intervals of mean dispersal kernels for forest and field habitats overlap over distances up to ≈50 m, they diverge over longer distances, and the longest distance we observed between the release point and a recaptured male was 297 m (before correcting for drift).

In the edge behavior experiment, in 65 trials divided between 4 different forest edges, 42 male gypsy moths chose the forest and 23 did not display a choice. A male gypsy moth was

never observed to choose the field over the forest. Of the 23 for which no choice was recorded, 3 were lost from view as they flew along the forest edge.

Our survey of wild gypsy moths captured a total of 331 male gypsy moths. Mean catch in non-forest traps was 1.9 moths per trap, with nearly half of total recapture outside of forest patches coming from the non-forest trap that was closest to a forest patch (Table 3). Mean catch in forest traps was 62.8 moths per trap, and trap catch tended to increase with the area of the forest patch (Table 3).

Simulation Model

In the first simulation experiment where we varied the amount and aggregation of suitable habitat (*H*), increasing the proportion of suitable habitat on the landscape increased rates of population persistence and spread (Table 1). Increasing the degree to which habitat patches were aggregated also facilitated gypsy moth spread (Table 1). When suitable habitat comprised 50% or more of the landscape, nearly all simulations persisted for 20 generations, but only when suitable habitat comprised 75% of the landscape and patches of suitable habitat were aggregated (H = 0.5, 0.75) did the simulated gypsy moth populations tend to spread more than a few grid cells into the landscape. In both of our alternate models, in which either mate finding or mortality was unaffected by landscape structure, extinction rates were reduced and the population tended to spread further into the landscape (Table 4). In simulations where larvae landing outside the forest did not die, there were no population extinctions.

In our second simulation experiment, in which we examined which landscape metrics were the most informative predictors of gypsy moth spread, four landscape metrics, in addition to the proportion of suitable habitat, were determined to be informative predictors of simulated gypsy moth spread. The metrics proportion of like adjacencies, effective mesh size, aggregation

index, and largest patch index were selected because AIC differences <10 indicated support for these models (Burnham and Anderson 2002) (Table 2). The relationships between the invasion distance and each landscape metric have similar non-linear shapes showing a threshold response of spread distance to landscape structure (Figure 2). Adjusted R^2 values of models containing the selected landscape metrics ranged from 0.279 to 0.290 (Table 2).

Empirical Spread Rates

Empirically estimated gypsy moth spread rates ranged from -7.5 to 11.5 km yr^{-1} with a mean (± SD) of 3.7 ± 4.0 km yr^{-1}. Comparing the predictive ability of landscape metrics selected from the simulation models, we found the full model containing the aggregation index had the lowest AIC value (AIC = 1241.6). We detected high concurvity (i.e., a generalization of colinearity that allows for nonlinear relationships) among elevation, elevational heterogeneity, and May maximum temperature, so we began our model selection procedure by removing one of these variables at a time until concurvity was reduced to acceptable levels. Based on backward selection, no further variables were removed. In the final model, having adjusted R^2 = 0.765, invasion rate was predicted by the aggregation index, May maximum temperature, host tree density, and the weighted mean invasion rate. Increases in the aggregation index had a positive effect on invasion rates while the aggregation index was <90, but above that value the confidence region for the relationship overlapped zero indicating no relationship (Figure 3). May maximum temperature had no directional relationship with invasion rate between ca. 20-23.5 °C, but showed an optimum around 24.6 °C (Figure 3). There was a negative effect of increasing host tree density, although the confidence region for this relationship overlapped zero for much of the range of host tree densities (Figure 3). Because the AIC values of the full models also supported the model containing the landscape metric proportion of like adjacencies (ΔAIC = -0.9), we

applied the same model selection procedure to the full model containing that variable. The same covariates were retained, the model fit similarly well (Adj. $R^2 = 0.763$) and relationships with all predictors had similar shapes. Including the distance-weighted mean invasion rate as a covariate reduced autocorrelation in the model residuals and had a modest influence on the overall model fit ($R^2 = 0.625$ for the final model without distance-weighted mean invasion rate). See Appendix C3 for additional details regarding the alternate model containing proportion of like adjacencies and corrections for spatial autocorrelation.

Discussion

In this study, we used incorporated field experiments, simulation modeling, and spatial analysis to demonstrate how landscape structure impacts population persistence and spread of the gypsy moth. Our field experiments showed that the landscape structure impacts mate finding because gypsy moths resist crossing edges from the forest to the matrix, and because of faster distance-decay in mate location probabilities in the non-forest matrix. A model incorporating these effects of landscape structure on mate finding, as well as mortality of larvae landing in the matrix, predicted increased likelihood of extinction and reduced spread rates as the proportion of forested habitat on the landscape decreases, and as the connectivity of forest patches is reduced. An analysis of empirical rates of gypsy moth spread in West Virginia and Virginia revealed relationships between landscape structure and the rate of range expansion that were consistent with our simulation predictions given that we used landscape metrics reflecting both forest area and connectivity.

Our alternate simulations, in which we manipulated effects of landscape structure on mate finding and larval mortality, indicated that both processes contributed to simulated effects of forest abundance and aggregatoion on gypsy moth spread and population persistence.

Dispersal mortality of larvae appeared to be particularly important given that our simulations predicted the fastest spread and no extinctions when mortality was not imposed on larvae landing in the non-forest matrix. Dispersal mortality in larvae may have high importance for two reasons. Because adult females are flightless, the failure of ballooning larvae to cross the matrix, and their removal from the population due to mortality, inhibited spread. When larvae in the non-forest matrix were killed, this also reduced the number of surviving adults, ostensibly increasing rates of mating failure. One caveat is that our assumptions that larvae disperse according to simple diffusion and that all those landing outside the forest perish may be simplifications. Gypsy moths certainly require suitable host trees to develop to adulthood, but certain land uses, for instance low to medium-density residential areas, may have lower but non-zero abundances of host trees. In addition, some other organisms that disperse largely passively are capable of modifying their buoyancy to land in favorable habitats (Koehl et al. 2007). Gypsy moth larvae produce silk threads to "balloon" on air currents, and could potentially alter their buoyancy to settle out when in proximity to potential host trees. Therefore, it is possible that our scenario that kills larvae landing in the matrix overestimates dispersal mortality.

Simulations from our alternate model in which forest edges were completely permeable and the matrix did not affect the mate-finding dispersal kernel indicate that the effects of forest abundance and aggregation on mate finding also contribute to patterns of spread and population persistence. Prior studies have shown that levels of protandry and temporal dispersion in maturation times used in this study (chosen because they are representative of conditions in our study area) result in a mating failure Allee effect (Robinet et al. 2007, 2008, Walter et al. 2014). The resistance of gypsy moths to crossing from forest into the matrix, the more rapid distance-decay of mate finding in the matrix, and dispersal mortality of larvae, then exacerbate mating

failure in landscapes where non-forest matrix is present. Our simulations predicted gypsy moth spread to be more rapid in landscapes with greater forest abundance and connectivity, even when mortality was not imposed on larvae landing in the matrix, suggesting strongly that the abundance and connectivity of forest influences the severity of mating failure Allee effects in the gypsy moth.

Our field experiments also showed the probability of a male gypsy moth locating a female to decay more rapidly in the non-forest matrix than in the forest. Although the confidence intervals for each kernel overlapped each other over short distances, they diverged over longer distances, and even small differences in the probability of long-distance dispersal have been shown to be important to spread (Kot et al. 1996, Clark 1998). These differences in mate-finding probability may reflect a combination of differences in dispersal behavior and increased rates of mortality. We did not attempt to quantify dispersal behavior *per se*, but we did not observe between-habitat differences in gypsy moth behavior during ≈20 minutes after their release, when many gypsy moths began to disperse from the release point. Causes of mortality in adult gypsy moths are not well quantified, but predation is likely to be important given that typical adult life spans of wild gypsy moths are around 3 days (Elkinton and Cardé 1980), whereas adult moths kept in the laboratory can live for more than two weeks. Although we are not aware of any published studies on predation of adult gypsy moths, birds feed on other life stages (Smith 1985) and we observed them to predate upon adults. As birds are visual predators, their rates of predation on gypsy moths may be higher in open habitats than in forest.

The simulation results also suggest an important role of human-mediated long-distance transport of egg masses in determining rates of spread. Across all levels of forest abundance and aggregation, median simulated spread distances tended to be low, but the 95th percentile of

spread distances increased dramatically when the proportion of forest and the aggregation of forest was high. Given the limited dispersal ability of gypsy moths, and the further limitations imposed by forest edges and the non-forest matrix, it is apparent that rapid spread occurs through successful establishment of populations initiated by long-distance transport (Liebhold et al. 1992, Liebhold and Tobin 2006). Increasing the area and connectivity of forest, then, has two positive effects on the success of such transport events. Increasing forest area improves the likelihood that the transported egg mass will arrive at a suitable location, while increasing forest connectivity improves the likelihood that males originating elsewhere are able to disperse to, and mate with, individuals originating from a long-distance transport event. Our simulations did predict rates of gypsy moth spread much slower than observed in our empirical analysis, which might suggest that long-distance transport is more common than represented in our simulations; however, overall rates of spread were also constrained by the spatial extent of our simulation landscapes. These were limited by the high computational costs of simulating individual, local-scale processes in such detail.

Despite the difference in scales, our analysis of real-world gypsy moth spread rates supported the predictions of our model. Two landscape metrics, the aggregation index and the proportion of like adjacencies, were significant components of models explaining >75% of the variability in gypsy moth spread in our study area. The importance of these variables, which reflect the total area of forest on the landscape as well as the aggregation or connectedness of forest, suggest that habitat area and aggregation contribute to real-world patterns of gypsy moth spread. The shape of the relationships between these landscape metrics and spread did differ between the empirical analysis (Figure 2) and simulations used to select which landscape metrics to investigate in the empirical analysis (Figure 3) but a likely explanation is that our simulated

landscapes covered a broad range of aggregation indices, whereas the empirical landscapes had uniformly high values of the aggregation index. Although positive effects of forest area and aggregation on gypsy moth spread may not seem surprising, human transport of egg masses is thought to be a crucial driver of gypsy moth spread (Liebhold et al. 1992, Bigsby et al. 2011). Gypsy moth spread might be expected to increase with decreasing forest area (at least above a minimum forested area) if these transport events occur more frequently in landscapes with more human land uses, but our results to do not support this prediction. Rather, they suggest that the local-scale processes of dispersal mortality and mate finding scale up to contribute to landscape-scale patterns.

In the empirical analysis, while controlling for the effects of May maximum temperature, host tree density, and spatial autocorrelation, we found that these covariates had interesting, sometimes unexpected, relationships with the invasion rate. We identified an optimum May maximum temperature for gypsy moth spread at ≈24.6 °C (Figure 3). Slowed spread in the warmest parts of our study area is consistent with recent research in the same region suggesting that supraoptimal temperatures during larval development, which typically occurs in May for much of our study area, have negative effects on development and may restrict spread (Tobin et al. 2014). Suboptimal temperatures could also negatively affect spread by slowing development and increasing reproductive asynchrony (Robinet et al. 2007, Walter et al. 2014). Finally, there was a negative relationship between invasion rate and host tree density over the most resource-poor landscapes, but only over a narrow range of host-tree densities. While the abundance of host trees is critical to the development of population outbreaks (Gottschalk 1993), other studies of spreading populations have found no relationship or slightly negative relationships between host tree density and population persistence and growth (Whitmire and Tobin 2006, Walter et al.

2014). One potential explanation is that high densities of host trees are not needed to support the low-density populations found at the invasion front.

In conclusion, our combination of field experiments, simulation modeling, and spatial analysis provides strong evidence that landscape structure impacts the spread of the gypsy moth in North America. Our results suggest that, although gypsy moth populations might persist in landscapes with very little forest, rapid gypsy moth spread requires landscapes where forest is abundant and highly aggregated, which has clear implications for the future spread of this invasion and management efforts to slow its advance. We provide evidence that these landscape-level patterns result because forest edges and the non-forest matrix reduce rates of mate finding and survivorship, exacerbating a mating-failure Allee effect in the gypsy moth. In addition, effects of landscape structure on movement and population vital rates occur in many species, suggesting that the mechanisms we describe may be widespread. Our findings also highlight cross-scale interactions in which local-scale processes (mortality, mate finding) impact landscape-level rates of invasion. In general, the effects of cross-scale interactions on the expansion or contraction of range boundaries are not well understood, but a combined approach involving field study, simulation modeling, and analysis of spatiotemporal data offers a powerful methodology for investigating these interactions.

Tables & Figures

Table 1: Selected dispersal kernels and their mean performance ranking. Kernel equations were fit to recapture data from each release and ranked by AIC value. Ranks were averaged across all replicates to determine which kernel best described the distance-decay of male gypsy moth mate-finding probabilities. The Laplace function could not be fit to data from several open field releases and was omitted from further consideration.

Kernel	Equation	Mean Rank
Gaussian	$\exp(a - bx^2)$	2.8
Fat-tailed	$\exp(a - b\sqrt{x})$	2.2
Laplace	$\exp(a - bx)$	-
Neg. exponential	$a\exp(-bx)$	2.4
Inverse power	ax^{-b}	2.6

Table 2: A selection of landscape metrics were evaluated to determine which are the most informative predictors of the effect of landscape structure on simulated gypsy moth spread. Generalized additive models (GAMs) containing each landscape metric individually were ranked according to their AIC value.

Name	Description	Rank	AIC	Adj. R^2
Proportion habitat	The proportion of the landscape comprised of suitable gypsy moth habitat.	1	1076.8	0.290
Proportion like adjacencies	Number of adjacent habitat cells divided by the total number of adjacent cells.	2	1082.7	0.289
Effective mesh size	Sum of squared habitat areas divided by total landscape area. Corresponds to the size of patches when habitat is divided into S patches, where S = the splitting index.	3	1084.9	0.289
Aggregation index	Number of like adjacencies normalized by the maximum possible number of adjacencies if habitat were maximally clumped into a single patch.	4	1085.0	0.279
Largest patch index	The percentage of the landscape occupied by the largest patch.	5	1085.4	0.289
Proportion core habitat	Proportion of core area on the landscape; core area represents the area of patches inside of a specified "edge depth," which was set to one grid cell.	6	1091.9	0.341
Patch cohesion index	Measures the physical connectedness of habitat by relating patch perimeter, patch area, and total landscape area.	7	1118.0	0.205
Landscape shape index	Sum of the length of the landscape boundary and all internal edge segments divided by the square root of the total landscape area.	8	1125.5	0.241
Patch density	Number of patches per unit of landscape area.	9	1146.1	0.124
Splitting index	Number of patches with a constant size when subdivided into S patches, where S is the value of the splitting index.	10	1175.8	0.068
Edge density	Length of habitat edge normalized by the area of the landscape.	11	1209.6	0.068

Table 3: We deployed pheromone-baited traps at several locations on Blandy Experimental Farm to ensure that our experimental results were consistent with male mate-finding patterns in a wild population. We report the total number of moths captured in 14 traps representing field, mid-succession, and forest habitats. These locations are described in terms of their dominant vegetation and either the distance to the nearest forest patch or the area of the forest patch the trap was placed in.

	Type	**Catch**	**Description**
1	Field	0	Abandoned field; 96 m from nearest forest
2	Field	1	Hay field; 112 m from nearest forest
3	Field	1	Corn field; 118 m from nearest forest
4	Field	2	Abandoned field; 237 m from nearest forest
5	Field	2	Hay field; 120 m from nearest forest
6	Field	7	Lawn grasses; 72 m from nearest forest
7	Mid-succession	1	Shrubs; buckthorn, Osage orange; 93 m from nearest forest
8	Mid-succession	1	Shrubs; buckthorn; 142 m from nearest forest
9	Mid-succession	2	Shrubs; buckthorn, Osage orange; 114 m from nearest forest
10	Forest	2	Mockernut hickory, black walnut; 2.6 ha
11	Forest	13	Black walnut, black locust, 5.7 ha
12	Forest	22	White oak, mockernut hickory, 5.0 ha
13*	Forest	74	White oak, black walnut, American elm; 23.3 ha
14*	Forest	203	White oak, mockernut hickory; 23.3 ha

* Traps 13 and 14 were located >350 m apart in the same large woodlot.

Table 4: Effects of proportion of suitable habitat and aggregation of habitat patches (*H*) on gypsy moth invasion rates using the main scenario and two alternate scenarios. In the "Alternate Mate Finding" model, there were no effects of landscape structure on male mate location probabilities. In the "Alternate Mortality" model, larvae landing outside the forest survived. For each combination of habitat proportion and *H*, we report the percent of simulations in which the population went extinct before 20 generations, and the 5th, 50th, and 95th percentile of gypsy moth invasion distances. In simulations that went extinct before 20 generations, the invasion distance was considered to be 0.

		Aggregation (*H*)											
	Habitat proportion	**0.25**				**0.5**				**0.75**			
		Ext.	5%	50%	95%	Ext.	5%	50%	95%	Ext.	5%	50%	95%
Main	**0.1**	32%	0	7	13	24%	0	7	13	26%	0	7	11
	0.25	10%	0	7	11	6%	1	7	11	12%	0	7	11
	0.5	6%	2	7	17	2%	4	7	14	6%	1	7	47
	0.75	0%	5	9	62	0%	5	10	113	0%	6	9	101
Alt. Mat. Find.	**0.1**	14%	0	7	13	16%	0	7	12	12%	0	9	14
	0.25	8%	0	7	28	12%	0	7	19	6%	0	9	11
	0.5	2%	4	8	12	2%	3	7	27	4%	3	8	47
	0.75	0%	7	11	151	0%	6	12	140	0%	7	13	147
Alt. Mort.	**0.1**	0%	7	17	21	0%	12	17	60	0%	10	18	76
	0.25	0%	10	15	67	0%	9	17	77	0%	11	16	83
	0.5	0%	11	16	56	0%	15	20	67	0%	12	17	98
	0.75	0%	16	22	147	0%	18	23	155	0%	17	24	163

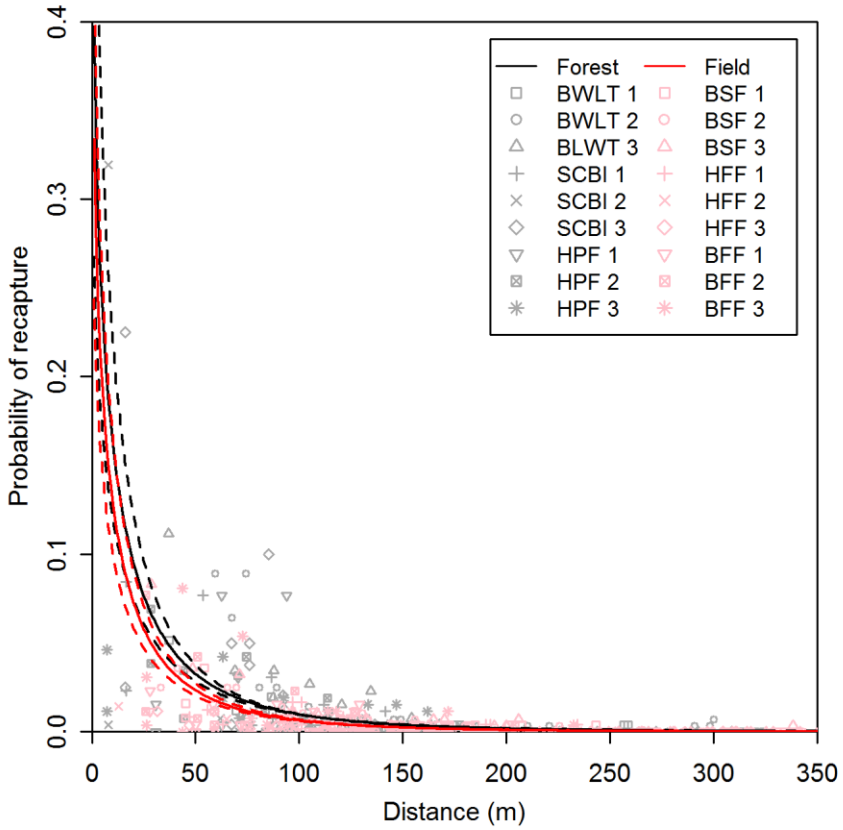

Figure 1: Mean (± 95% confidence intervals) gypsy moth mate finding kernels in forest (black) and field (red) habitats, as estimated from mass-release-recapture experiments. Points represent proportion recapture at individual traps, with distances corrected for drift. Point characters identify separate trials.

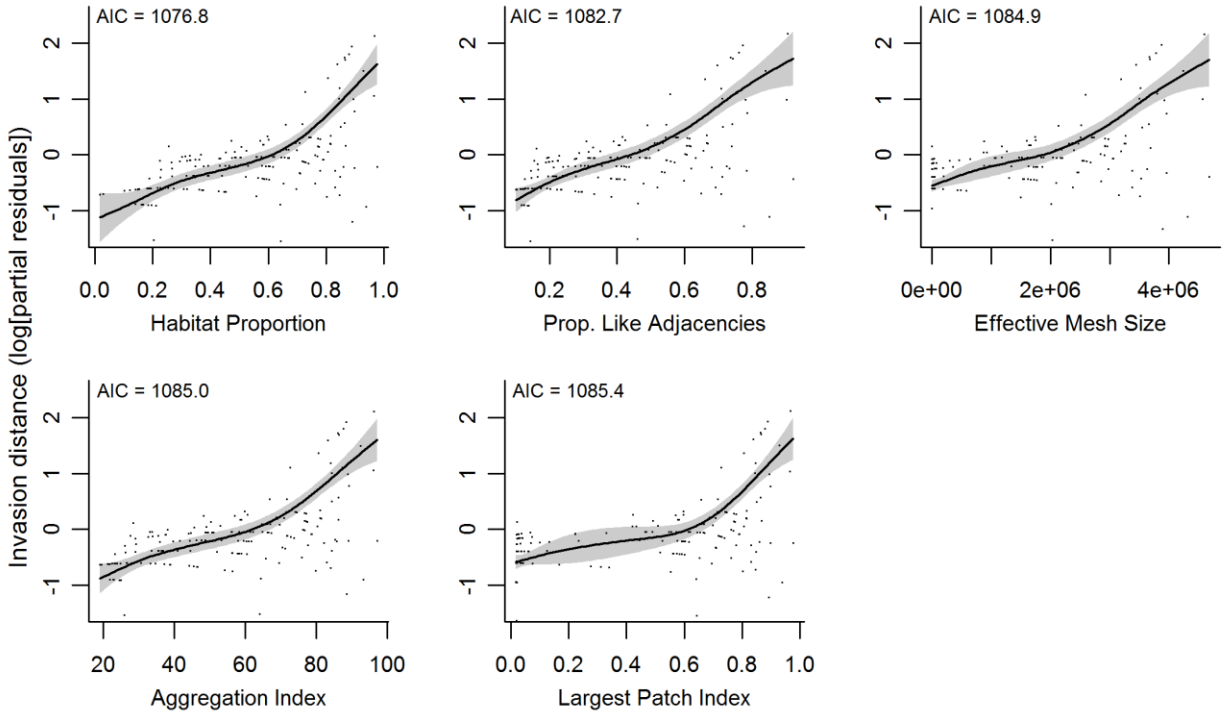

Figure 2: GAM fitted relationships between simulated gypsy moth invasion rates and landscape metrics selected based on AIC values.

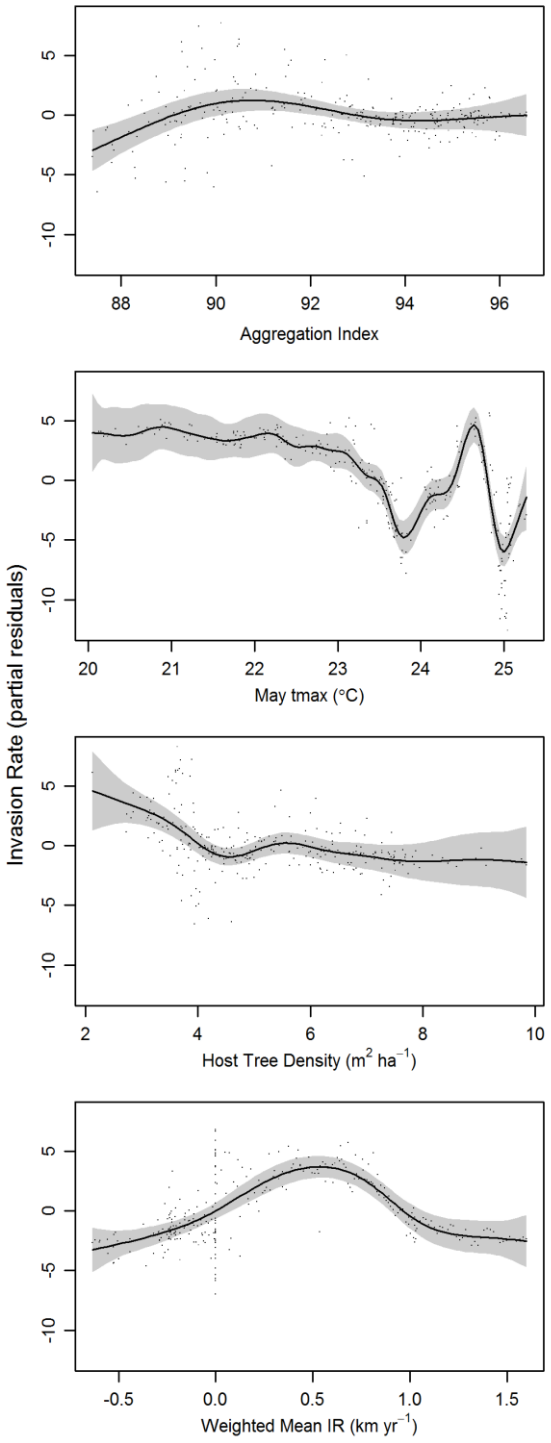

Figure 3: GAM fitted relationships between empirically estimated gypsy moth invasion rates and the aggregation index (spline with 3.2 df), May maximum temperature (20.3 df), elevational heterogeneity (SD of elevation; 2.1 df), and host tree density (6.9 df).

5. Spatial variation in Allee effect severity impacts patterns of range expansion[4]

Abstract

Allee effects are thought to slow the range expansion of spreading populations and contribute to stable range boundaries. Recent studies have found that the severity of Allee effects may vary spatiotemporally due to effects of heterogeneity in environmental conditions on demographic processes. However, theoretical studies have largely considered the severity of Allee effects to be fixed across time and space, and it is not clear what patterns of spread should result when Allee effects do vary. In this study, we use a spatially explicit population dynamic model to explore how varying the severity of Allee effects and the spatial configuration of their variations on the landscape affect resulting patterns of range expansion. We show that spatial variations in the severity of Allee effects can influence patterns of spread, with different landscape configurations producing different spread patterns. Impacts of spatial variation in Allee effect severity on spread depended on an interaction between Allee effects, long-distance dispersal, and the shape of the spreading front. Allee effects limited the growth of nascent populations at the invasion front, lengthening the distance over which population density declined from high density in long-established populations to zero at the range boundary, and patterns of spread were affected most strongly when the Allee effect was sufficiently severe that nascent populations at the range boundary rarely received enough immigrants to overcome the Allee threshold. When this condition was met, linearly increasing gradients in Allee severity produced decelerating patterns of spread. Patchy variations in Allee severity induced variability in spread patterns, as patches with low Allee severity facilitated rapid spread but high severity patches inhibited spread; however, spread may be enhanced when the scale of patchiness is

[4] This study was conducted in collaboration with Derek Johnson, Patrick Tobin, and Kyle Haynes.

extremely fine relative to the dispersal capabilities of an organism. These results highlight spatial variations in the severity of Allee effects as a potentially underappreciated mechanism underlying heterogeneity in rates of range expansion.

Introduction

The Allee effect is a potentially widespread density-dependent phenomenon affecting small or low-density populations. The concept, originally developed to describe how cooperation among animals of the same species could improve average per-capita fitness (Allee 1931), has come to refer to any positive correlation between population size and individual fitness (Stephens et al. 1999, Courchamp et al. 1999). Allee effects are potentially widespread because they have been detected in species spanning several taxa of plants and animals, and because of the ubiquity of ecological processes that can give rise to Allee effects (Kramer et al. 2009). Known mechanisms of Allee effects include mate (or pollen) limitation, inbreeding depression, breakdown of cooperative defensive or feeding behaviors, and failure to satiate predators (Kramer et al. 2009).

When the positive correlation between population size and individual fitness translates into an increase in the population growth rate with increasing population size, this is termed a demographic Allee effect. It is also possible for increases in population size to improve aspects of individual fitness without also increasing the population growth rate; this is termed a component Allee effect (Stephens et al. 1999). This study concerns demographic Allee effects, which can be further characterized as weak or strong. In the case of a strong Allee effect, there is a threshold population size, termed the Allee threshold, below which the population growth rate is below the replacement rate and the population is likely to decline to extinction (Wang and Kot 2001, Taylor and Hastings 2005, Courchamp et al. 2008). Although the Allee threshold is

particularly important, the magnitude of the impact of Allee effects on a population is also affected by the rate at which increases in population size increase the population growth rate (i.e., the slope of the relationship between population size and growth rate). We use the terminology "severity" of the Allee effect to describe the *combination* of Allee threshold and slope and to differentiate from the "strength" of the Allee effect, which by convention denotes whether or not there is an Allee threshold.

Allee effects may be important in a variety of scenarios including population outbreaks (Bjørnstad et al. 2010, Régnière et al. 2013) and extinction risks of endangered species (Courchamp et al. 2008), and a particularly rich body of theory predicts that Allee effects may slow the spread of biological invasions and set stable range boundaries (Kot et al. 1996, Wang and Kot 2001, Keitt et al. 2001). These general predictions have been supported by empirical studies of range expansion in systems including the house finch invasion of North America (Veit and Lewis 1996), invasive spread of cordgrass in Washington, USA (Taylor et al. 2004), and wolf recolonization in Yellowstone National Park, USA (Hurford et al. 2006). Theoretical models have largely considered Allee effect severity a fixed quantity, but recent evidence has highlighted how the Allee threshold may vary spatiotemporally due to heterogeneity in environmental conditions (Tobin et al. 2007b, Kramer and Drake 2010, Kramer et al. 2011, Walter et al. 2014). For example, Kramer et al. (2010) experimentally demonstrated that the presence of a type-II predator can produce a demographic Allee effect and used a model to predict how the presence of refugia could alter the Allee threshold. In addition, Walter et al. (2014) found that effects of topography on temperature produced spatial variability in reproductive asynchrony in the gypsy moth, leading to variations in the severity of a mating failure Allee effect.

Due to the variability present in real-world landscapes it may be particularly simplistic to treat Allee effect severity as constant through space when investigating how Allee effects impact range boundary dynamics, whether the species in question is an exotic invader or is shifting its range in response to climate change. Landscape structure may impact several mechanisms giving rise to Allee effects. Its effects on movement could alter rates of mate finding (Wiens 1976, Lamberson et al. 1999), while landscape characteristics may also impact the spatial distribution of natural enemies (Yahner and Smith 1991, Cronin and Reeve 2014). Moreover, gradients in climate due to topography and latitude impact phenology and survivorship, in some cases leading to mating failure (Rhainds and Fagan 2010, Lynch et al. 2014, Walter et al. 2014). Consequently, variation in the severity of Allee effects related to spatial heterogeneity in environmental conditions is a likely component of the dynamics of low-density populations found near the edge of a species range, but the effects of spatial variability in Allee effect severity on range dynamics have received little attention and are not well understood.

This study explores how spatial variability in the severity of Allee effects impacts range expansion using a model simulating population dynamics and spread. We compare patterns of range expansion in landscapes having different spatial configurations of Allee effect variability to spread in environments with a constant Allee effect. We considered landscapes with random variations in Allee effect severity, increasing linear gradients in Allee effect severity, and two scenarios with variations in Allee effect severity that simulate landscape patchiness: one in which low positive spatial autocorrelation in Allee effect severity simulated fine-scale patchiness, and one in which high positive spatial autocorrelation simulated patches that were coarser in scale. For each of these five landscape configurations, we also considered how the

average severity of Allee effects and the range of Allee effect severities present on the landscape impact spread.

In real landscapes, continuous gradients in Allee effect severity could result if, for example, there are elevational or latitudinal gradients in mating success (Rhainds and Fagan 2010, Lynch et al. 2014, Walter et al. 2014), predation pressure (McKinnon et al. 2010), or other biotic interactions (Schemske et al. 2009). Other types of landscape heterogeneity, for example variations in habitat type, often result in patchy configurations, and the spatial scale of landscape patchiness–relative to the scale of dispersal–may impact habitat occupancy (Hanski et al. 1994) and rates of movement (With and Crist 1995) of a focal species as well as its natural enemies. Hence, habitat patchiness plays a potentially important role in mediating ecological interactions, such as predation (Bernstein et al. 1988), that may impact the severity of Allee effects. Although random, non-autocorrelated variation in Allee effect severity is unlikely in nature, randomly-generated landscapes without autocorrelation in habitat type have often provided null models for investigating the effects of landscape patchiness on ecological processes (Gardner et al. 1987, With and Crist 1995). Consequently, we include it as a null model for Allee effect variation.

Methods

We examined effects of spatial variability in Allee effects using a discrete-time logistic growth population model with an asymptotic Allee effect, extended in two dimensions of discrete space:

$$N_{i,t} = rN_{i,t-1}\left(1 - \frac{N_{i,t-1}}{K}\right)\left(\frac{N_{i,t-1}}{c_i + N_{i,t-1}}\right) + S + L. \qquad \text{(eqn. 1)}$$

Here, the population size N at location i and time t depends on the rate of population growth, r,

the population size N_i at time t-1, the carrying capacity K, the Allee effect parameter c, and the net contributions of short-distance (S) and long-distance (L) dispersal. Short-distance dispersal was implemented by transporting a constant fraction f_s of the source population to an adjacent grid cell (using 8-cell adjacency) with probability p_s. Similarly, long-distance dispersal transported a constant fraction f_l of the source population to a new grid cell with probability p_l; however, in this case the displacement of dispersers in the x and y directions was determined by independently drawing values from a Gaussian distribution having zero mean and unit variance and multiplying these values by the parameter d_l to control the scale of long-distance dispersal.

We included both short and long-distance dispersal processes to simulate stratified diffusion, which is likely to be a feature of range expansion in many systems and can have a strong influence on patterns of spread (Shigesada et al. 1995, Shigesada and Kawasaki 1997). Our method of modeling long-distance dispersal by transporting a constant fraction of the population to a new location approximates accidental transport by humans, a common component of biological invasions (e.g., Suarez et al. 2001, Davis et al. 2004, Muirhead et al. 2006, Johnson et al. 2006). We assume that the likelihood of a long-distance dispersal event occurring does not change with population density, but that the number of dispersers increases with the density of the source populations. Modeling short-distance dispersal by transporting a fraction of the source population to a neighboring cell assumes no distance-decay in short-distance dispersal and does not allow for the possibility of some dispersers from a source population to immigrate to different locations. However, similar representations of dispersal are not uncommon in models with space represented on a discrete grid (e.g., Allstadt et al. 2009, Ferreira et al. 2014), and, moreover, making these assumptions has the advantage of minimizing computational requirements.

The parameter *c*, controlling the severity of the Allee effect, was specified to vary spatially in four different patterns: random fluctuations, a linearly increasing gradient, fine-scale patches, and coarse-scale patches. Random fluctuations in *c* were generated by independently drawing values from a uniform distribution. In landscapes with linear gradients in Allee effect severity, *c* increased incrementally from one end of the landscape to the other. Landscapes with patchy variations in *c* were generated using a version of the midpoint displacement algorithm (Saupe 1988) modified to produce rectangular landscapes. Using this algorithm, the dimensions of landscapes are constrained to multiples of 2^n+1, where *n* is an integer, so landscapes were given dimensions of 33x99. In the midpoint displacement algorithm, the parameter *H* controlled the degree of autocorrelation in values of *c* between nearby locations and thus the scale of patchiness. We set $H = 0.2$ to create landscapes with fine-scale spatial variations in Allee effect severity, and $H = 0.8$ for landscapes with coarse-scale variations in Allee effect severity. For each spatial pattern, we created landscapes where values of *c* spanned the intervals 0-5 ("low" severity), 5-10 ("high" severity), and 0-10 ("high variability" in severity). We compared results from simulations in which *c* varied spatially to simulations where *c* remained constant across the landscape. In the constant Allee parameter scenario, *c* was set at 2.5, 7.5, and 5.0. These values correspond to the average values of *c* in the low, high, and high variability scenarios, respectively.

The values of all other population dynamic and dispersal parameters remained constant throughout each simulation. We began with simulations where the intrinsic rate of population growth $r = 2$, the carrying capacity $K = 200$, the probability of short-distance dispersal $p_s = 0.2$, the fraction of the source population moving via short-distance dispersal $f_s = 0.1$, the probability of long-distance dispersal $p_l = 0.05$, the fraction of the source population transported by long-

distance dispersal $f_l = 0.1$, and the scale of long-distance dispersal $d_l = 10$. The values in this main parameter set are not specific to any particular species, but are thought to be within a range of reasonable values for a variety of organisms. We also investigated the sensitivity of our model results to variability in each parameter by running simulations in which one parameter at a time was assigned a value higher or lower than that "main value" used above (Table 1). It is important to note that varying *r*, and to a lesser degree *K*, changes the Allee threshold density produced by a given value of *c* (Figure 1).

Simulations were initialized with all grid cells in the column $y = 1$ having 25 individuals. Simulations were run for up to 250 generations, with spread in the *y* direction measured by fitting a smoothing spline to the mean population density in each column *y*; the range boundary was determined as the largest value of *y* where the expected density was ≥ 1 individual. We ran 50 replicate simulations for each combination of landscape configuration and range of Allee effect severity and population/dispersal parameter set. In the random and patchy landscape configurations, a new landscape was randomly generated for every replicate.

Results

Increasing the parameter *c*, controlling the severity of Allee effects, slowed the rate of spread, and patterns of spread were affected by the spatial configuration of variation in *c* (Figure 2, Figure 3). Relative to simulations with constant Allee effect severity, the rate of spread was faster in landscapes with random variations in *c*, and this held true regardless of the range of Allee effect severity. With the exception of the landscapes with random variability in *c*, patterns of spread among landscape configurations with low Allee effect strength ($0 \leq c \leq 5$, or $c = 2.5$) were nearly identical. In contrast, spatial variability in Allee effect severity caused patterns of spread to differ from equivalent homogenous landscapes in the high severity ($5 \leq c \leq 10$) and

high variability ($0 \leq c \leq 10$) scenarios (Figure 2). The mean rate of spread in landscapes with patchy variations in Allee effect severity was very similar to the mean rate of spread in constant severity landscapes, but the greater degree of variability among replicates indicates that the specific configuration of an individual landscape, despite being randomly generated and having equal scales of patchiness, can substantially impact spread (Figure 3). Large effects of landscape configuration on patterns of spread were observed in the linear gradient landscapes with high Allee effect severity and with high variability in Allee effect severity (Figure 1). Here, increasing c as spread proceeded into the landscape resulted in deceleration in the spread rate, with the spread rate decelerating most strongly after passing ≈60 grid cells into landscapes where $5 \leq c \leq 10$ and ≈80 grid cells into landscapes where $0 \leq c \leq 10$ (Figure 2).

Our sensitivity analyses suggest that patterns of spread are most strongly affected by the parameters determining population growth (r), carrying capacity (K), and long-distance dispersal (p_l, f_l, and d_l). Generally, increasing any of these parameters caused the invasion to spread more quickly, but altering these parameters also changed how variability in Allee effect strength shaped spread patterns (Figure 4; Appendix A). For example, there were no differences between the low gradient ($0 \leq c \leq 5$) and the comparable constant $c = 2.5$ scenarios when the main parameter set was used, but we did observe nonlinear spread trajectories (similar to those in the high and high variability scenarios using the main parameter set) when we reduced r, K, or f_l. By the same token, a nonlinear spread trajectory was not observed in the high severity gradient landscape when using high values of r, K, and f_l. When the intrinsic rate of population growth was low ($r = 1.5$), there was almost no spread in constant landscapes with $c = 5.0$ or $c = 7.5$, producing Allee thresholds at $N_{i,t} = 2.2$ and $N_{i,t} = 2.6$ individuals, respectively, but populations did spread in landscapes with variability in Allee effect severity (Figure 4; Appendix A). Effects

of varying other parameters also depended on Allee effect strength; for example, varying the scale of long-distance dispersal (d_l) had a larger impact on the spread rate when Allee effect severity was low than in the high severity or high variability in severity scenarios. In simulations where there was no long-distance dispersal ($p_l = 0$), the population spread slowly and at a constant rate, even in simulations where the spatial pattern of Allee effect severity caused non-linear patterns of spread. The proportion of the population dispersing short distances (f_s) had no detectable impact on spread trajectories (Figure 3; Appendix A). See Appendix A for additional plots from our sensitivity analyses.

Discussion

In our simulations, spatial variations in the severity of Allee effects were shown to influence spatiotemporal patterns of spread, and these influences were most sensitive to interactions between the range of Allee effect severities present on the landscape, the population growth rate, the carrying capacity, and long-distance dispersal. Increasing the severity of Allee effects has been shown to slow rates of spread (Wang and Kot 2001, Keitt et al. 2001, Wang et al. 2002), but these and other studies have considered Allee effect severity a constant value. Consistent with these predictions, mean rates of spread in simulated landscapes with varying Allee effect severity were similar to those observed in simulations with an equivalent constant Allee effect severity (Figure 1), but this study demonstrates that spatial variability in Allee effect severity can drive deviations from the mean predictions (Figures 1-2). Hence, variations in the severity of Allee effects may be an underappreciated source of variability in patterns of range expansion.

An important insight from our results is that impacts of spatial variability in Allee effect severity on spread are strongly influenced by an interaction between the Allee threshold, the

shape of the spreading front, and the size of nascent populations formed by long-distance dispersal. In accordance with other predictions of spread patterns where stratified diffusion is present (Shigesada et al. 1995, Muirhead et al. 2006), long-distance dispersal appeared to be the major driver of advance of the invasion front (Figure 4; Appendix A). Spread is most rapid when nascent populations formed by long-distance dispersal are able to grow quickly and themselves become sources of immigrants, but Allee effects cause these populations to grow slowly or become extinct if the number of immigrants is insufficient to overcome the Allee threshold. Consequently, when considering the shape of the spreading front, the distance over which population density declines from a high set by the carrying capacity to zero in locations that have yet to be successfully colonized increases as the severity of Allee effects increases. In our simulations, when Allee effect severity was sufficiently high, that distance became large relative to the scale of long-distance dispersal, and the density of source populations near enough to send immigrants ahead of the spreading front was not high enough for founding population sizes to exceed the Allee threshold.

For example, with our main parameter set when c was low (i.e. $0 \leq c \leq 5$), landscape configuration had very little impact on spread (Figure 2), even though with $r = 2$ and $K = 200$, $c = 2.5$ produces a strong Allee effect with a threshold at 1.4 individuals, because with $d_l = 10$ high-density populations behind the spreading front were near enough to the leading edge that their long-distance dispersers, in groups larger than the Allee threshold, were regularly able to reach the leading edge. When we increased c, effects of landscape configuration on spread became apparent (Figure 2, Figure 3), but the sensitivity of spread patterns to changes in K, d_l, and f_l at all levels of c corroborate our interpretation of the interaction between the Allee threshold, the shape of the spreading front, and the size of nascent populations formed by long-

distance dispersal. Increasing either of these parameters led to faster spread overall and a reduction in sensitivity to variations in *c*, while decreasing these parameters led to slower overall rates of spread and greater sensitivity to variations in *c* (Figure 4). Neither d_l nor f_l have any effect on the Allee threshold, and *K* has an inconsequentially small effect (Figure 1),

Although with our main parameter set there were generally no impacts of landscape configuration on spread when Allee effect severity was low, we did observe one exception in that spread was always most rapid in landscapes with random, uncorrelated variations in Allee effect severity, regardless of the range of *c* (Figure 2). This scenario was examined as a potential null model and is generally not thought to be representative of how Allee effect severity would vary in real landscapes, although it may be possible for the configuration of landscapes to appear random at certain spatial scales, although whether or not an organism perceived the landscape as varying randomly would depend on the scale of its movements.

In comparison to the random variation scenario, simulations with patchy variations in Allee effect severity, regardless of whether that variation was fine or coarse in spatial scale, the mean spread trajectories were similar to those produced by a spatially constant Allee effect (Figure 2). However, plots of individual replicate simulations reveal a large degree of variability between replicates in simulations where *c* was large enough to produce strong Allee effects (Figure 3), with variability being highest when variations in Allee effect severity were coarse in scale. These findings suggest that specific characteristics of a heterogeneous landscape can dramatically influence patterns of spread. Spread may be stalled by encountering areas where local environmental conditions lead to high Allee effect severity or enhanced where local environmental conditions support rapid growth of nascent populations, and the effect may be

particularly dramatic when the scale of patchiness is large relative to the dispersal capabilities of the organism.

Although random variations in Allee effect severity are thought to be unlikely in nature, in combination our results point to an important role for the scale of patchiness in determining spread patterns. Where variations in *c* were random and uncorrelated, the scale of patchiness was extremely fine and from any location on the landscape dispersers are as likely to encounter a relatively favorable patch (i.e. a patch with a less severe Allee effect) as a relatively unfavorable one. This may be particularly important when nascent populations formed by long-distance dispersal that are unconstrained by Allee effects are able to rapidly increase in density and ultimately contribute dispersers. Even when dispersers populate an unfavorable patch there are better patches nearby where populations can grow quickly and produce larger numbers of emigrants, provided that the population in the unfavorable patch can persist long enough to colonize the favorable one.

In contrast, where the scale of patchiness grows (i.e., where variations in Allee effect severity are positively autocorrelated), the probability of dispersers landing in a favorable or unfavorable patch is location-dependent. From any location, short-distance dispersers will find similar conditions to their former location, while long-distance dispersers–depending on the scale of patchiness and dispersal capabilities of the organism–may be likely to encounter very different conditions. This can of course allow spread out of less favorable patches or for spread to "jump" across an unfavorable area, but it also means that long-distance dispersers from favorable patches could be more likely to land in unfavorable patches where the nascent population may grow slowly or even go extinct if the founding population size is below the Allee threshold. Given that the mean spread trajectory for simulations in patchy landscapes was very similar to that of

spread in landscapes with an equivalent constant Allee parameter (Figure 2), it appears that these effects tend to balance each other. We did also observe that some individual configurations, although randomly-generated and having statistically the same level of patchiness, particularly favor or restrict spread (Figure 3).

Given evidence of elevational and latitudinal trends in factors that could give rise to Allee effects (Schemske et al. 2009, Rhainds and Fagan 2010, McKinnon et al. 2010, Walter et al. 2014), we investigated how linearly increasing gradients affected spread. Using our main parameter set, when the range of c included values sufficiently large to produce strong Allee effects, increasing linear gradients in Allee effect severity resulted in decelerating rates of spread (Figure 2). Initially, the invasion spread faster than in corresponding landscapes with a constant Allee parameter, but as spread progressed further into the landscape the spread rate decreased, eventually becoming markedly slower than spread in the constant landscapes. This is perhaps the most dramatic example of the interaction we observed between the Allee threshold, the shape of the spreading front, and the size of nascent populations formed by long-distance dispersal. Using the main parameter set, spread decelerated rapidly after reaching the distance into the landscape where $c \approx 8$, producing an Allee threshold at $N_{i,t} \approx 2.25$ individuals. This switch from relatively fast to slow spread suggests that $c \approx 8$ is a transition zone in which the distance over which the populations transitions from high density to zero is becoming so long that long-distance dispersers from high-density populations are rarely reaching the invasion front. Because both the long-distance dispersal kernel and the decline in population density moving from high-density established populations to the range boundary nonlinear, the effect of increasing c on patterns of spread is also nonlinear.

In all landscape configurations and Allee severity levels, patterns of spread depended strongly on the intrinsic rate of growth (r), the carrying capacity (K), and parameters controlling long-distance dispersal (f_l, p_l, d_l). For a given value of c, the intrinsic rate of growth (r) has a large impact on the Allee threshold (Figure 1). Decreasing r resulted in increased Allee effect severity and, in some cases, very slow rates of spread (Figure 3; Appendix A). The parameters K, f_l, and d_l all influence the size of nascent populations ahead of the invasion front formed by long-distance dispersal, impacting whether or not they are able to overcome the Allee threshold and persist. To an extent, the importance of long-distance dispersal to our model results reflects our strategy of modeling long-distance dispersal as transporting a constant fraction of the source population to a new grid cell. While this may be a reasonable approximation when long-distance dispersal is the result of accidental transport by humans, rates of dispersal could also be density dependent, particularly if stratified diffusion occurs because of factors intrinsic to the population such as stage structure, or if increasing population density leads to increasing rates of encounter between humans and the spreading species.

To design a tractable study, we held all parameters besides c constant in our simulations. It stands to reason, however, that in real landscapes factors such as the intrinsic rate of growth, the carrying capacity, or the probability of individuals dispersing out of a source population could also vary geographically and that variations in these other parameters could be correlated or uncorrelated with Allee effect severity. Examining these effects lay beyond the scope of this study and is particularly complicated by an extremely limited understanding of how factors like density-independent mortality or competition interact with mechanisms generating Allee effects to determine population dynamics.

In summary, our results indicate that spatial variability in the severity of Allee effects can have a strong impact on range expansion, but species-specific characteristics and effects of environmental heterogeneity on other aspects of demography are also important. One important implication of these results is that when an environment is relatively unfavorable to low-density populations (i.e. the Allee effect is very severe), but is capable of supporting higher-density populations (i.e. the carrying capacity is relatively high), variations resulting in patches with lower Allee effect severity can act as stepping-stones and sources of immigrants that can facilitate range expansion. In an applied context, this could pose a challenge to efforts to restrict the spread of invasive species, but could also be a boon to those seeking to assist northward or upslope migrations of species in light of climate change since creation of a small number of very good habitat patches could lead to range expansion.

Although variability in Allee effect severity has been empirically detected in a very small number of studies to date, the degree of variability in the various processes that drive Allee effects and determine their severity makes it incredibly unlikely that Allee effect severity *does not* vary in nature. In fact, this may be one reason why demographic Allee effects have proven difficult to confirm in natural populations. Arguably, the difficulty of empirically studying Allee effects may have slowed progress toward understanding the causes and consequences of their variability, but observing spread patterns consistent with our predictions may provide indirect evidence of this phenomenon and suggest further studies to elucidate the mechanisms driving spatial heterogeneity in patterns of spread.

Tables & Figures:

Table 1: Parameter values used in the main simulations and sensitivity analyses.

Parameter	Low	Main	High
r	1.5	2	3
K	100	200	400
p_s	0.05	0.2	0.4
f_s	0.05	0.1	0.2
p_l	0	0.05	0.1
f_l	0.05	0.1	0.2
d_l	5	10	15

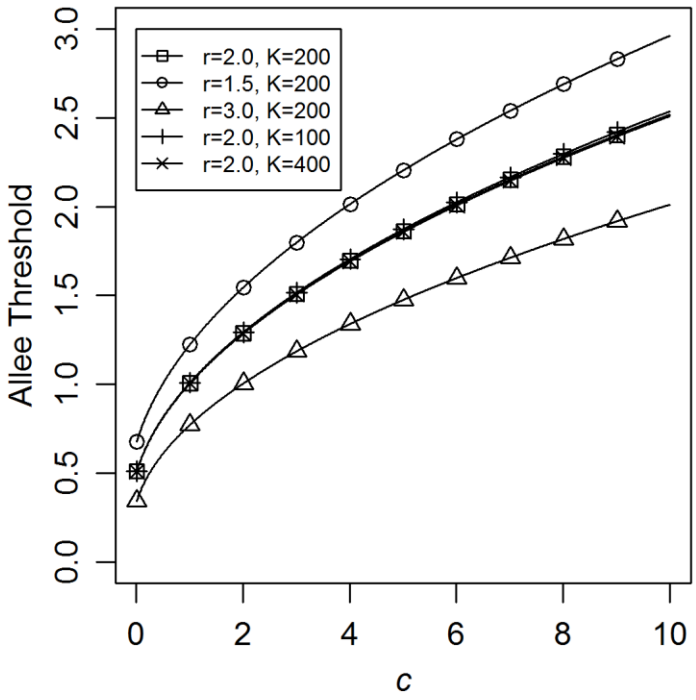

Figure 1: Relationships between *c* and the Allee threshold density for combinations of *r* and *K* used in our simulations. Our main parameter values were $r = 2$ and $K = 200$.

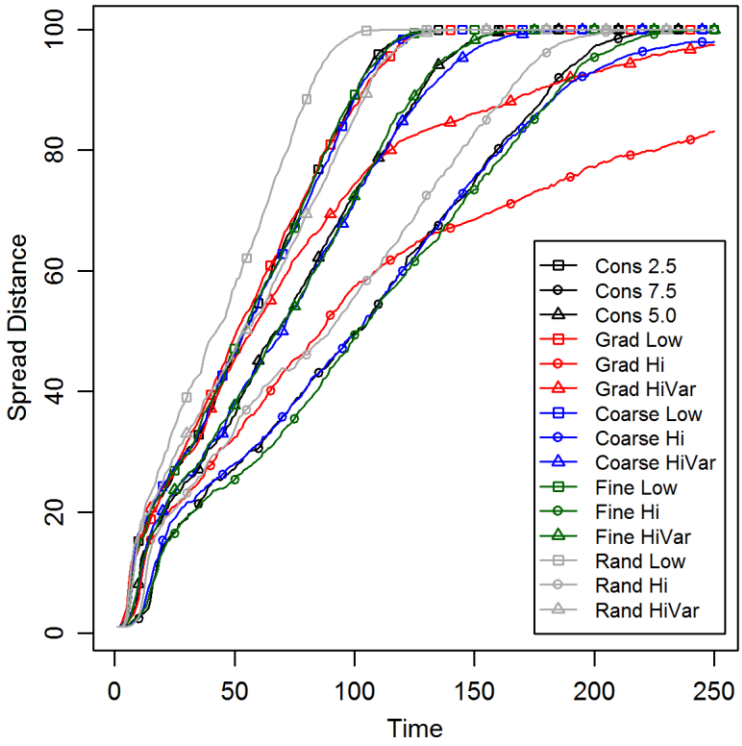

Figure 2: Mean trajectories for spread into landscapes with different spatial configurations and levels of variability in Allee effect severity. Legend labels denote the landscape configuration followed by the severity of the Allee effect; for example, "Cons 2.5" denotes the spatially constant Allee severity, with $c = 2.5$, and "Grad Low" denotes the gradient configuration with low Allee severity. The apparent slowing in the rate of spread as the invasion approached the end of the landscape ($y = 99$) is an artifact resulting from replicates that already reached the end of the landscape having nowhere further to spread.

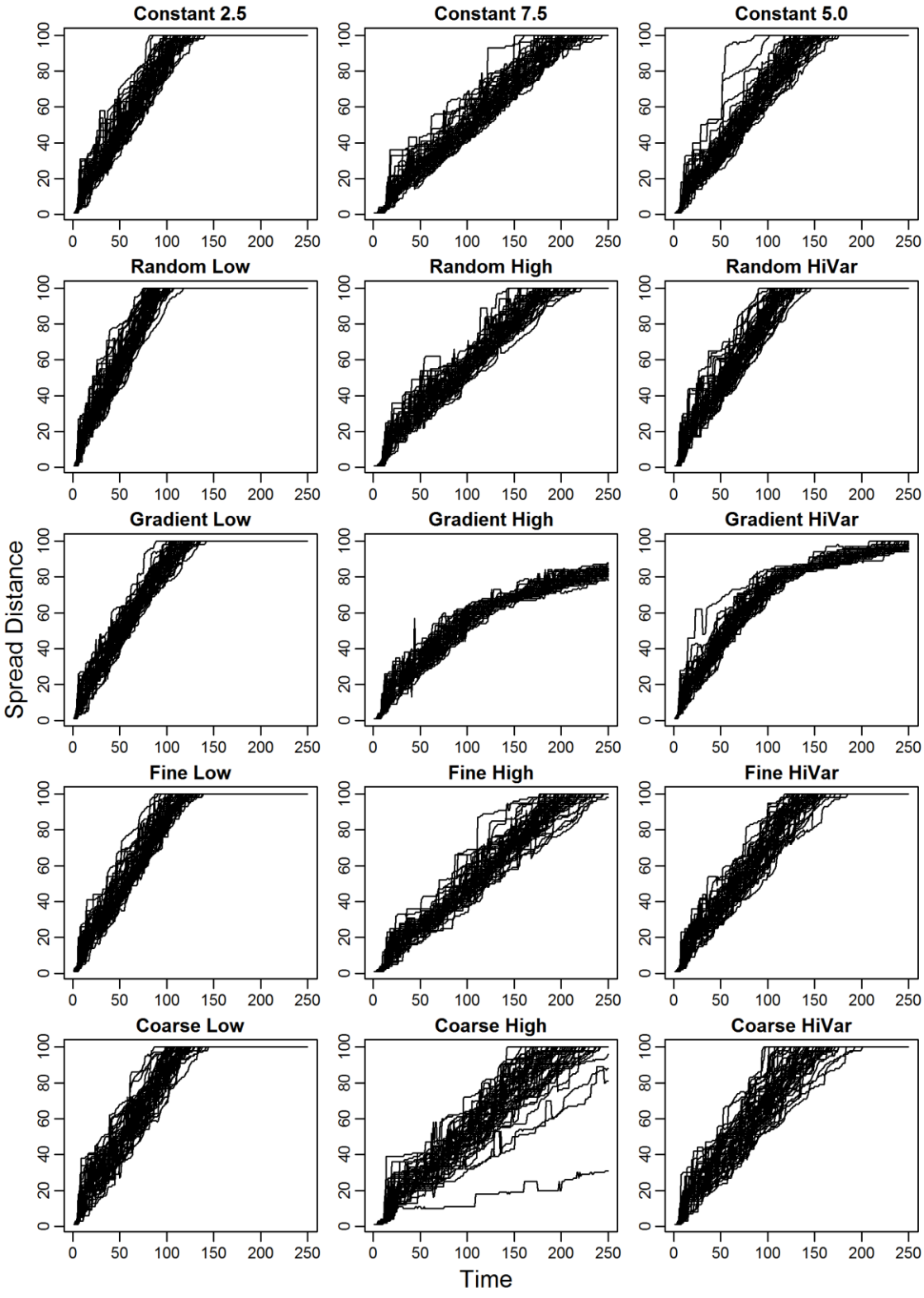

Figure: 3 Spread trajectories for individual replicate simulations revealing variability from mean spread trajectories.

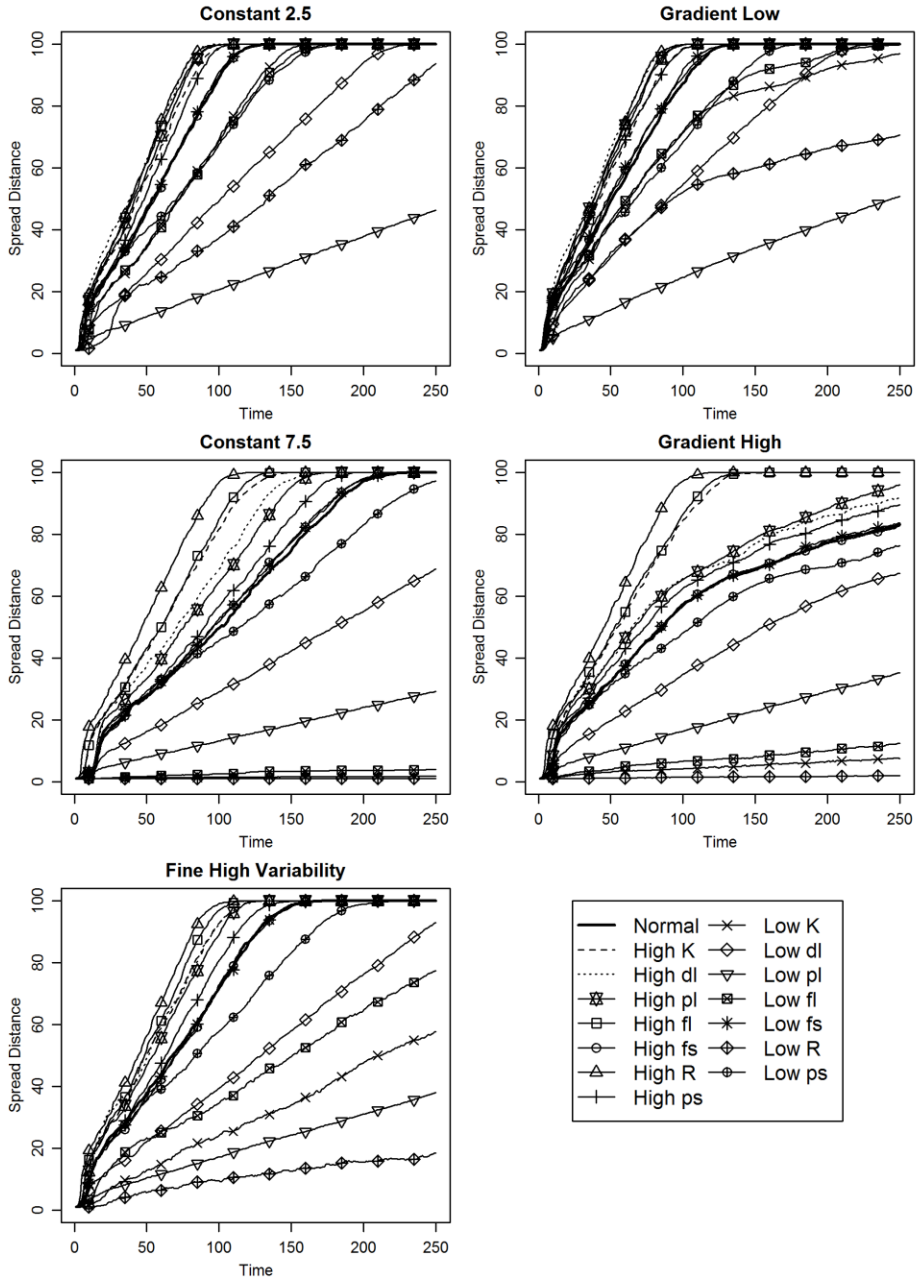

Figure 4: A selection of mean spread trajectories showing sensitivity of spread patterns to variations in model parameters in landscapes having different configurations and levels of variability in Allee effect severity. Sensitivity analyses were conducted by varying one parameter at a time, selecting one value of each parameter that was higher and lower than our main parameter values. Numerical parameter values can be found in Table 1. Additional sensitivity plots can be found in Appendix A.

6. Conclusions

In combination, the studies comprising this dissertation indicate that spatiotemporal patterns in gypsy moth spread are explained in part by a population cycles and spatial variations in the severity of Allee effects. In Chapter 2, using a combination of time-series analysis and simulation models incorporating population cycles, Allee effects, and stratified dispersal, I found that temporal fluctuations in gypsy moth spread appear to be driven by population cycles in established populations. This projects suggests that longer-established populations are linked to nascent populations near the invasion front by human-mediated long-distance transport, which results in cyclical fluctuations in the number of immigrants provided to the invasion front by established populations. Outbreaks push the invasion front forward by providing larger numbers of immigrants that allow some nascent populations to overcome Allee effects, while the range retracts following an outbreak crash when a dearth of immigrants to the invasion front causes population growth rates to decline and local extinctions to occur, likely in concert with strong Allee effects in those populations. The apparent importance of outbreaks to gypsy moth range expansion suggests that spread could be reduced by increasing efforts to suppress outbreaks. Further study is needed to quantify how great a reduction in outbreaking populations is needed to cause a substantial reduction in spread, and whether or not such an approach is economically feasible.

Geographical patterns in gypsy moth spread result in part from spatial variations in the severity of Allee effects. Previous research yielded empirical evidence for regional variations in the severity of Allee effects in the gypsy moth (Tobin et al. 2007b), but the mechanisms underlying the observed variations remained unknown. In Chapter 3, I used a combination of simulation modeling and an empirical analysis of growth rates in nascent populations to show

how elevation and hilliness drive variations in the severity of mating failure Allee effects. In Chapter 4, I incorporated field experiments, simulations of mating and spread in heterogeneous environments, and an empirical analysis of gypsy moth spread rates to show how landscape structure drives variations in mating success, Allee effect severity, and the rate of spread. These findings improve predictions of future gypsy moth spread, suggesting that, all else being equal, spread should occur most rapidly in areas where forest habitat is abundant and well-connected, and in flat, low-elevation landscapes. Future research should investigate the relative importance of these two factors, as well as the contributions of additional mechanisms of Allee effects that may vary spatially, such as predation by small mammals. Tobin et al. (2007) also observed temporal variability in the Allee threshold, which topography and landscape structure do not explain given that these characteristics vary over time scales larger than observed fluctuations in the Allee threshold. Further study should also consider what processes give rise to these temporal patterns.

Chapters 3, 4 and 5 of this dissertation represent three of the first studies regarding variability in the severity of Allee effects, including the first studies to identify ways that spatial environmental heterogeneity can drive such variations (Chapters 3 & 4). Because many species have temperature-dependent developmental rates, and the movements of many species are affected by landscape structure, the mechanisms of variability in Allee dynamics described in this dissertation are likely to occur in other taxa. Considering also the variety of ecological processes that can give rise to Allee effects (Kramer et al. 2009), variations in the severity of Allee effects are likely be widespread. These studies, including Chapter 5 in which I simulated spread through landscapes with spatially varying Allee effect severity, also show how these variations affect spatiotemporal patterns of range expansion, prompting the hypothesis that

variations in the severity of Allee effects are an underappreciated source of variability in the dynamics of range expansion. Species whose ranges are changing may include those responding to changes in climate in addition to invasive species, making a robust understanding of such dynamics critical.

Further research, however, is needed to inform a working understanding of the processes that give rise to variations in the severity of Allee effects and the impacts of such variations on the persistence and growth of populations. The Allee effect severity realized by a population may result from the interaction of multiple mechanisms of Allee effects and other sources of demographic variability–such as density-independent mortality, rates of immigration and emigration, or drivers of negative density dependence–that may vary in space and time. These interactions have received little attention, arguably in part because the difficulty of detecting Allee effects in real-world populations has obscured their significance. Given the importance of low-density populations to range expansion as well as the conservation of threatened species, one implication of varying Allee effect severity is that management plans, which currently cannot explicitly consider such variability, may not be equally effective across space and time. Improving understanding of how and why Allee effects vary spatiotemporally may at worst allow management plans to predict and account for their effects, but may also suggest particular interventions that compensate for potential variations.

References

Allee, W. C. 1931. Animal Aggregations. The University of Chicago Press, Chicago, IL.

Allstadt, A., T. Caraco, and G. Korniss. 2009. Preemptive spatial competition under a reproduction-mortality constraint. Journal of Theoretical Biology 258:537–49.

Allstadt, A. J., K. J. Haynes, A. M. Liebhold, and D. M. Johnson. 2013. Long-term shifts in the cyclicity of outbreaks of a forest-defoliating insect. Oecologia 172:141–51.

Andow, D. A., P. M. Kareiva, S. A. Levin, and A. Okubo. 1990. Spread of invading organisms. Landscape Ecology 4:177–188.

Angulo, E., G. W. Roemer, L. Berec, J. Gascoigne, and F. Courchamp. 2007. Double Allee effects and extinction in the island fox. Conservation Biology 21:1082–91.

Anselin, L., and A. K. Bera. 1998. Spatial dependence in linear regression models with an introduction to spatial econometrics. Pages 237–289 *in* A. Ullah and D. E. Giles, editors. Handbook of Applied Economic Statistics. Marcel Dekker, New York.

Aukema, J. E., B. Leung, K. Kovacs, C. Chivers, K. O. Britton, J. Englin, S. J. Frankel, R. G. Haight, T. P. Holmes, A. M. Liebhold, D. G. McCullough, and B. Von Holle. 2011. Economic impacts of non-native forest insects in the continental United States. PloS One 6:e24587.

Berec, L., E. Angulo, and F. Courchamp. 2007. Multiple Allee effects and population management. Trends in Ecology & Evolution 22:185–91.

Berec, L., and T. Mrkvička. 2013. Neglecting uncertainty behind Allee effect estimation may generate false predictions of population extinction risk. Oikos 122:845–856.

Bernstein, C., A. Kacelnik, and J. R. Krebs. 1988. Individual decisions and the distribution of predators in a patchy environment. Journal of Animal Ecology 57:1007–1026.

Berryman, A. 1991. The gypsy moth in North America: a case of successful biological control? Trends in Ecology & Evolution 6:110–111.

Bigsby, K. M., P. C. Tobin, and E. O. Sills. 2011. Anthropogenic drivers of gypsy moth spread. Biological Invasions 13:2077–2090.

Bjørnstad, O. N., A. M. Liebhold, and D. M. Johnson. 2008. Transient synchronization following invasion: revisiting Moran's model and a case study. Population Ecology 50:379–389.

Bjørnstad, O. N., C. Robinet, and A. M. Liebhold. 2010. Geographic variation in North American gypsy moth cycles: subharmonics, generalist predators, and spatial coupling. Ecology 91:106–18.

Bonte, D., H. Van Dyck, J. M. Bullock, A. Coulon, M. Delgado, M. Gibbs, V. Lehouck, E. Matthysen, K. Mustin, M. Saastamoinen, N. Schtickzelle, V. M. Stevens, S. Vandewoestijne, M. Baguette, K. Barton, T. G. Benton, A. Chaput-Bardy, J. Clobert, C. Dytham, T. Hovestadt, C. M. Meier, S. C. F. Palmer, C. Turlure, and J. M. J. Travis. 2012. Costs of dispersal. Biological Reviews 87:290–312.

Brooks, R. T., H. R. Smith, and W. M. Healey. 1998. Small mammal abundance at three elevations on a mountain in central Vermont, USA, a sixteen-year record. Forest Ecology and Management 110:181–193.

Burnham, K. P., and D. R. Anderson. 2002. Model Selection and Multimodel Inference. 2nd Ed. Springer, New York.

Calabrese, J. M., and W. F. Fagan. 2004. Lost in time, lonely, and single: reproductive asynchrony and the Allee effect. The American Naturalist 164:25–37.

Calabrese, J. M., L. Ries, S. F. Matter, D. M. Debinski, J. N. Auckland, J. Roland, and W. F. Fagan. 2008. Reproductive asynchrony in natural butterfly populations and its consequences for female matelessness. The Journal of Animal Ecology 77:746–56.

Cazelles, B., K. Cazelles, and M. Chavez. 2014. Wavelet analysis in ecology and epidemiology: impact of statistical tests. Journal of the Royal Society Interface 11:20130585.

Cazelles, B., M. Chavez, G. C. De Magny, S. Hales, and J. Gue. 2007. Time-dependent spectral analysis of epidemiological time-series with wavelets. Journal of the Royal Society Interface 4:625–636.

Chang, F., C.-J. Chen, and C.-J. Lu. 2004. A linear-time component-labeling algorithm using contour tracing technique. Computer Vision and Image Understanding 93:206–220.

Clark, J. S. 1998. Why trees migrate so fast: confronting theory with dispersal biology and the paleorecord. The American Naturalist 152:204–24.

Clark, K. L., N. Skowronski, and J. Hom. 2010. Invasive insects impact forest carbon dynamics. Global Change Biology 16:88–101.

Collingham, Y. C., and B. Huntley. 2000. Impacts of habitat fragmentation and patch size upon migration rates. Ecological Applications 10:131–144.

Contarini, M., K. S. Onufrieva, K. W. Thorpe, K. F. Raffa, and P. C. Tobin. 2009. Mate-finding failure as an important cause of Allee effects along the leading edge of an invading insect population. Entomologia Experimentalis et Applicata 133:307–314.

Courchamp, F., L. Berec, and J. Gascoigne. 2008. Allee effects in ecology and conservation. Oxford University Press, Oxford, UK.

Courchamp, F., T. Clutton-Brock, and B. Grenfell. 1999. Inverse density dependence and the Allee effect. Trends in Ecology & Evolution 14:405–410.

Cronin, J. T. 2003. Movement and spatial population structure of a prairie planthopper. Ecology 84:1179–1188.

Cronin, J. T., and J. D. Reeve. 2014. An integrative approach to understanding host–parasitoid population dynamics in real landscapes. Basic and Applied Ecology 15:101–113.

Davis, H. G., C. M. Taylor, J. C. Civille, and D. R. Strong. 2004. An Allee effect at the front of a plant invasion: Spartina in a Pacific estuary. Journal of Ecology 92:321–327.

Deutsch, C. V, and A. G. Journel. 1992. GSLIB: a geostatistical software library and user's guide. Oxford University Press, Oxford, UK.

Doane, C. C. 1976. Flight and mating behavior of the gypsy moth. Pages 127–136 *in* J. F. Anderson and H. K. Kaya, editors. Perspectives in Forest Entomology. Academic Press, New York.

Doane, C. C., and M. L. McManus. 1981. The gypsy moth: research toward integrated pest management. United States Department of Agriculture, Washington, DC.

Dwyer, G., J. Dushoff, J. S. Elkinton, and S. A. Levin. 2000. Pathogen-driven outbreaks in forest defoliators revisited: building models from experimental data. The American Naturalist 156:105–120.

Dwyer, G., J. Dushoff, and S. H. Yee. 2004. The combined effects of pathogens and predators on insect outbreaks. Nature 430:341–345.

Dwyer, G., and J. S. Elkinton. 1993. Using simple models to predict virus epizootics in gypsy moth populations. Journal of Animal Ecology 62:1–11.

Dwyer, G., J. S. Elkinton, and J. P. Buonaccorsi. 1997. Host heterogeneity in susceptibility and disease dynamics: tests of a mathematical model. The American Naturalist 150:685–707.

Ehler, L. E. 1998. Invasion biology and biological control. Biological Control 13:127–133.

Elkinton, J. S., and R. T. Cardé. 1980. Distribution, dispersal, and apparent survival of male gypsy moths as determined by capture in pheromone-baited traps. Environmental Entomology 9:729–737.

Elkinton, J. S., and R. T. Cardé. 1983. Efficiency of two gypsy moth (Lepidoptera: Lymantriidae) pheromone-baited traps. Environmental Entomology 12:1519–1525.

Elkinton, J. S., and R. T. Cardé. 1988. Effects of intertrap distance and wind direction on the interaction of gypsy moth (Lepidoptera, Lymantriidae) pheromone-baited traps. Environmental Entomology1 17:764–769.

Elkinton, J. S., W. M. Healy, J. P. Buonaccorsi, G. H. Boettner, A. M. Hazzard, H. R. Smith, and A. M. Liebhold. 1996. Interactions among gypsy moths, white-footed mice, and acorns. Ecology 77:2332–2342.

Elkinton, J. S., and A. M. Liebhold. 1990. Population dynamics of gypsy moth in North America. Annual Review of Entomology 35:571–596.

Elkinton, J. S., A. M. Liebhold, and R.-M. Muzika. 2004. Effects of alternative prey on predation by small mammals on gypsy moth pupae. Population Ecology 46:171–178.

Fagan, W. F., M. A. Lewis, M. G. Neubert, and P. van den Driessche. 2002. Invasion theory and biological control. Ecology Letters 5:148–157.

Farge, M. 1992. Wavelet transforms and their applications to turbulence. Annual Review of Fluid Mechanics 24:395–457.

Ferreira, C. P., L. Esteva, W. a C. Godoy, and F. L. Cônsoli. 2014. Landscape diversity influences dispersal and establishment of pest with complex nutritional ecology. Bulletin of Mathematical Biology 76:1747–61.

Fisher, R. A. 1937. The wave of advance of advantageous genes. Annals of Eugenics 7:255–369.

Frank, K. L., P. C. Tobin, H. W. Thistle, and L. S. Kalkstein. 2013. Interpretation of gypsy moth frontal advance using meteorology in a conditional algorithm. International Journal of Biometeorology 57:459–73.

Fry, J. A., G. Xian, S. Jin, J. A. Dewitz, C. G. Homer, L. Yang, C. A. Barnes, N. D. Herold, and J. D. Wickham. 2011. Completion of the 2006 National Land Cover Database for the conterminous United States. Photogrammetric Engineering and Remote Sensing 77:858–864.

Gardner, R. H., B. T. Milne, M. G. Turner, R. V O'Neill, B. T. Mime, and R. V. O. Neill. 1987. Neutral models for the analysis of broad-scale landscape pattern. Landscape Ecology 1:19–28.

Gascoigne, J., L. Berec, S. Gregory, and F. Courchamp. 2009. Dangerously few liaisons: a review of mate-finding Allee effects. Population Ecology 51:355–372.

Gascoigne, J. C., and R. N. Lipcius. 2004. Allee effects driven by predation. Journal of Applied Ecology 41:801–810.

Gottschalk, K. W. 1993. Silvicultural guidelines for forest stands threatened by the gypsy moth. USDA Forest Service General Technical Report NE-171, Radnor, PA.

Gray, D. R. 2004. The gypsy moth life stage model: landscape-wide estimates of gypsy moth establishment using a multi-generational phenology model. Ecological Modelling 176:155–171.

Gray, D., F. Ravlin, and J. Braine. 2001. Diapause in the gypsy moth: a model of inhibition and development. Journal of Insect Physiology 47:173–184.

Gregory, S. D., C. J. A. Bradshaw, B. W. Brook, and F. Courchamp. 2010. Limited evidence for the demographic Allee effect from numerous species across taxa. Ecology 91:2151–61.

Grenfell, B. T., O. N. Bjørnstad, and J. Kappey. 2001. Travelling waves and spatial hierarchies in measles epidemics. Nature 414:716–723.

Hajek, A. E., and P. C. Tobin. 2009. North American eradications of Asian and European gypsy moth. Pages 71–89 *in* A. E. Hajek, T. R. Glare, and M. O'Callaghan, editors. Use of Microbes for Control and Eradication of Invasive Arthropods. Springer, Dordrecht.

Hamilton, D. J., and M. J. Lechowicz. 1991. Host effects on the development and fecundity of gypsy moth, *Lymantria dispar* L., reared under field conditions. Canadian Journal of Zoology 69:2217–2224.

Hanski, I., M. Kuussaari, and M. Nieminen. 1994. Metapopulation structure and migration in the butterfly *Melitaea cinxia*. Ecology 75:747–762.

Hanski, I., P. Turchin, E. Korpimaki, and H. Henttonen. 1993. Population oscillations of boreal rodents: regulation by mustelid predators leads to chaos. Nature 364:232–235.

Hargis, C. D., J. A. Bissonette, and J. L. David. 1998. The behavior of landscape metrics commonly used in the study of habitat fragmentation. Landscape Ecology 13:167–186.

Hastie, T., and R. Tibshirani. 1986. Generalized additive models. Statistical Science 1:297–318.

Hastings, A., K. Cuddington, K. F. Davies, C. J. Dugaw, S. Elmendorf, A. Freestone, S. Harrison, M. Holland, J. Lambrinos, U. Malvadkar, B. A. Melbourne, K. Moore, C. M. Taylor, and D. Thomson. 2005. The spatial spread of invasions: new developments in theory and evidence. Ecology Letters 8:91–101.

Haynes, K. J., O. N. Bjørnstad, A. J. Allstadt, and A. M. Liebhold. 2013. Geographical variation in the spatial syncrhony of a forest-defoliating insect: isolation of environmental and spatial drivers. Proceedings of the Royal Society Biological Sciences 280:20122373.

Haynes, K. J., and J. T. Cronin. 2006. Interpatch movement and edge effects: the role of behavioral responses to the landscape matrix. Oikos 113:43–54.

Haynes, K. J., A. M. Liebhold, and D. M. Johnson. 2009. Spatial analysis of harmonic oscillation of gypsy moth outbreak intensity. Oecologia 159:249–56.

Haynes, K. J., A. M. Liebhold, and D. M. Johnson. 2012. Elevational gradient in the cyclicity of a forest-defoliating insect. Population Ecology 54:239–250.

Hoffman Gray, R., C. G. Lorimer, P. C. Tobin, and K. F. Raffa. 2008. Preoutbreak dynamics of a recently established invasive herbivore: roles of natural enemies and habitat structure in stage-specific performance of gypsy moth (Lepidoptera: Lymantriidae) populations in northeastern Wisconsin. Environmental Entomology 37:1174–84.

Hurford, A., M. Hebblewhite, and M. A. Lewis. 2006. A spatially explicit model for an Allee effect: why wolves recolonize so slowly in Greater Yellowstone. Theoretical Population Biology 70:244–54.

Isaaks, E. H., and R. M. Srivastava. 1989. An introduction to applied geostatistics. Oxford University Press, Oxford, UK.

Johnson, D. M., U. Büntgen, D. C. Frank, K. Kausrud, K. J. Haynes, and A. M. Liebhold. 2010. Climatic warming disrupts recurrent Alpine insect outbreaks. Proceedings of the National Academy of Sciences of the United States of America 107:20576–20581.

Johnson, D. M., A. M. Liebhold, and O. N. Bjørnstad. 2006a. Geographical variation in the periodicity of gypsy moth outbreaks. Ecography 29:367–374.

Johnson, D. M., A. M. Liebhold, P. C. Tobin, and O. N. Bjørnstad. 2006b. Allee effects and pulsed invasion by the gypsy moth. Nature 444:361–3.

Kauffman, M. J., N. Varley, D. W. Smith, D. R. Stahler, D. R. MacNulty, and M. S. Boyce. 2007. Landscape heterogeneity shapes predation in a newly restored predator-prey system. Ecology letters 10:690–700.

Keitt, T. H., M. A. Lewis, and R. D. Holt. 2001. Allee effects, invasion pinning, and species' borders. The American Naturalist 157:203–16.

Kim, Y. J., and C. Gu. 2004. Smothing spline Gaussian regression: more scalable computation via efficient approximation. Journal of the Royal Statistical Society B (Statistical Methodology) 66:337–356.

Koehl, M., J. Strother, M. Reidenbach, J. Koseff, and M. Hadfield. 2007. Individual-based model of larval transport to coral reefs in turbulent, wave-driven flow: behavioral responses to dissolved settlement inducer. Marine Ecology Progress Series 335:1–18.

Kot, M., M. A. Lewis, and P. van den Driessche. 1996. Dispersal data and the spread of invading organisms. Ecology 77:2027–2042.

Kramer, A. M., B. Dennis, A. M. Liebhold, and J. M. Drake. 2009. The evidence for Allee effects. Population Ecology 51:341–354.

Kramer, A. M., and J. M. Drake. 2010. Experimental demonstration of population extinction due to a predator-driven Allee effect. The Journal of Animal Ecology 79:633–639.

Kramer, A. M., O. Sarnelle, and J. Yen. 2011. The effect of mating behavior and temperature variation on the critical population density of a freshwater copepod. Limnology and Oceanography 56:707–715.

Lamberson, R. H., R. McKelvey, B. R. Noon, and C. Voss. 1999. A dynamic analysis of northern spotted owl viability in a fragmented forest landscape. Conservation Biology 6:505–512.

Larsen, E., J. M. Calabrese, M. Rhainds, and W. F. Fagan. 2013. How protandry and protogyny affect female mating failure: a spatial population model. Entomologia Experimentalis et Applicata 146:130–140.

Leung, B., J. M. Drake, and D. M. Lodge. 2004. Predicting invasions: propagule pressure and the gravity of Allee effects. Ecology 85:1651–1660.

Lewis, M. A., and P. Kareiva. 1993. Allee dynamics and the spread of invading organisms. Theoretical Population Biology 43:141–158.

Liebhold, A. M., and J. S. Elkinton. 1989. Characterizing spatial patterns of gypsy moth regional defoliation. Forest Science 35:557–568.

Liebhold, A. M., K. W. Gottschalk, E. R. Luzader, D. A. Mason, and D. B. Twardus. 1997. Gypsy Moth in the United States: An Atlas. USDA Forest Service General Technical Report NE-233.

Liebhold, A. M., K. W. Gottschalk, R.-M. Muzika, M. E. Montgomery, R. Young, K. O'Day, and B. Kelley. 1995. Suitability of North American Tree Species to the Gypsy Moth: A Summary of Field and Laboratory Tests. USDA Forest Service General Technical Report NE-211.

Liebhold, A. M., J. A. Halverson, and G. A. Elmes. 1992. Gypsy moth invasion in North America: a quantitative analysis. Journal of Biogeography 19:513–520.

Liebhold, A. M., V. C. Mastro, and P. W. Schaefer. 1989. Learning from the legacy of Leopold Trouvelot. Bulletin of the Entomological Society of America 35:20–22.

Liebhold, A. M., and P. C. Tobin. 2006. Growth of newly established alien populations: comparison of North American gypsy moth colonies with invasion theory. Population Ecology 48:253–262.

Lockwood, J. L., M. F. Hoopes, and M. P. Marchetti. 2007. Invasion Ecology. Blackwell, Oxford, UK.

Logan, J. A., P. A. Casagrande, and A. M. Liebhold. 1991. Modeling environment for simulation of gypsy moth (Lepidoptera: Lymantriidae) larval phenology. Environmental Entomology 20:1516–1525.

Lubina, J. A., and S. A. Levin. 1988. The spread of a reinvading species: range expansion in the California sea otter. The American Naturalist 131:526–543.

Lynch, H. J., M. Rhainds, J. M. Calabrese, S. Cantrell, C. Cosner, and W. F. Fagan. 2014. How climate extremes — not means — define a species' geographic range boundary via a demographic tipping point. Ecological Monographs 84:131–149.

Mack, R. N., D. Simberloff, W. M. Lonsdale, H. Evans, M. Clout, and F. A. Bazzaz. 2000. Biotic invasions: causes, epidemiology, global consequences, and control. Ecological Applications 10:689–710.

Manderino, R., T. O. Crist, and K. J. Haynes. 2014. Lepidoptera-specific insecticide used to suppress gypsy moth outbreaks may benefit non-target forest Lepidoptera. Agricultural and Forest Entomology 16:359–368.

Mason, C. J., and M. L. McManus. 1981. Larval dispersal of the gypsy moth. Pages 161–202 *in* C. C. Doane and M. L. McManus, editors. The gypsy moth: research toward integrated pest management. USDA Forest Service, Technical Bulletin 1584, Washington, DC.

Mastro, V. C. 1981. Evaluation of disparlure-baited traps. Pages 549–554 *in* C. C. Doane and M. L. McManus, editors. The gypsy moth: research toward integrated pest management. USDA Forest Service, Technical Bulletin 1584, Washington, DC.

Matter, S. F., T. Roslin, and J. Roland. 2005. Predicting immigration of two species in contrasting landscapes: effects of scale, patch size and isolation. Oikos 111:359–368.

McGarigal, K., S. A. Cushman, M. C. Neel, and E. Ene. 2002. FRAGSTATS: Spatial pattern analysis for categorical maps.

McKinnon, L., P. A. Smith, E. Nol, J. L. Martin, F. I. Doyle, K. F. Abraham, H. G. Gilchrist, R. I. G. Morrison, and J. Bêty. 2010. Lower predation risk for migratory birds at high latitudes. Science 327:326–7.

Milenkovic, M., V. Ducic, and B. Milovanovic. 2010. The influence of the solar flux at 2.8 GHz on outbreaks of gypsy moth (*Lymantria dispar* L.) (Lepidoptera: Lymantriidae) in Serbia. Archives of Biological Sciences 62:1021–1025.

Mooney, H. A., and R. J. Hobbs. 2000. Invasive species in a changing world. Island Press, Washington, DC.

Morbey, Y. E., and R. C. Ydenberg. 2001. Protandrous arrival timing to breeding areas: a review. Ecology Letters 4:663–673.

Morin, R. S., A. M. Liebhold, E. R. Luzader, A. J. Lister, K. W. Gottschalk, and D. B. Twardus. 2005. Mapping host-species abundance of three major exotic forest pests. USDA Forest Service Research Paper NE-726.

Muirhead, J. R., B. Leung, C. Overdijk, D. W. Kelly, K. Nandakumar, K. R. Marchant, and H. J. MacIsaac. 2006. Modelling local and long-distance dispersal of invasive emerald ash borer *Agrilus planipennis* (Coleoptera) in North America. Diversity and Distributions 12:71–79.

Neubert, M. G., and H. Caswell. 2000. Demography and dispersal: calculation and sensitivity analysis of invasion speed for structured populations. Ecology 81:1613–1628.

Neubert, M. G., M. Kot, and M. A. Lewis. 2000. Invasion speeds in fluctuating environments. Proceedings of the Royal Society Biological Sciences 267:1603–10.

Pe'er, G., D. Saltz, H.-H. Thulke, and U. Motro. 2004. Response to topography in a hilltopping butterfly and implications for modelling nonrandom dispersal. Animal Behaviour 68:825–839.

Peltonen, M., A. M. Liebhold, O. N. Bjørnstad, and D. W. Williams. 2002. Spatial synchrony in forest insect outbreaks: roles of regional stochasticity and dispersal. Ecology 83:3120–3129.

Pimentel, D., R. Zuniga, and D. Morrison. 2005. Update on the environmental and economic costs associated with alien-invasive species in the United States. Ecological Economics 52:273–288.

Post, E., S. A. Levin, Y. Iwasa, and N. C. Stenseth. 2001. Reproductive asynchrony increases with environmental disturbance. Evolution 55:830–834.

Prism Climate Group. 2012. United States average May maximum temperature, 1981-2010 (800m; BIL). Oregon State University.

R Core Team. 2014. R: A language and environment for statistical computing. R Foundation for Statistical Computing.

Régnière, J., J. Delisle, D. S. Pureswaran, and R. Trudel. 2013. Mate-finding allee effect in spruce budworm population dynamics. Entomologia Experimentalis et Applicata 146:112–122.

Regniere, J., and R. Saint-Amant. 2008. BioSIM 9 - User's Manual. Natural Resources Canada, Canadian Forest Service, Laurentian Forestry Centre, Quebec, QC.

Regniere, J., and A. A. Sharov. 1998. Phenology of *Lymantria dispar* (Lepidoptera: Lymantriidae), male flight and the effect of moth dispersal in heterogeneous landscapes. International Journal of Biometeorology 41:161–168.

Rhainds, M., and W. F. Fagan. 2010. Broad-scale latitudinal variation in female reproductive success contributes to the maintenance of a geographic range boundary in bagworms (Lepidoptera: Psychidae). PloS One 5:e14166.

Riscassi, A. L., and T. M. Scanlon. 2009. Nitrate variability in hydrological flow paths for three mid-Appalachian forested watersheds following a large-scale defoliation. Journal of Geophysical Research 114:G02009.

Robinet, C., D. R. Lance, K. W. Thorpe, K. S. Onufrieva, P. C. Tobin, and A. M. Liebhold. 2008. Dispersion in time and space affect mating success and Allee effects in invading gypsy moth populations. The Journal of Animal Ecology 77:966–73.

Robinet, C., A. M. Liebhold, and D. Gray. 2007. Variation in developmental time affects mating success and Allee effects. Oikos 116:1227–1237.

Saupe, D. 1988. Algorithms for random fractals. Pages 71–136 *in* H. O. Petigen and D. Saupe, editors. The Science of Fractal Images. Springer, New York.

Scanlon, T. M., S. M. Ingram, and A. L. Riscassi. 2010. Terrestrial and in-stream influences on the spatial variability of nitrate in a forested headwater catchment. Journal of Geophysical Research 115:G02022.

Schauber, E. M. 2001. Models of mast seeding and its ecological effects on gypsy moth populations and Lyme disease risk. Ph.D. Dissertation. The University of Connecticut, Storrs.

Schauber, E. M., R. S. Ostfeld, and C. G. Jones. 2004. Type 3 functional response of mice to gypsy moth pupae: is it stabilizing? Oikos 107:592–602.

Schemske, D. W., G. G. Mittelbach, H. V. Cornell, J. M. Sobel, and K. Roy. 2009. Is there a latitudinal gradient in the importance of biotic interactions? Annual Review of Ecology, Evolution, and Systematics 40:245–269.

Schwalbe, C. P. 1981. The use of attractants in traps. Pages 542–548 *in* C. C. Doane and M. L. McManus, editors. The gypsy moth: research toward integrated pest management. USDA Forest Service, Technical Bulletin 1584, Washington, DC.

Sharov, A. A., A. M. Liebhold, and E. Anderson. 1997. Correlations of counts of gypsy moths (Lepidoptera: Lymantriidae) in pheromone traps with landscape characteristics. Forest Science 43:483–490.

Sharov, A. A., A. M. Liebhold, and F. W. Ravlin. 1995a. Prediction of gypsy moth (Lepidoptera, Lymantriidae) mating success from pheromone trap counts. Environmental Entomology 24:1239–1244.

Sharov, A. A., B. C. Pijanowski, A. M. Liebhold, and S. H. Gage. 1999. What affects the rate of gypsy moth (Lepidoptera: Lymantriidae) spread: winter temperature or forest susceptibility? Agricultural and Forest Entomology 1:37–45.

Sharov, A. A., E. A. Roberts, A. M. Liebhold, and F. W. Ravlin. 1995b. Gypsy moth (Lepidoptera: Lymantriidae) spread in the central Appalachians: three methods for species boundary estimation. Environmental Entomology 24:1529–1538.

Sheehan, K. A. 1992. User's guide for GMPHEN: gypsy moth phenology model. USDA Forest Service, Northeast Research Station, Radnor, PA.

Shigesada, N., and K. Kawasaki. 1997. Biological Invasions: Theory and Practice. Oxford University Press, New York.

Shigesada, N., K. Kawasaki, and Y. Takeda. 1995. Modeling stratified diffusion in biological invasions. The American Naturalist 146:229–251.

Simberloff, D., J.-L. Martin, P. Genovesi, V. Maris, D. a Wardle, J. Aronson, F. Courchamp, B. Galil, E. García-Berthou, M. Pascal, P. Pyšek, R. Sousa, E. Tabacchi, and M. Vilà. 2013. Impacts of biological invasions: what's what and the way forward. Trends in Ecology & Evolution 28:58–66.

Skellam, J. G. 1951. Random dispersal in theoretical populations. Biometrika 38:196–218.

Skelsey, P., K. A. With, and K. A. Garrett. 2012. Why dispersal should be maximized at intermediate scales of heterogeneity. Theoretical Ecology 6:203–211.

Smith, H. R. 1985. Wildlife and the gypsy moth. Wildlife Society Bulletin 13:166–174.

Stamps, J. A., M. Buechner, and V. V Krishnan. 1987. The effects of edge permiability and habitat geometriy on emigration from patches of habitat. The American Naturalist 129:533–552.

Stenseth, N. C., A. Mysterud, G. Ottersen, J. W. Hurrell, K.-S. Chan, and M. Lima. 2002. Ecological effects of climate fluctuations. Science 297:1292–6.

Stephens, P. A., W. J. Sutherland, and R. P. Freckleton. 1999. What is the Allee effect? Oikos 87:185–190.

Suarez, A. V, D. A. Holway, and T. J. Case. 2001. Patterns of spread in biological invasions dominated by long-distance jump dispersal: insights from Argentine ants. Proceedings of the National Academy of Sciences of the United States of America 98:1095–100.

Symonides, E., J. Silvertown, and V. Andreasen. 1986. Population cycles caused by overcompensating density-dependence in an annual plant. Oecologia 71:156–158.

Taylor, C. M., H. G. Davis, J. C. Civille, F. S. Grevstad, C. A. Z. M. Taylor, and A. Hastings. 2004. Consequences of an Allee Effect in the Invasion of a Pacific estuary by *Spartina alterniflora*. Ecology 85:3254–3266.

Taylor, C. M., and A. Hastings. 2005. Allee effects in biological invasions. Ecology Letters 8:895–908.

Tcheslavskaia, K., C. C. Brewster, and A. A. Sharov. 2002. Mating successs of gypsy moth (Lepidoptera: Lymantriidae) females in Southern Wisconsin. Great Lakes Entomologist 35:1–7.

Thompson, L. M. 2014. Forest edges enhance mate-finding in the European gypsy moth, *Lymantria dispar*. M.S. Thesis. Virginia Commonwealth University.

Tobin, P. C., B. B. Bai, D. A. Eggen, and D. S. Leonard. 2012. The ecology, geopolitics, and economics of managing *Lymantria dispar* in the United States. International Journal of Pest Management 58:195–210.

Tobin, P. C., L. L. Berec, and A. M. Liebhold. 2011. Exploiting Allee effects for managing biological invasions. Ecology Letters 14:615–624.

Tobin, P. C., and L. M. Blackburn. 2008. Long-distance dispersal of the gypsy moth (Lepidoptera: Lymantriidae) facilitated its initial invasion of Wisconsin. Environmental Entomology 37:87–93.

Tobin, P. C., D. R. Gray, and A. M. Liebhold. 2014. Supraoptimal temperatures influence the range dynamics of a non-native insect. Diversity and Distributions 20:813–823.

Tobin, P. C., K. T. Klein, and D. S. Leonard. 2009a. Gypsy moth (Lepidoptera: Lymantriidae) flight behavior and phenology based on field-deployed automated pheromone-baited traps. Environmental Entomology 38:1555–62.

Tobin, P. C., A. M. Liebhold, and E. A. Roberts. 2007a. Comparison of methods for estimating the spread of a non-indigenous species. Journal of Biogeography 34:305–312.

Tobin, P. C., K. S. Onufrieva, and K. W. Thorpe. 2013. The relationship between male moth density and female mating success in invading populations of *Lymantria dispar*. Entomologia Experimentalis et Applicata 146:103–111.

Tobin, P. C., C. Robinet, D. M. Johnson, S. L. Whitmire, O. N. Bjørnstad, and A. M. Liebhold. 2009b. The role of Allee effects in gypsy moth, *Lymantria dispar* (L.), invasions. Population Ecology 51:373–384.

Tobin, P. C., A. A. Sharov, A. M. Liebhold, D. S. Leonard, E. A. Roberts, and M. R. Learn. 2004. Management of the gypsy moth through a decision algorithm under the STS project. American Entomologist 50:200–209.

Tobin, P. C., S. L. Whitmire, D. M. Johnson, O. N. Bjørnstad, and A. M. Liebhold. 2007b. Invasion speed is affected by geographical variation in the strength of Allee effects. Ecology Letters 10:36–43.

Torrence, C., and G. P. Compo. 1998. A practical guide to wavelet analysis. Bulletin of the American Meteorological Society 79:61–78.

Turchin, P. 1998. Quantitative analysis of movement. Sinauer, Sunderland, MA.

Ugeno, M. A. S. 2013. A semiparametric Bayesian method for detecting Allee effects 94:1196–1204.

United States Geologic Survey. 2002. National elevation dataset. http://nationalmap.gov.

USDA Forest Service. 2008. Forest type groups of the United States. http://fsgeodata.fs.fed.us/rastergateway/forest_type/.

USDA Forest Service. 2013. Insect and disease detection survey data explorer. http://foresthealth.fs.usda.gov/portal/Flex/IDS.

USDA Forest Service. 2014. European Gypsy Moth North America Quarantine. http://www.aphis.usda.gov/plant_health/plant_pest_info/gypsy_moth/downloads/gypmoth.pdf.

Vandermeer, J., B. Hoffman, S. L. Krantz-ryan, U. Wijayratne, J. Buff, and V. Franciscus. 2001. Effect of habitat fragmentation on gypsy moth (*Lymantria dispar* L.) dispersal: the quality of the matrix. The American Midland Naturalist 145:188–193.

Veit, R. R., and M. A. Lewis. 1996. Dispersal, population growth, and the Allee effect: dynamics of the house finch invasion of eastern North America. The American Naturalist 148:255–274.

Vercken, E., A. M. Kramer, P. C. Tobin, and J. M. Drake. 2011. Critical patch size generated by Allee effect in gypsy moth, *Lymantria dispar* (L.). Ecology Letters 14:179–86.

Vitousek, P. M., C. M. D'Antonio, L. L. Loope, and R. G. Westbrooks. 1996. Biological invasions as global environmental change. American Scientist 84:218–228.

Walter, J. A., M. S. Meixler, T. Mueller, W. F. Fagan, P. C. Tobin, and K. J. Haynes. 2014. How topography induces reproductive asynchrony and alters gypsy moth invasion dynamics. The Journal of Animal Ecology.

Wang, M., and M. Kot. 2001. Speeds of invasion in a model with strong or weak Allee effects. Mathematical Biosciences 171:83–97.

Wang, M., M. Kot, and M. G. Neubert. 2002. Integrodifference equations, Allee effects, and invasions. Mathematical Biology 168:150–168.

Whiteman, C. D. 2000. Mountain Meteorology: Fundementals and Applications. Oxford University Press, New York.

Whitmire, S. L., and P. C. Tobin. 2006. Persistence of invading gypsy moth populations in the United States. Oecologia 147:230–237.

Wiens, J. A. 1976. Population responses to patchy environments. Annual Review of Ecology and Systematics 7:81–120.

With, K. A. 2002. The landscape ecology of invasive spread. Conservation Biology 16:1192–1203.

With, K. A., and T. O. Crist. 1995. Critical thresholds in species' responses to landscape structure. Ecology 76:2446–2459.

Wood, S. N. 2006. Generalized additive models: an introduction with R. Chapman and Hall/CRC, Boca Raton, FL, USA.

Wood, S. N. 2008. Fast Stable Direct Fitting and Smoothness Selection for Generalized Additive Models. Journal of the Royal Statistical Society B (Statistical Methodology) 70:495–518.

Wood, S. N., and N. H. Augustin. 2002. GAMs with integrated model selection using penalized regression splines and applications to environmental modelling. Ecological Modelling 157:157–177.

Yahner, R. H., and H. R. Smith. 1991. Small mammals abundance and habitat relationships on deciduous forested sites with different susceptibility to gypsy moth defoliation. Environmental Management 15:113–120.

Appendices

Appendix A1: Sensitivity of spread model results to dispersal parameters (Chapter 2)

We performed additional simulations to investigate how varying short and long-distance dispersal parameters affects invasion pulses. *Sr* and *Lr* correspond to the probability of short and long distance dispersal occurring. The proportion of the population dispersing to a different location is controlled by p_{sr} and p_{lr} for short and long-distance dispersal, respectively, and *Ld* affects the distance of long-distance dispersal. The parameter values presented in the manuscript were: *Sr* = 0.1, p_{sr} = 0.01, *Lr* = 0.01, p_{lr} = 0.1, and *Ld* = 15. Here we present two cases, a 6-year (*P* = 0.16) and a 10-year (*P* = 0.85) population cycle, both with normal cycle strength ($\lambda = 76.4$). As in the manuscript, simulations were run for 250 years with 150 years of run-up time and all figures represent the average (with 95% confidence intervals) global wavelet spectra from 100 model iterations.

In general, varying dispersal parameters did not affect the period lengths at which invasion pulses occurred (Figures A1, A2). Thus, these properties appear to be a consequence of population fluctuations alone. However, the magnitude of peaks in wavelet power indicating pulsed invasion behavior were sensitive to the probability of long-distance dispersal (*Lr*), and somewhat less so to the proportion of the source population dispersing (p_{lr}) with wavelet power of invasion pulses at the full population cycle length declining as *Lr* and p_{lr} increased. At the same time, the magnitude of a peak at ≈2 years increased, possibly reflecting the increased influence of stochasticity when long-distance dispersal occurred more commonly. This was particularly apparent for the 6-year population cycle length (Figure A1). Varying short-distance dispersal parameters had no significant impact on model results.

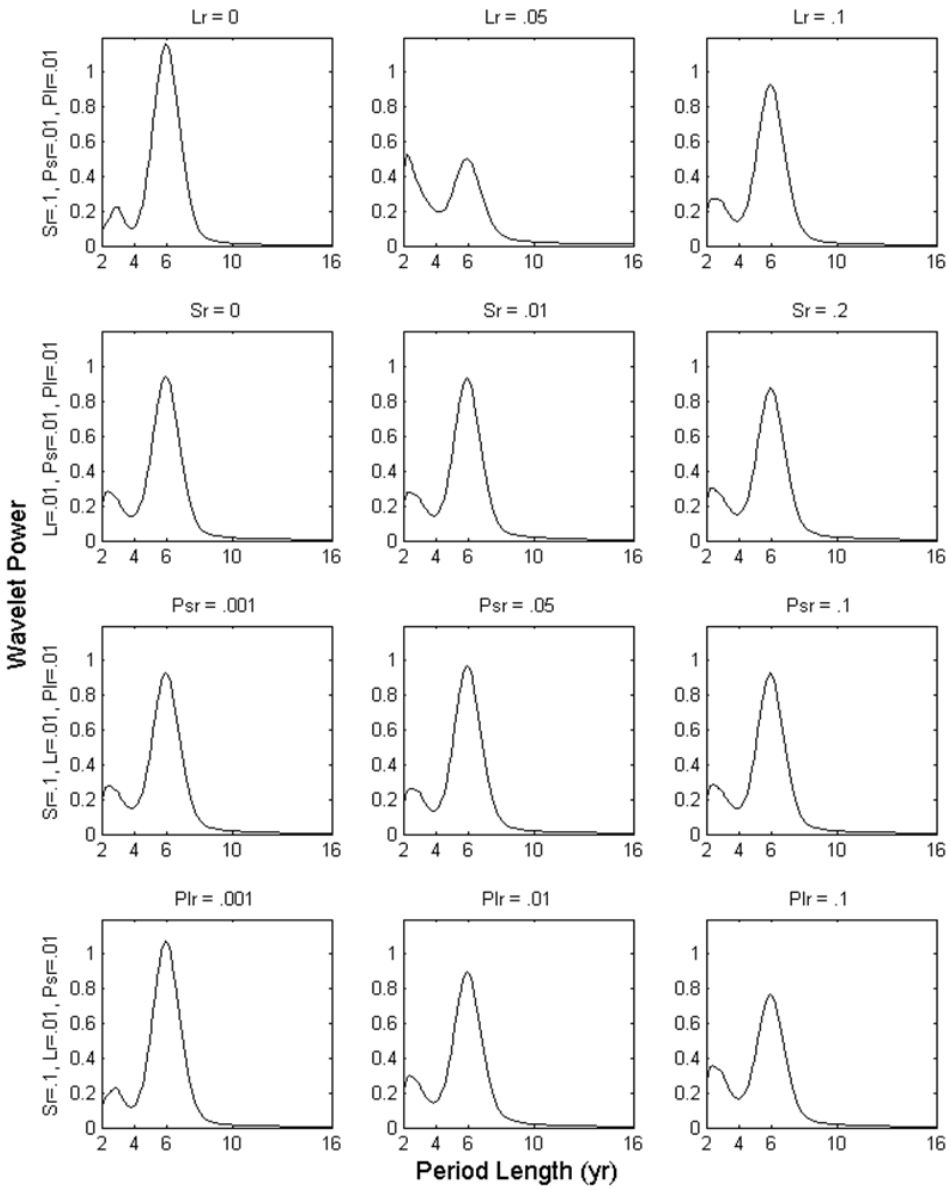

Figure A1.1: Averaged global wavelet spectra of invasion rate where $\lambda = 74.6$ and $P = 0.16$ (6-year period, normal cycle strength), showing effects of variation in *Lr*, *Sr*, p_{sr}, and p_{lr}. All rows have 3 parameters held constant, which are indicated by the *y*-axis labels, and the plot title indicates the varied parameter. The *y*-axes scale is wavelet power. For reference, parameter values in the center plot in the bottom row are those presented in the main manuscript.

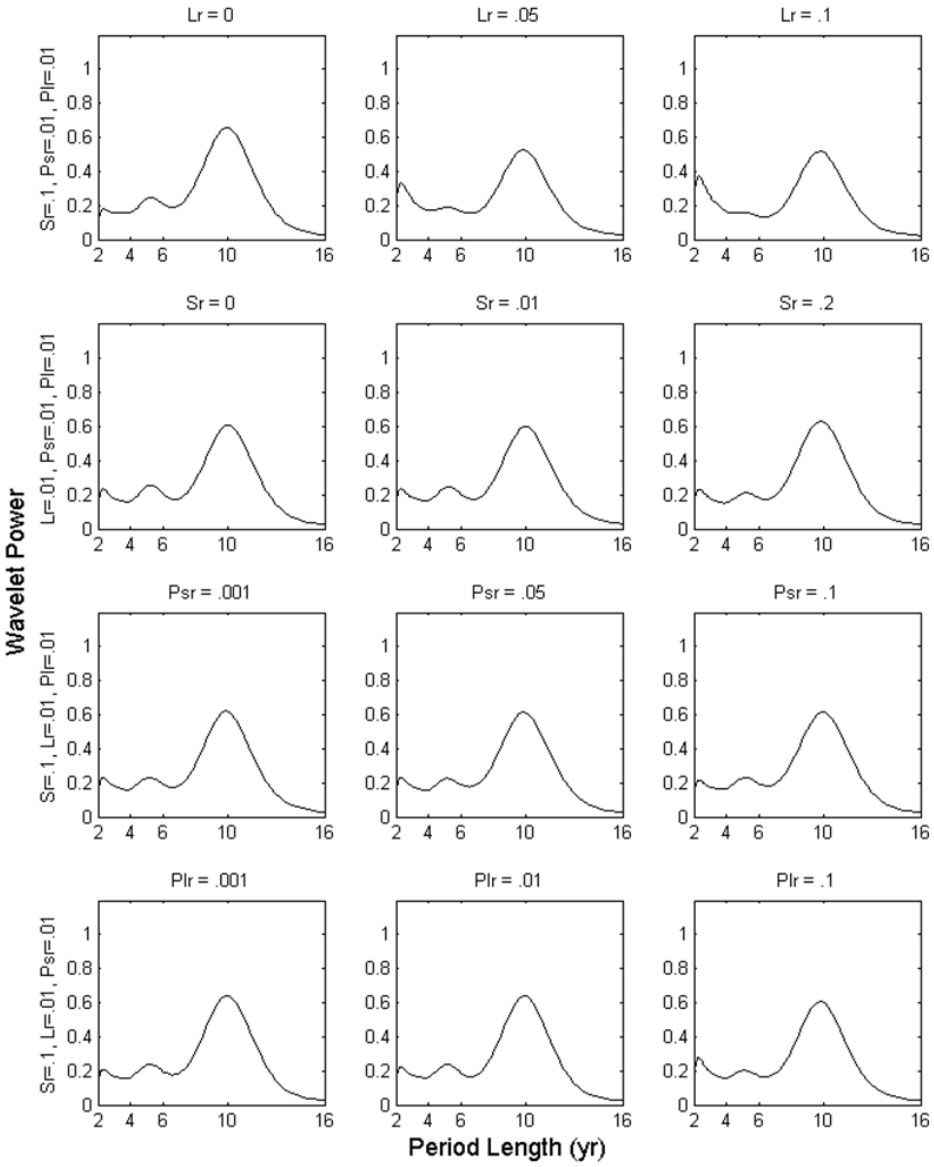

Figure A1.2: Averaged global wavelet spectra of invasion rate for a population with $\lambda = 74.6$ and $P = .85$ (10-year period, normal cycle strength) showing effects of variation in *Lr*, *Sr*, p_{sr}, and p_{lr}. All rows have 3 parameters held constant, which are indicated by the *y*-axis labels, and the plot title indicates the varied parameter. The *y*-axes scale is wavelet power. For reference, parameter values in the center plot in the 3rd row from the top are those presented in the main manuscript.

Appendix A2: Sensitivity of spread model results to range boundary threshold (Chapter 2)

We assessed the sensitivity of our results to variability in the population density threshold defining the range boundary. In the model, gypsy moth population densities fluctuated over 4 orders of magnitude, with the order of magnitude of population density at the nadir of population cycles declining from 10^{-5} to 10^{-7} as predator density, *P*, increased. We examined periodic fluctuations in the location of the range boundary when the range boundary was set at 10^{-5}, 10^{-6}, 10^{-7}, 10^{-8}, and 10^{-9} (Figure B1). The intrinsic rate of increase, λ, was set to 74.6 and we varied *P* to cause the population to cycle with 6, 8, 10, and 12 year periods. The population density defining the range boundary affected the detected periodicity in invasion pulses when it exceeded the density at the nadir of population cycles. In these cases, the period length at which wavelet power peaked tended to be shifted toward shorter period lengths (Figure B1).

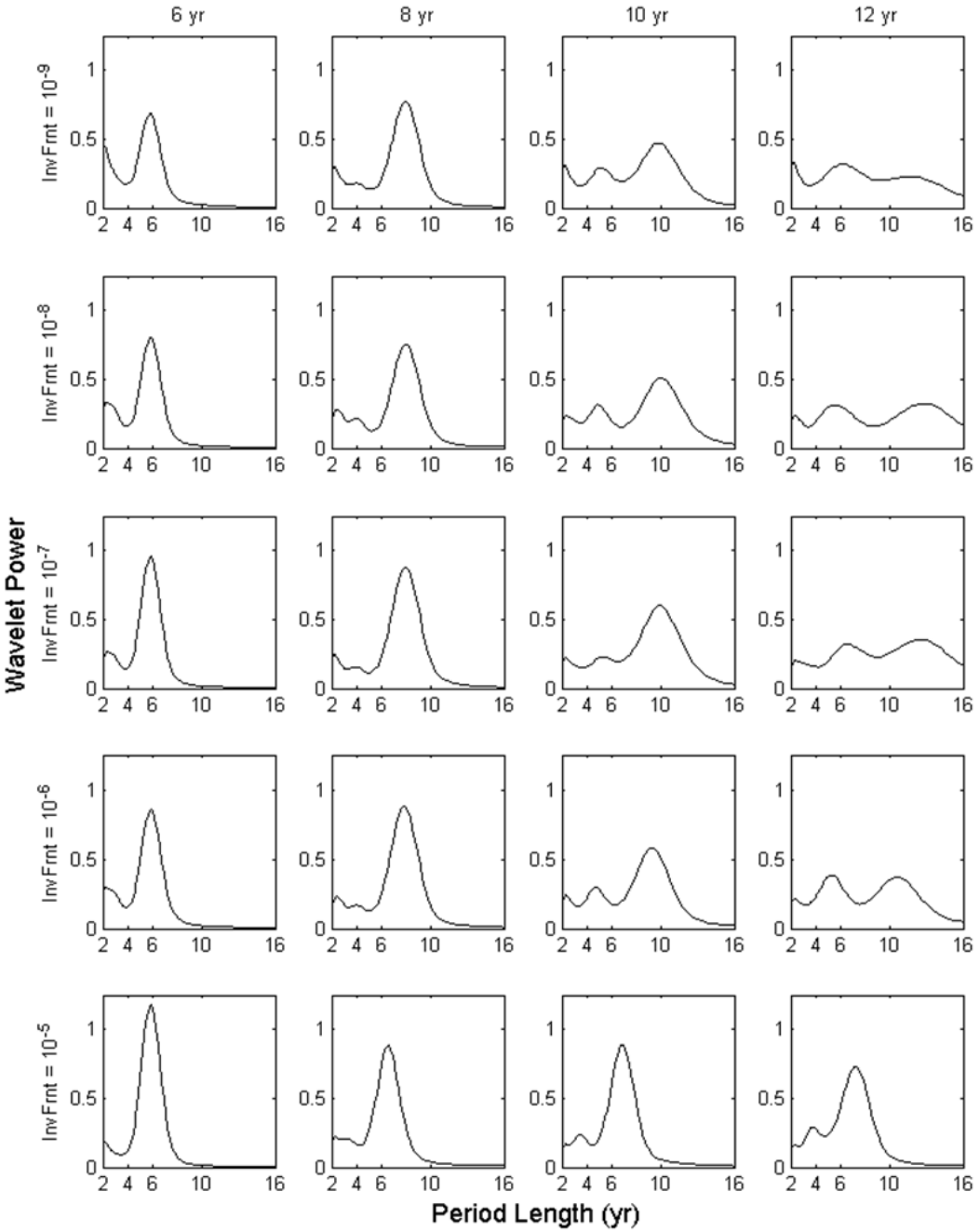

Figure A2.1: Sensitivity of model results to the choice of population density threshold defining the range boundary. Columns have common period length; rows have common range boundary threshold.

Appendix B1: Additional detail regarding data filtering (Chapter 3)

In our empirical analysis (see *Growth Rates in Field Populations* in methods, Chapter 3), we excluded grid cells meeting certain non-mutually-exclusive criteria, primarily removing grid cells in which gypsy moth was present at the beginning of our study period or cells with too little data. We excluded cells where $N > 0$ in the first year in which data were available for that cell (12,694 grid cells) and cells that had fewer than 3 years with $N > 0$ after the last year in which $N = 0$ (40,905 grid cells), which included cells where a zero was recorded in the last year of the time series (22,704 grid cells). In total, 22,850 out of 76,449 cells (29.9%) were retained for analysis. The construction of our time series did remove instances that could be of interest because gypsy moth populations declined to zero; however, we observed that populations for which $N = 0$ at the end of the study period (1988-2009) were predominantly located well beyond the leading edge of the invasion front. These populations were likely more susceptible to extinction than those in cells along the invasion front because dispersal limitation caused founder population sizes and rescue effects to decline with increasing distance from the established population (Whitmire and Tobin 2006, Vercken et al. 2011).

Appendix B2: Spatial autocorrelation in population growth rates (Chapter 3)

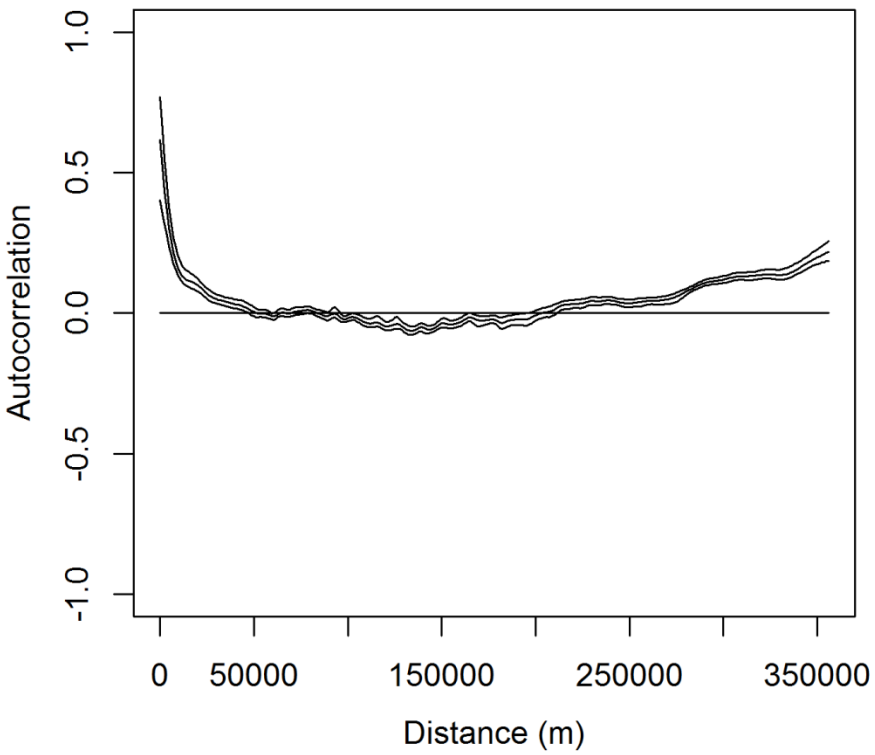

Figure B2.1: Spatial autocorrelation in gypsy moth population growth rates was assessed using a spline correlogram. The mean spline estimate of autocorrelation decayed to zero over 57,629 meters, with the lower 95% confidence boundary reaching zero at 47,926 meters. To account for spatial autocorrelation, we used the distance-decay of spatial autocorrelation to inform computation of the distance-weighted mean population growth rate and included this as a term in the GAM analysis.

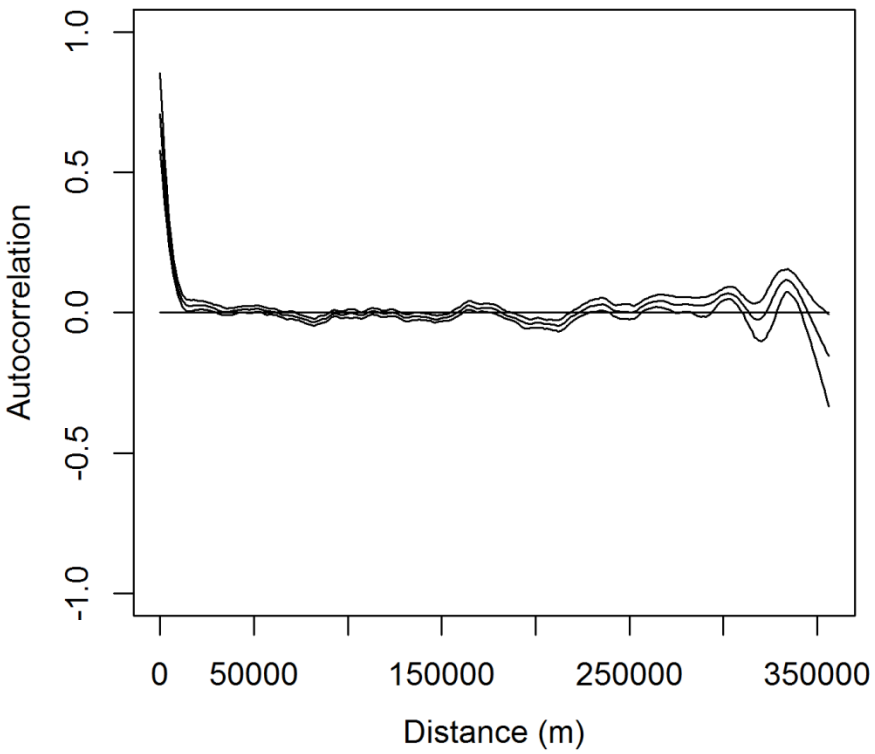

Figure B2.2: Inclusion of the distance-weighted mean growth rate effectively reduced spatial autocorrelation in the GAM model residuals. The mean spline estimate of autocorrelation decayed to zero over 63,773 meters, but the lower 95% confidence boundary reached zero in only 28,267 meters. Autocorrelation in the model residuals declined more rapidly with increases in distance than in the raw population growth rates.

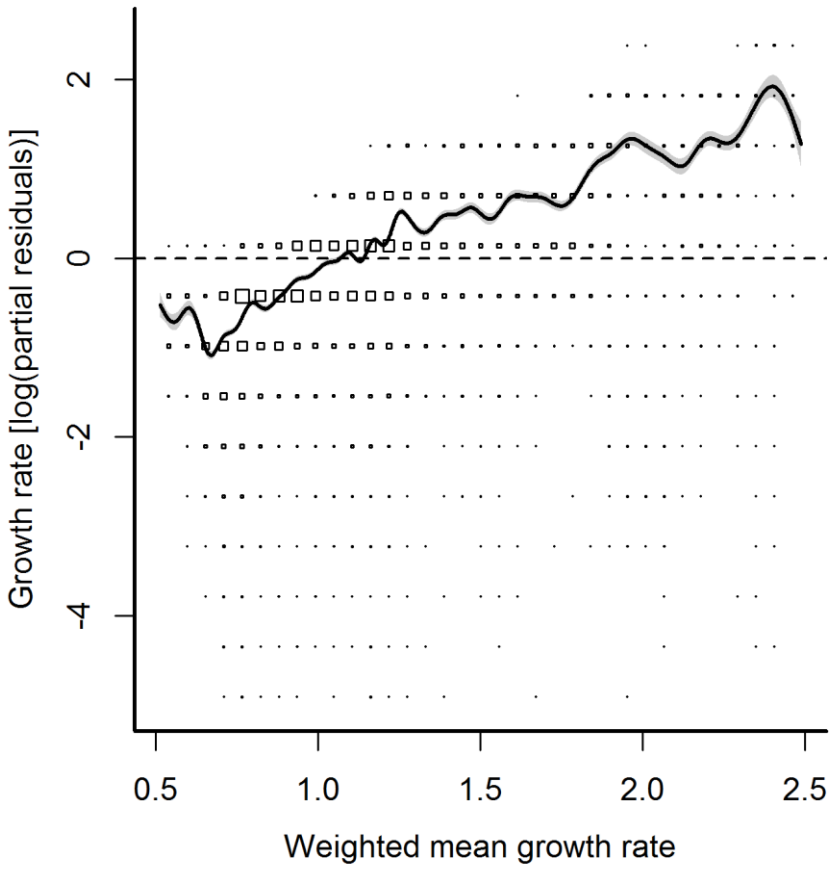

Figure B2. 3: GAM fitted spline relationship between gypsy moth population growth rates and the distance-weighted mean growth rate (estimated spline degrees of freedom = 44.4). Grey regions are confidence bounds (± 2 standard errors). X-axes are scaled in units of the linear predictor; Y-axes are partial residuals on a logarithmic scale. Partial residuals were binned using equal-width intervals and are plotted using squares scaled proportionally to the number of residuals in that bin.

Appendix B3: Details of custom geographic projection (Chapter 3)

Base projection: Albers
False Easting: 0
False Northing: 0
Central Meridian: -85.0
Standard Parallel 1: 34.0
Standard Parallel 2: 47.0
Latitude of Origin: 0
Linear Unit: Meter

Appendix B4: Model selection for effects of elevation and latitude on phenology (Chapter 3)

Table B4.1: We considered combinations of linear, quadratic, and exponential effects of elevation and latitude on day of peak male gypsy moth maturation. The best model was selected by minimizing AIC values and are presented according to rank.

Rank	Model	AIC
1	Peak ~ northing^2 + northing + elevation^2 + elevation	384852.4
2	Peak ~ northing^2 + northing + exp(elevation)	386617.0
3	Peak ~ northing + elevation^2 + elevation	387394.0
4	Peak ~ northing + exp(elevation)	389235.0
5	Peak ~ northing^2 + northing + elevation	407934.7
6	Peak ~ northing + elevation	410600.5
7	Peak ~ exp(northing) + elevation^2 + elevation	493892.0
8	Peak ~ exp(northing) + exp(elevation)	499503.3
9	Peak ~ elevation^2 + elevation	505083.1
10	Peak ~ exp(elevation)	510939.6
11	Peak ~ exp(northing) + elevation	515822.6
12	Peak ~ elevation	525620.9
13	Peak ~ northing^2 + northing	626800.1
14	Peak ~ northing	627329.2
15	Peak ~ exp(northing)	631343.9

Table B4.2: We considered combinations of linear, quadratic, and exponential effects of elevation and latitude on temporal dispersion of male gypsy moth maturation. The best model was selected by minimizing AIC values and are presented according to rank.

Rank	Model	AIC
1	Dispersion ~ northing^2 + northing + exp(elevation)	-12836.60
2	Dispersion ~ northing + exp(elevation)	-12417.54
3	Dispersion ~ northing^2 + northing + elevation^2 + elevation	-11717.69
4	Dispersion ~ northing + elevation^2 + elevation	-11390.31
5	Dispersion ~ northing^2 + northing + elevation	-292.96
6	Dispersion ~ northing + elevation	220.29
7	Dispersion ~ exp(northing) + elevation^2 + elevation	45759.39
8	Dispersion ~ exp(northing) + exp(elevation)	50521.26
9	Dispersion ~ elevation^2 + elevation	53291.42
10	Dispersion ~ exp(elevation)	58474.03
11	Dispersion ~ exp(northing) + elevation	63320.75
12	Dispersion ~ elevation	70318.83
13	Dispersion ~ northing^2 + northing	146750.53
14	Dispersion ~ northing	147395.99
15	Dispersion ~ exp(northing)	152148.47

Table B4.3: We considered combinations of linear, quadratic, and exponential effects of elevation and latitude on gypsy moth protandry. The best model was selected by minimizing AIC values and are presented according to rank. Note that a common model selection criterion indicates substantial support for several candidate models because that difference in AIC values is < 2 (Burnham and Anderson 2002), but only one model could be used in our simulations.

Rank	**Model**	**AIC**
1	Protandry ~ northing + elevation	86.61
2	Protandry ~ northing + exp(elevation)	86.62
3	Protandry ~ exp(elevation)	87.21
4	Protandry ~ elevation	87.77
5	Protandry ~ northing + elevation^2 + elevation	88.50
6	Protandry ~ northing^2 + northing + exp(elevation)	88.59
7	Protandry ~ northing^2 + northing + elevation	88.60
8	Protandry ~ elevation^2 + elevation	89.17
9	Protandry ~ exp(northing) + exp(elevation)	89.21
10	Protandry ~ exp(northing) + elevation	89.76
11	Protandry ~ northing^2 + northing + elevation^2 + elevation	90.48
12	Protandry ~ exp(northing) + elevation^2 + elevation	91.16
13	Protandry ~ northing	113.42
14	Protandry ~ exp(northing)	113.81
15	Protandry ~ northing^2 + northing	115.42

Appendix B5: plots of population growth rate vs. elevation and hilliness (Chapter 3)

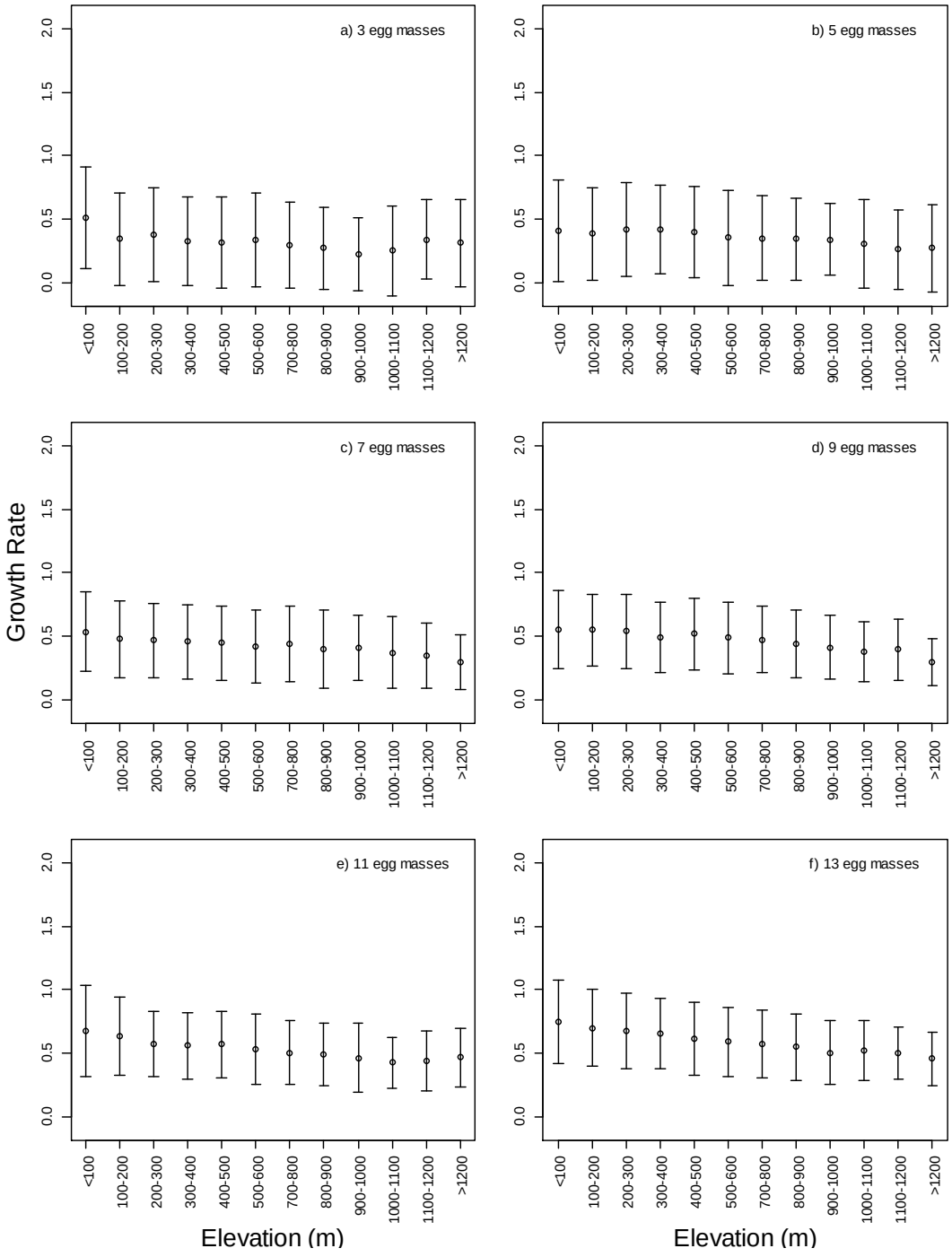

Figure B5.1**:** Effect of elevation on population growth rates for a range of egg mass densities. The population growth rate generally declined with increases in elevation, and the decline in population growth rate tended to strengthen as the number of introduced egg masses increased.

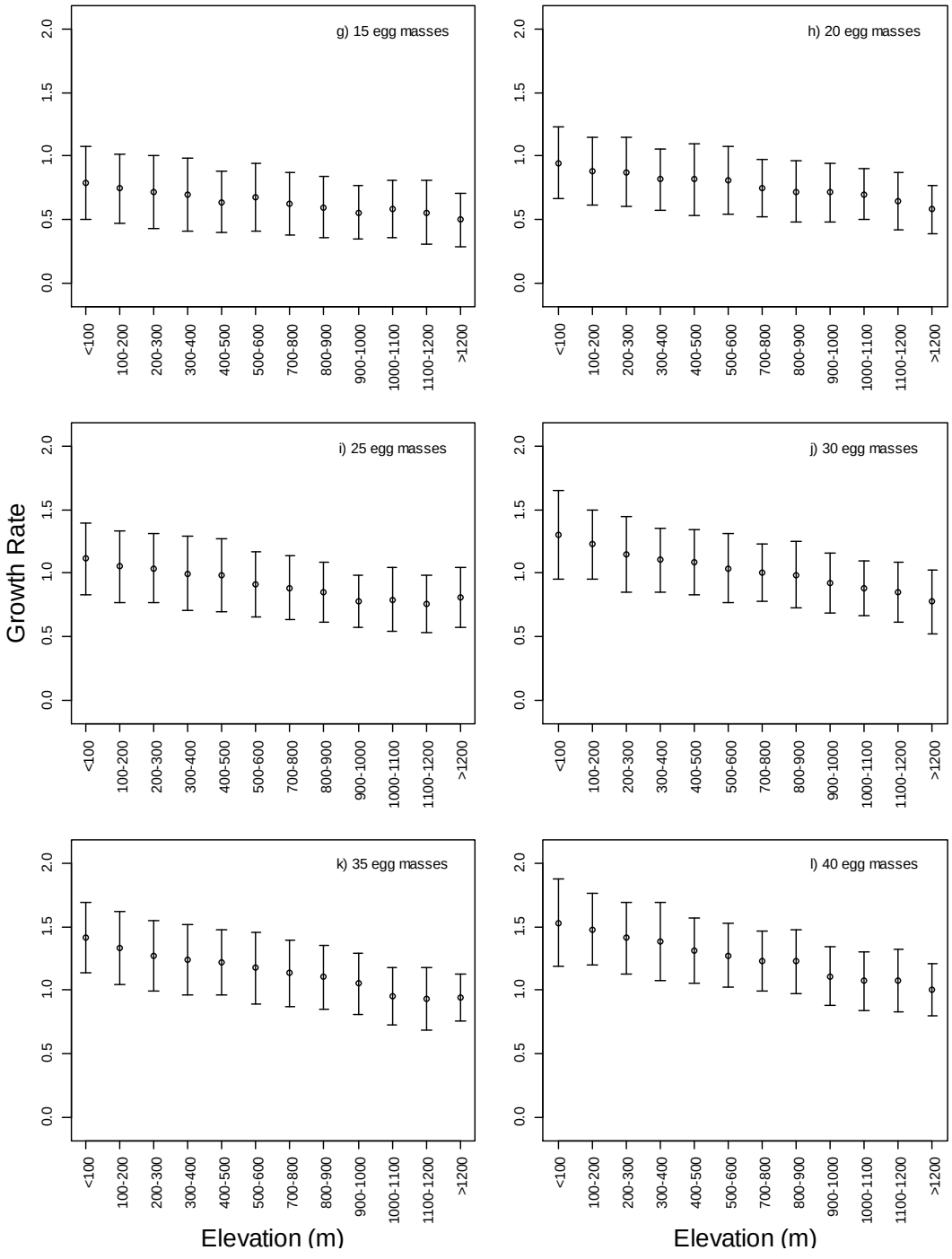

Figure B5.2: Effect of elevation on population growth rates for a range of egg mass densities. The population growth rate generally declined with increases in elevation, and the decline in population growth rate tended to strengthen as the number of introduced egg masses increased.

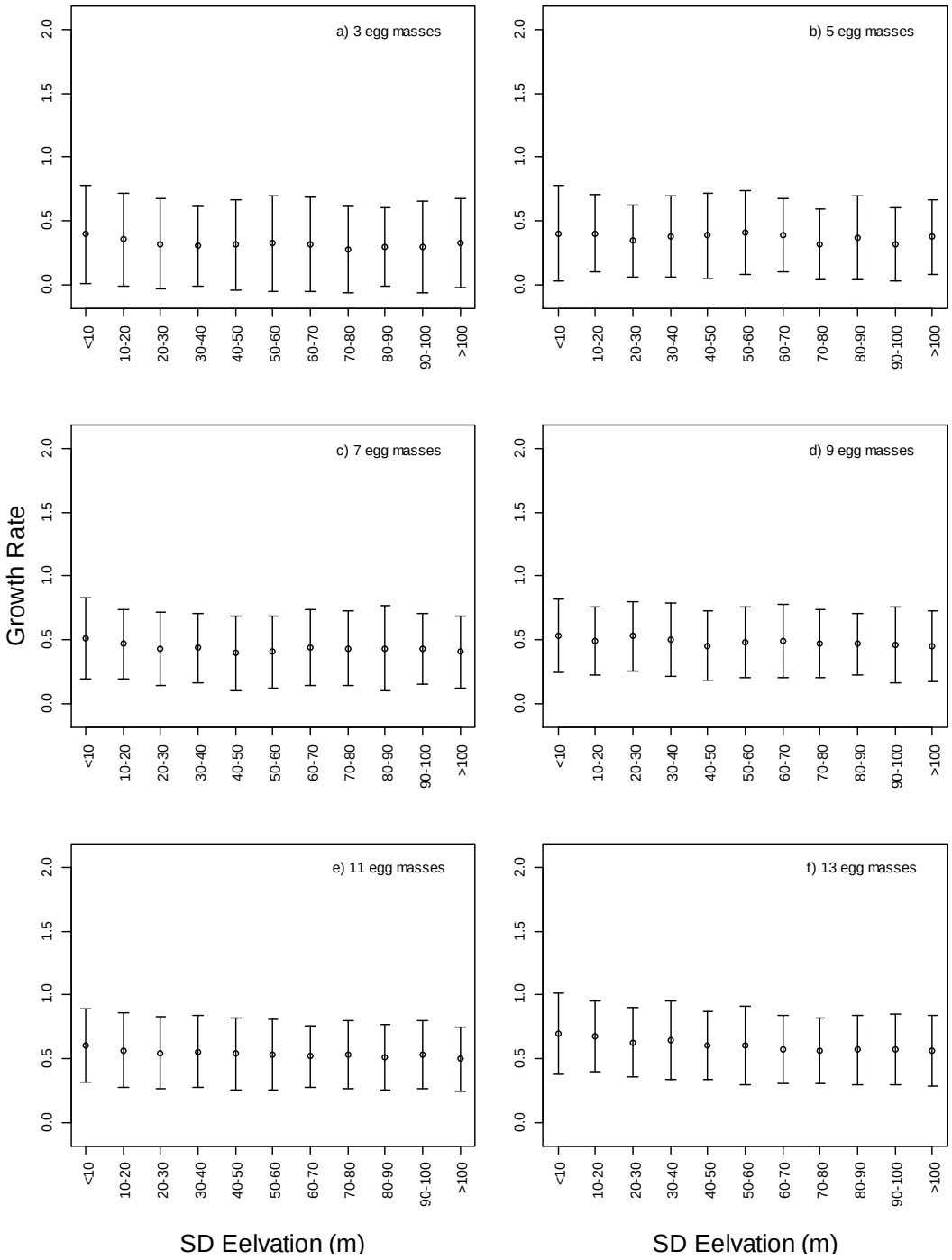

Figure B5.3: Effect of elevational heterogeneity (SD Elevation) on gypsy moth population growth rates. The population growth rate declined with increases elevational heterogeneity), although more modestly than with increases in elevation, and with the effect of elevational heterogeneity only becoming apparent at higher egg mass densities.

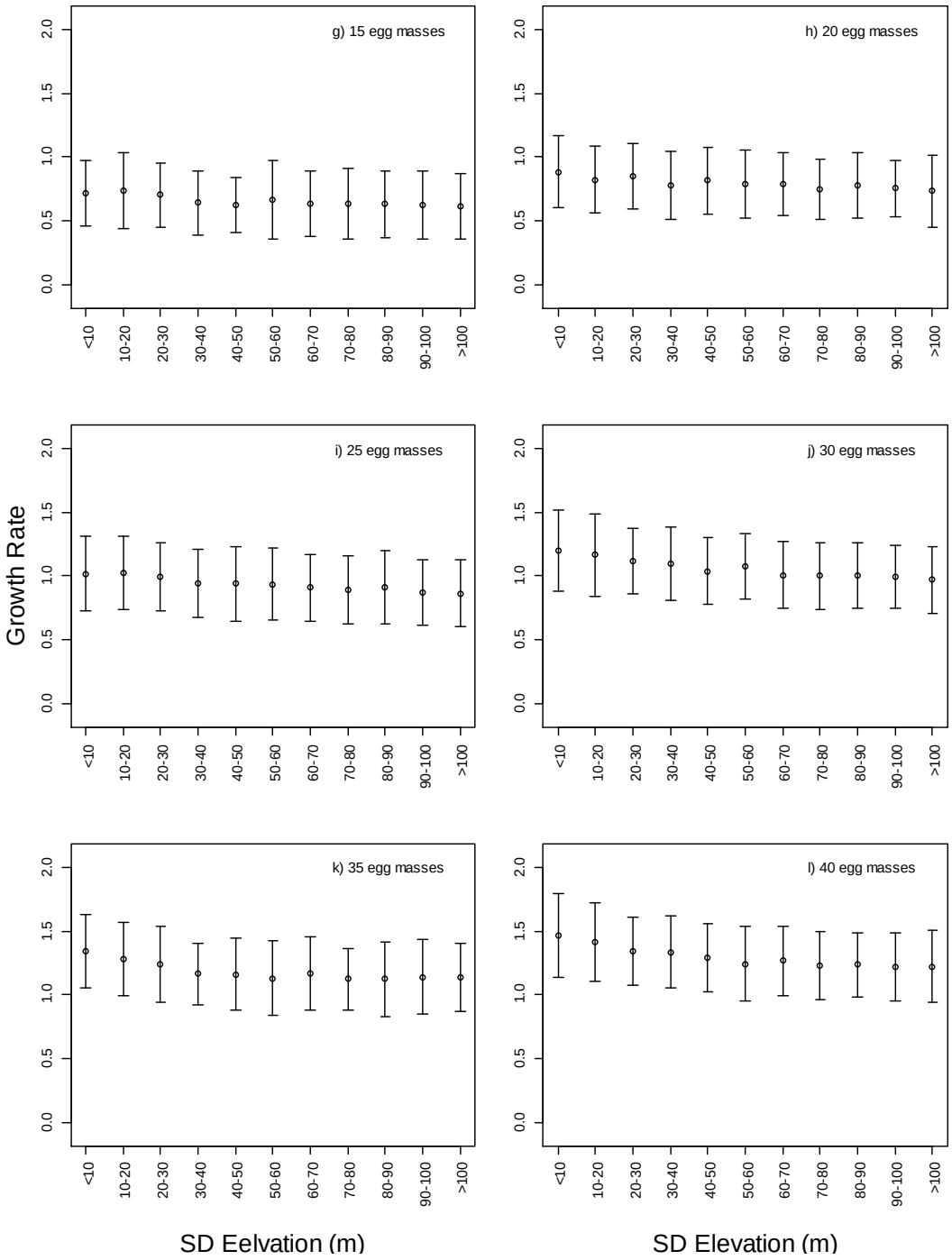

Figure B5.4: Effect of elevational heterogeneity (SD Elevation) on gypsy moth population growth rates. The population growth rate declined with increases elevational heterogeneity), although more modestly than with increases in elevation, and with the effect of elevational heterogeneity only becoming apparent at higher egg mass densities.

Appendix C1: The effect of grid size on dispersal kernel equation fits (Chapter 4)

When determining which kernel equation best described the distance-decay of gypsy moth mate-finding probabilities, we considered whether a different kernel equation could fit best in each habitat type, but we found that we were unable to reach a robust conclusion. The fat-tailed kernel performed best overall and in the non-forest matrix, but the Gaussian and negative exponential equations performed best in the forest (Table C1.1). Since the main difference between the fat-tailed kernel and the Gaussian or negative exponential equations is the higher probability of long-distance dispersal events predicted by the fat-tailed kernel, we suspected that this difference in performance might be explained by the fact that forest trap arrays were generally smaller than our non-forest matrix arrays. To test this, we ran our model evaluation procedure on the non-forest matrix datasets, while omitting traps further than a 5×5 array (matching 2 out of 3 forest releases). Using this restricted dataset, the Gaussian and negative exponential equations performed best (Table C1.1). Hence, we concluded that the stronger performance of the Gaussian and negative exponential functions in the forest releases stemmed from the absence of data on rare long-distance dispersal events and proceeded using the fat-tailed kernel, which performed best overall.

Table C1.1: Selected dispersal kernel equations and their mean rank in forest trials, open field trials, a restricted version of the open field data, and their overall mean rank averaged across all trials. The restricted open field dataset limits the array size to 5×5 traps to investigate the influence of differences in array size between field and forest habitats. The Laplace function could not be fit to data from several open field releases and was omitted from further consideration.

		Mean Rank			
	Equation	**Forest**	**Field**	**Restricted**	**Overall**
Gaussian	$\exp(a - bx^2)$	2.2	3.3	2.3	2.8
Fat-tailed	$\exp(a - b\sqrt{x})$	2.4	1.9	2.4	2.2
Laplace	$\exp(a - bx)$	2.7	-	-	-
Neg. exponential	$a\exp(-bx)$	2.2	2.6	2.2	2.4
Inverse power	ax^{-b}	3.1	2.2	2.9	2.6

Appendix C2: Edge choice release apparatus (Chapter 4)

Figure C2.1: We used the platform and pulley apparatus above to release experimental gypsy moths at forest edges to estimate the likelihood that they would cross forest edges. A release cup containing a single moth was attached with velcro to the platform and released by pulling the string to raise the lid. This apparatus allowed the experimenter to remain ≈5 m away, minimizing the effect of the experimenter's presence on moth behavior. Prior to release, moths selected for experimentation (virgin, <24 hours since eclosion) were stored in a dark cooler to keep them calm.

Appendix C3: Alternate model explaining empirical gypsy moth spread (Chapter 4)

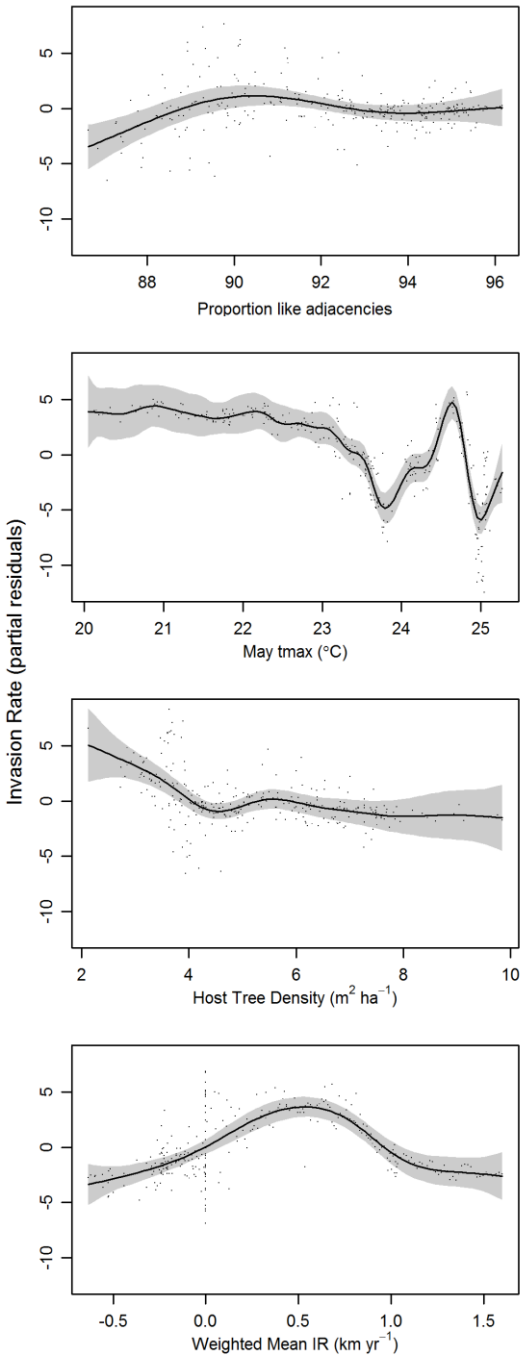

Figure C3.1: Our model selection procedure also indicated strong support (ΔAIC = -0.9) for the model containing the proportion like adjacencies landscape metric. The same predictors were retained after accounting for concurvity, and the model adjusted R^2 = 0.763.

Appendix D: Sensitivity of spread patterns to population dynamic and dispersal parameters (Chapter 5)

In our simulations, the values of all parameters except *c* were held constant over space, but to examine the sensitivity of our results to other model parameters we ran sets of simulations in which we specified one parameter at a time to have a value higher or lower than the "main" value. For reference, the table showing these main and alternate parameter values is reproduced below (Table D1). As with the main parameter set, 50 replicate simulations in each landscape configuration and Allee effect severity level were conducted for each alternate parameter value. The following plots show mean spread trajectories, grouped by Allee effect severity level (Figures D1-D3).

Table D1: Parameter values used in the main simulations and sensitivity analyses.

Parameter	**Low**	**Main**	**High**
r	1.5	2	3
K	100	200	400
p_s	0.05	0.2	0.4
f_s	0.05	0.1	0.2
p_l	0	0.05	0.1
f_l	0.05	0.1	0.2
d_l	5	10	15

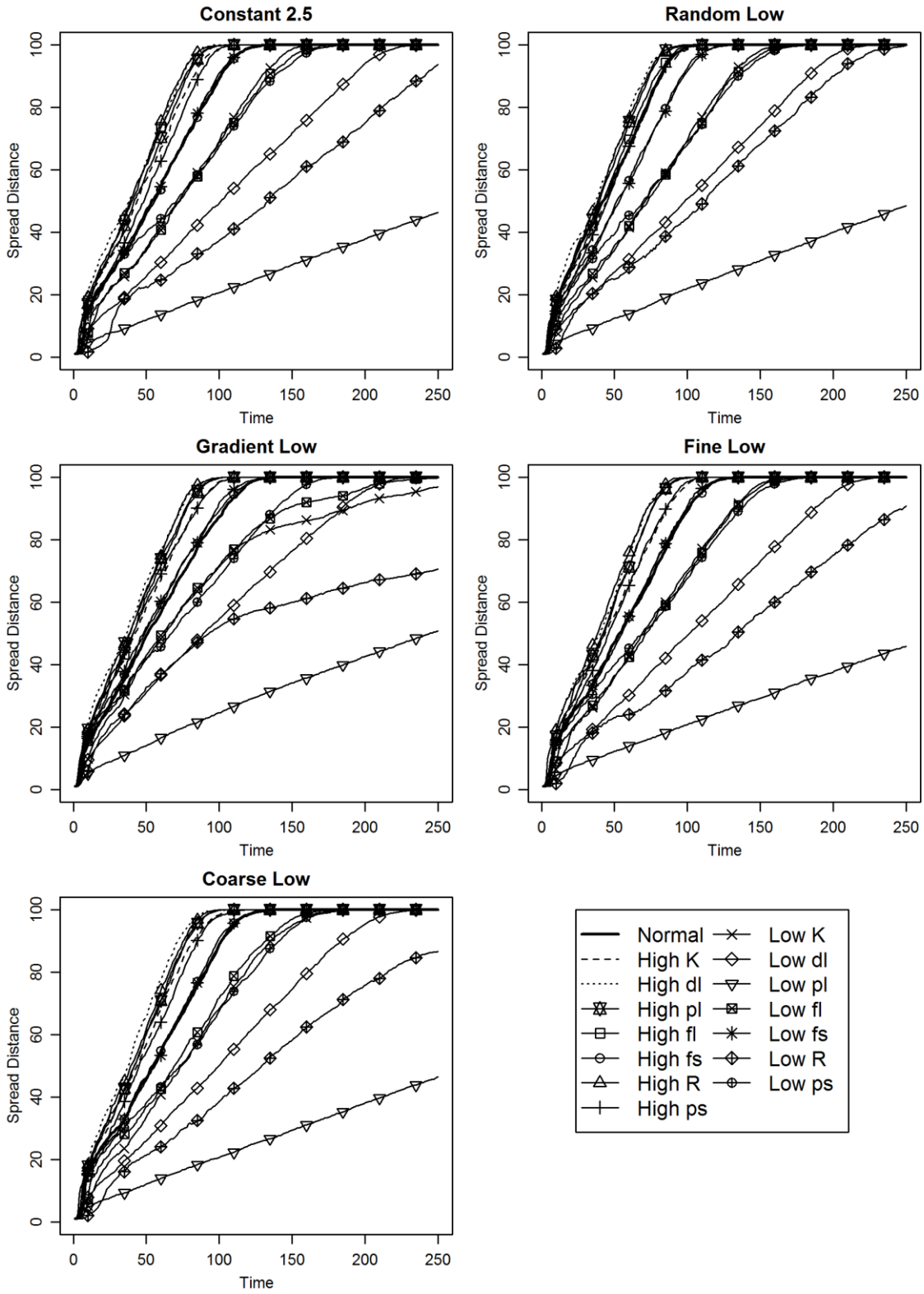

Figure D1: Sensitivity analysis plots for the low Allee effect severity scenario ($0 \leq c \leq 5$).

Plotted spread trajectories represent the mean of 50 replicate simulations.

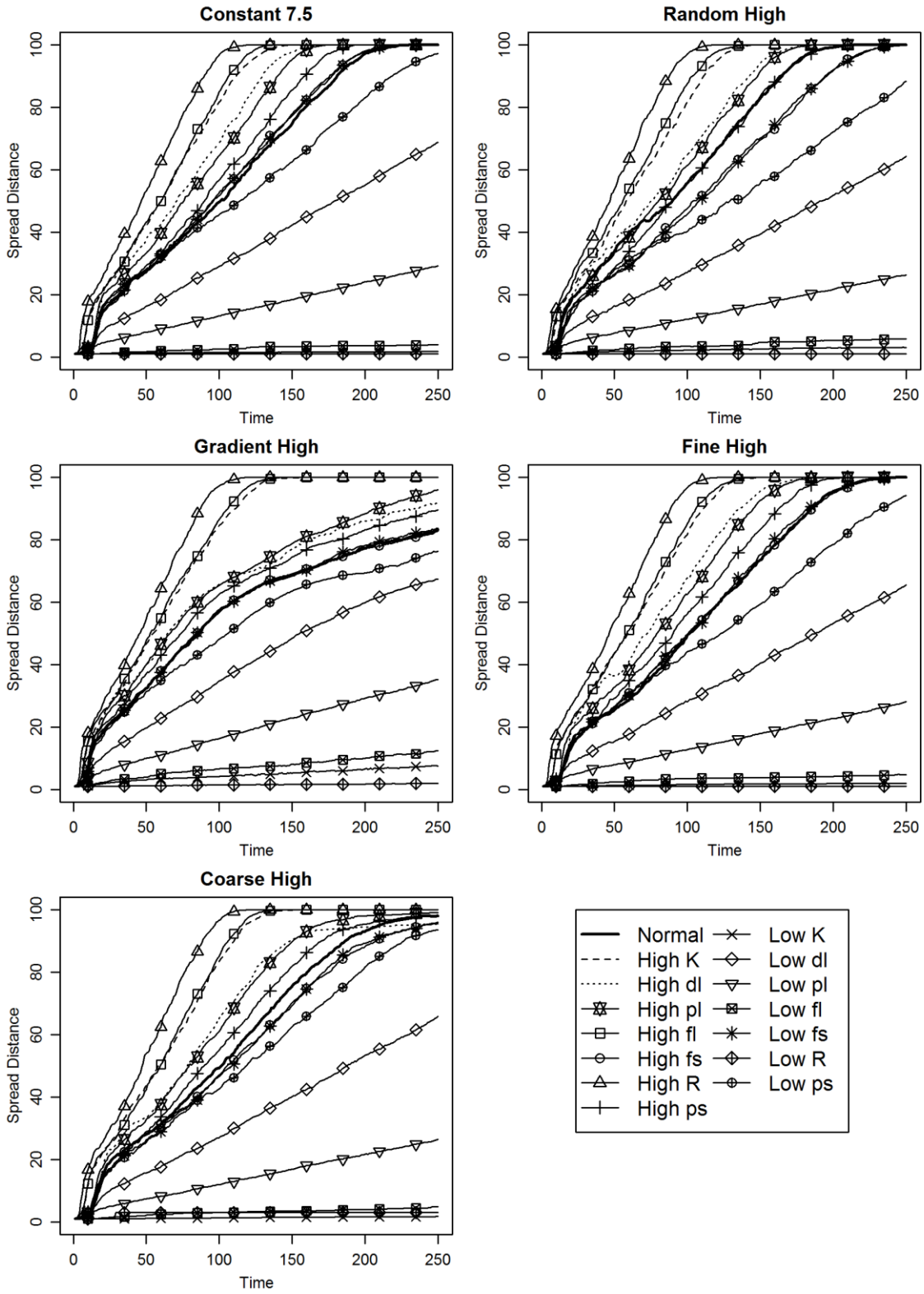

Figure D2: Sensitivity analysis plots for the high Allee effect severity scenario ($5 \leq c \leq 10$).

Plotted spread trajectories represent the mean of 50 replicate simulations.

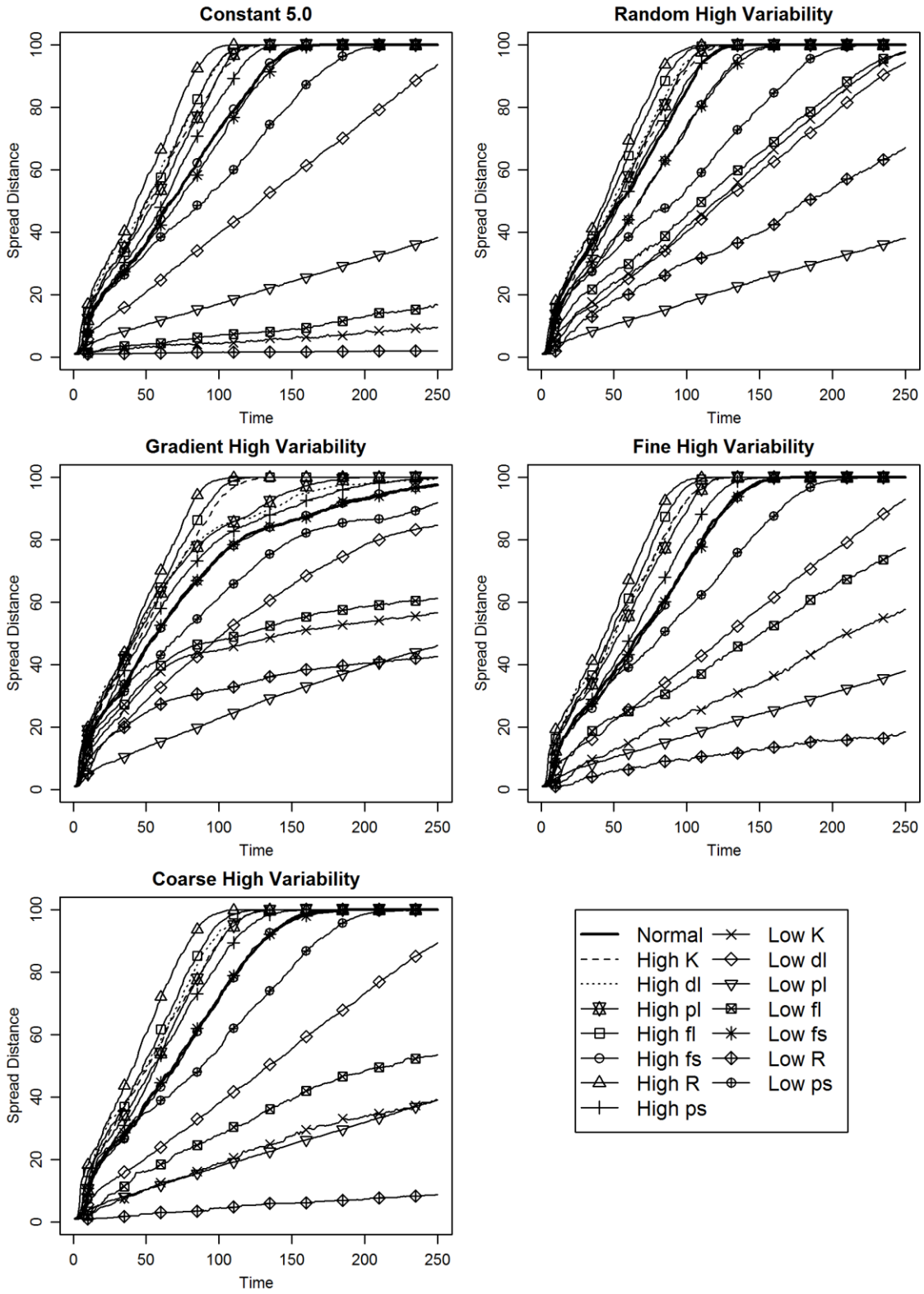

Figure D3: Sensitivity analysis plots for the high variability in Allee effect severity scenario ($0 \leq c \leq 10$). Plotted spread trajectories represent the mean of 50 replicate simulations.